

**Salinity responsiveness of aquaporins in osmoregulatory organs of larval
mosquito *Aedes aegypti***

Lidiya Misyura

A THESIS SUBMITTED TO THE FACULTY OF GRADUATE STUDIES IN PARTIAL
FULFILLMENT OF THE REQUIREMENTS FOR THE DEGREE OF MASTER OF SCIENCE

Graduate Program in Biology
York University
Toronto, Ontario

© Lidiya Misyura, 2018

II. ABSTRACT

Aedes aegypti mosquitoes harbour and transmit arboviral diseases such as chikungunya, dengue, yellow fever, and Zika. The aquatic larvae typically reside in freshwater environments that impose an osmotic challenge of water accumulation in their hemolymph across larval surfaces. Natural phenomena and anthropogenic activities salinize freshwater environments which larvae are able to exploit and successfully complete development in up to 30% seawater. Understanding water regulation under various osmoregulatory challenges is crucial to understanding this disease vector's physiology. Generally, water crosses cellular membranes through transmembrane proteins named aquaporins (AQPs) and *A. aegypti* possess six AQP homologues (AaAQP). This is the first comprehensive study examining the expression of AQPs in *A. aegypti* and their response to changes in environmental salinity within the osmoregulatory organs. An entomoglyceroporin, AaAQP5, is the most abundant AaAQP expressed in the osmoregulatory organs with the most AaAQPs expression found in the Malpighian tubules and anal papillae when compared to other osmoregulatory organs assessed in this study. Changes in transcript and protein abundance were observed in AaAQP1, AaAQP3, AaAQP4, AaAQP5, and AaAQP6 suggesting that the larvae modulate AaAQP expression to regulate water balance with changes to aquatic environmental salinity. Additionally, it was revealed that AaAQPs change their localization between the cytosol and the membrane in osmoregulatory organ epithelia in response to environmental salinity as a potential means of regulating membrane permeability through AaAQP insertion into the membrane. The results provide a basis of understanding for the role of AQPs in the osmoregulatory processes of *A. aegypti* larvae which, through further studies may identify new targets for the development of novel mosquito control agents for larvae prior to their emergence into the disease vector adult life stage.

III. STATEMENT OF CONTRIBUTIONS

This thesis was written by Lidiya Misyura with editing provided by Dr. Andrew Donini. Dissections for RNA extraction were performed by Lidiya Misyura and assisted by Elia Grieco Guardian. All the subsequent experiments, data analysis, and presentation of data were performed by Lidiya Misyura. Figure 1 was created by Lecia Szyca and edited by Lidiya Misyura. Figures 2-33 were created by Lidiya Misyura.

IV. ACKNOWLEDGEMENTS

Firstly, I would like to sincerely thank my supervisor, Dr. Andrew Donini, for giving me a chance to prove myself in his lab and allowing me to become the researcher I am today. Thank you for your continuous support, knowledge, guidance, patience, and encouragement throughout my Master's. There are not enough thank yous to convey my gratitude.

I would like to express my appreciation to my advisor Dr. Scott Kelly for his continuous support, and wisdom throughout my Master's. Thank you for generously allowing me to use equipment to complete the research. I can truly say this Master's would not have been possible without his guidance.

I would also like to thank my Dr. Jean-Paul Paluzzi for allowing me to use his equipment and showing me how to use the notorious Geneious software. Thank you for the encouragement and guidance during my Master's.

Thank you to Dr. Adegoke for his time to read my thesis, provide constructive comments, and attend my defence.

I would like to thank past and present members of the Donini lab (Heath MacMillan, Sima Jonusaite, Andrea Durant, Gil Yerushalmi, Fargol Nowghani, Elia Grieco Guardian, and Amanda Jass)! I'd like to thank each and every one of you for the unbelievable support, kindness, humor, and brilliance throughout my Master's. Thank you Heath MacMillan for always being available to answer questions and for sharing new ideas to help my research. Thank you Sima Jonusaite for sharing your vast knowledge, for always offering advice, and showing me new techniques. Thank you Andrea Durant for being such an incredible supporter, teaching me techniques, and helping me with ideas for troubleshooting the pesky western blots. Thank you Gil Yerushalmi for brightening the day with your humour, for your support through the tough times, always being a friend, and of course providing transportation. Thank you Fargol Nowghani and Amanda Jass for your constant optimism and support. Thank you Elia Grieco Guardian for being such a wonderful student, for your support, and willingness to help.

Thank you Helen Chasiotis for your patience in teaching me the most of what I know in the lab, and for your encouragement even after finishing your postdoctoral fellowship.

Thank you members of the Kelly lab (Chun Chih Chen and Ana Laura Cuciureanu) as well as members Paluzzi lab (David Rocco, Azizia Wahedi, Farwa Sajadi, Aryan Lajevardi, and Andreea Matei) of the for making my Master's exceptionally enjoyable.

Finally, thank you to my family for the endless support, I could not have done this Master's without you.

V. TABLE OF CONTENTS

II. ABSTRACT	ii
III. STATEMENT OF CONTRIBUTIONS	iii
IV. ACKNOWLEDGEMENTS	iv
V. TABLE OF CONTENTS	v
VI. LIST OF TABLES	viii
VII. LIST OF FIGURES	ix
VIII. ABBREVIATIONS	xii
1. INTRODUCTION	1
1.1 Global Impact of <i>Aedes aegypti</i> and Mosquito Control	1
1.2 Aquatic Environments of <i>Aedes aegypti</i> .	2
1.3 Aquaporins	4
1.3.1 Aquaporin Structure	5
1.3.2 Aquaporin Regulation	6
1.3.3 Aquaporin Evolution and Diversification	8
1.3.4 <i>Aedes aegypti</i> Aquaporins	10
AaAQP1	11
AaAQP2	11
AaAQP3	12
AaAQP4	12
AaAQP5	13
AaAQP6	13
1.4 <i>Aedes aegypti</i> Larval Osmoregulatory Organs	16
1.4.1 Midgut	16
Gastric caeca	16
Anterior and Posterior Midgut	18
1.4.2 Malpighian Tubules	20
1.4.3 Hindgut	23
1.4.4 Anal Papillae	24
1.5 Objectives and Hypotheses	27
2. MATERIALS AND METHODS	30
2.1 Animal Care	30
2.2 Total RNA Extraction and cDNA Synthesis	30
2.3 Quantitative real-time PCR (qRT-PCR)	31
2.4 Immunohistochemistry	33
2.5 Protein Processing, Electrophoresis, and Western Blotting	34
2.6 Statistical Analysis	36
3. RESULTS	37

3.1 AaAQP transcript expression profile in the osmoregulatory organs of FW and BW reared <i>A. aegypti</i> larvae	37
3.2 Osmoregulatory organ AaAQP transcript expression profile of FW and BW reared <i>A. aegypti</i> larvae.	40
3.3 AaAQP transcript abundance in response to BW	43
3.4 AaAQP Protein Abundance in the Osmoregulatory Organs of <i>A. aegypti</i> Larvae.	45
3.4.1 AaAQP1	45
3.4.2 AaAQP4	48
3.4.3 AaAQP5	50
3.5 Immunolocalization of AaAQP1, AaAQP4, and AaAQP5 in the osmoregulatory organs of <i>Aedes aegypti</i> larvae	53
3.5.1 Gastric Caeca	53
3.5.2 Anterior Midgut	57
3.5.3 Posterior Midgut	61
3.5.4 Hindgut and Malpighian Tubules	65
3.5.5 Anal Papillae	69
4. DISCUSSION	73
4.1 Overview	73
4.2 AaAQPs in the Gastric Caeca	74
4.2.1 Transcript Abundance	75
4.2.2 Protein Expression	77
4.2.3 What AaAQP Expression May Indicate About Gastric Caeca Functions	79
4.3 AaAQPs in the Anterior Midgut.	81
4.3.1 Transcript Abundance	81
4.3.2 Protein Expression and Localization	83
4.4 AaAQPs in the Posterior Midgut	91
4.4.1 Transcript Abundance	91
4.4.2 Protein Expression and Localization	91
4.5 AaAQPs in the Hindgut	93
4.5.1 AaAQP1	95
4.5.2 AaAQP4	96
4.5.3 AaAQP5	97
4.6 AaAQPs in the Malpighian Tubules	99
4.6.1 AaAQP1	101
4.6.2 AaAQP4	103
4.6.3 AaAQP5	105
4.6.4 AQP Function in the Malpighian tubules	107
4.7 AaAQPs in the Anal Papillae	109
4.7.1 Transcript Abundance	110
4.7.2 AaAQP1	111

4.7.3 AaAQP4	112
4.7.1 AaAQP5	114
4.8 Conclusions	118
5. REFERENCES	120

VI. LIST OF TABLES

Table 1: <i>Aedes aegypti</i> aquaporin predicted molecular mass. _____	11
Table 2: <i>Aedes aegypti</i> adult and larval aquaporin expression, properties, and phylogeny overview. _____	14
Table 3: Ingredients and their corresponding concentration in larval <i>A. aegypti</i> artificial physiological saline, adapted from Clark and Bradley (1996) and Donini et al. (2006). _____	31
Table 4: Primers and their characterization utilized in qPCR. Primers for AaAQP1-6 and 18S rRNA were designed and reported previously (Akhter et al., 2017; Jonusaite et al., 2016; Marusalin et al., 2012). _____	32
Table 5: Antibody concentration used for western blotting. Antibodies were diluted in 5% skimmed milk and TBS-T. _____	36

VII. LIST OF FIGURES

Figure 1: Osmoregulatory organs of larval <i>Aedes aegypti</i> .	4
Figure 2: Schematic diagram illustrating membrane transport proteins in the distal and proximal gastric caeca of larval <i>Aedes aegypti</i> .	18
Figure 3: Schematic diagram illustrating membrane transport proteins in the anterior and posterior midgut of larval <i>Aedes aegypti</i> .	20
Figure 4: Schematic diagram illustrating membrane transport proteins in the Malpighian tubules of larval <i>Aedes aegypti</i> .	23
Figure 5: Schematic diagram illustrating the role of membrane transport proteins in the rectum of larval <i>Aedes aegypti</i> .	24
Figure 6: Schematic diagram illustrating membrane transport proteins in the anal papillae of larval <i>Aedes aegypti</i> .	27
Figure 7: Aquaporin (AQP) mRNA abundance profiles in osmoregulatory organs of freshwater (A,C,E,G,I,K) and brackish water (B,D,F,H,J,L) reared <i>Aedes aegypti</i> larvae.	39
Figure 8: <i>Aedes aegypti</i> osmoregulatory organ aquaporin (AaAQP) mRNA abundance of freshwater (A,C,E,G,I,K) and brackish water (B,D,F,H,J,L) reared larvae.	42
Figure 9: mRNA abundance of aquaporin (AQP) genes in the osmoregulatory organs of larval <i>Aedes aegypti</i> in response to brackish water (30% seawater, dark blue bars) relative to freshwater reared larvae (light blue bars).	44
Figure 10: Protein abundance of AaAQP1 in the gastric caeca (A), anterior midgut (B), posterior midgut (C), Malpighian tubules (D), hindgut (E), and anal papillae (F) of freshwater (FW, light blue bars) and brackish water (BW, 30% seawater, dark blue bars) reared larval <i>Aedes aegypti</i> .	47
Figure 11: Protein abundance of AaAQP4 in the gastric caeca (A), anterior midgut (B), posterior midgut (C), Malpighian tubules (D), hindgut (E), and anal papillae (F) of freshwater (FW, light blue bars) and brackish water (BW, 30% seawater, dark blue bars) reared larval <i>Aedes aegypti</i> .	49
Figure 12: Protein abundance of AaAQP5 in the gastric caeca (A), anterior midgut (B), posterior midgut (C), Malpighian tubules (D), hindgut (E), and anal papillae (F) of freshwater (FW, light blue bars) and brackish water (BW, 30% seawater, dark blue bars) reared larval <i>Aedes aegypti</i> .	52
Figure 13: Immunolocalization of AaAQP1 in the gastric caeca of larval <i>A. aegypti</i> reared in freshwater (FW) and brackish water (BW) using V-type H ⁺ -ATPase (VA) as a membrane marker.	54
Figure 14: Immunolocalization of AaAQP4 in the gastric caeca of larval <i>A. aegypti</i> reared in freshwater (FW) and brackish water (BW) using V-type H ⁺ -ATPase (VA) as a membrane marker.	55
Figure 15: Immunolocalization of AaAQP5 in the gastric caeca of larval <i>A. aegypti</i> reared in freshwater (FW) and brackish water (BW) using V-type H ⁺ -ATPase (VA) as a membrane marker.	56
Figure 16: Immunolocalization of AaAQP1 in the anterior midgut of larval <i>A. aegypti</i> reared in freshwater (FW) and brackish water (BW) using V-type H ⁺ -ATPase (VA) as a basolateral membrane marker.	58

Figure 17: Immunolocalization of AaAQP4 in the anterior midgut of larval <i>A. aegypti</i> reared in freshwater (FW) and brackish water (BW) using V-type H ⁺ -ATPase (VA) as a basolateral membrane marker. _____	59
Figure 18: Immunolocalization of AaAQP5 in the anterior midgut of larval <i>A. aegypti</i> reared in freshwater (FW) and brackish water (BW) using V-type H ⁺ -ATPase (VA) as a basolateral membrane marker. _____	60
Figure 19: Immunolocalization of AaAQP1 in the posterior midgut of larval <i>A. aegypti</i> reared in freshwater (FW) and brackish water (BW) using V-type H ⁺ -ATPase (VA) as an apical membrane marker. _____	62
Figure 20: Immunolocalization of AaAQP4 in the posterior midgut of larval <i>A. aegypti</i> reared in freshwater (FW) and brackish water (BW) using V-type H ⁺ -ATPase (VA) as an apical membrane marker. _____	63
Figure 21: Immunolocalization of AaAQP5 in the posterior midgut of larval <i>A. aegypti</i> reared in freshwater (FW) and brackish water (BW) using V-type H ⁺ -ATPase (VA) as an apical membrane marker. _____	64
Figure 22: Immunolocalization of AaAQP1 in the Malpighian tubules and hindgut of larval <i>A. aegypti</i> reared in freshwater (FW) and brackish water (BW) using V-type H ⁺ -ATPase (VA) as an apical membrane marker. _____	66
Figure 23: Immunolocalization of AaAQP4 in the Malpighian tubules and hindgut of larval <i>A. aegypti</i> reared in freshwater (FW) and brackish water (BW) using V-type H ⁺ -ATPase (VA) as an apical membrane marker. _____	67
Figure 24: Immunolocalization of AaAQP5 in the Malpighian tubules and hindgut of larval <i>A. aegypti</i> reared in freshwater (FW) and brackish water (BW) using V-type H ⁺ -ATPase (VA) as an apical membrane marker. _____	68
Figure 25: Immunolocalization of AaAQP1 in the anal papillae of larval <i>A. aegypti</i> reared in freshwater (FW) and brackish water (BW) using V-type H ⁺ -ATPase (VA) as an apical membrane marker. _____	70
Figure 26: Immunolocalization of AaAQP4 in the anal papillae of larval <i>A. aegypti</i> reared in freshwater (FW) and brackish water (BW) using V-type H ⁺ -ATPase (VA) as an apical membrane marker. _____	71
Figure 27: Immunolocalization of AaAQP5 in the anal papillae of larval <i>A. aegypti</i> reared in freshwater (FW) and brackish water (BW) using V-type H ⁺ -ATPase (VA) as an apical membrane marker. _____	72
Figure 28: Updated schematic diagram illustrating membrane transport proteins in the distal and proximal gastric caeca of larval <i>Aedes aegypti</i> . _____	81
Figure 29: Updated schematic diagram illustrating membrane transport proteins in the anterior and posterior midgut of larval <i>Aedes aegypti</i> in freshwater habitat. _____	88
Figure 30: Topology predictions of unfolded putative AaAQPs in the plasma membrane using TMPred and Protter software (Hofmann, 1993; Omasits et al., 2014). _____	90

Figure 31: Updated schematic diagram illustrating the role of membrane transport proteins in the hindgut of larval <i>Aedes aegypti</i> .	99
Figure 32: Updated schematic diagram illustrating membrane transport proteins in the Malpighian tubules of larval <i>Aedes aegypti</i> .	109
Figure 33: Updated schematic diagram illustrating membrane transport proteins in the anal papillae of larval <i>Aedes aegypti</i> .	117

VIII. ABBREVIATIONS

AQP	Aquaporin
AaAQP	<i>Aedes aegypti</i> aquaporin
FW	Freshwater
BW	Brackish water (30% seawater unless otherwise stated)
5-HT	5-Hydroxytryptamine
AeNHE3	<i>Aedes aegypti</i> Na ⁺ /H ⁺ exchanger 3
AeNHE8	<i>Aedes aegypti</i> Na ⁺ /H ⁺ exchanger 8
VA	V-type H ⁺ ATPase
NKA	Na ⁺ /K ⁺ ATPase
NPA	Asparagine-proline-alanine
DRIP	<i>Drosophila</i> integral proteins
BIB	Big brain
PRIP	<i>Pyrocoelia rufa</i> integral protein
GC	Gastric caeca
AMG	Anterior midgut
PMG	Posterior midgut
HG	Hindgut
MT	Malpighian tubules
AP	Anal papillae
WB	Whole body

1. INTRODUCTION

1.1 Global Impact of *Aedes aegypti* and Mosquito Control

Aedes aegypti mosquitoes are arboviral vectors for human diseases including Zika, chikungunya, dengue, and yellow fever (Bhatt et al., 2013). *A. aegypti* inhabit tropical and subtropical regions of the world, thriving in populous urban areas where they propagate disease (Kraemer et al., 2015). Viruses are spread from host to host via the salivary gland of hematophagous adult female mosquitoes which require a blood meal for vitellogenesis (Chamberlain and Sudia, 1961). Efforts to prevent disease transmission have been directed at curtailing host-insect interactions or reducing larval breeding grounds and adult mosquito densities (Peter et al., 2005). Recently, the sterile insect technique has been implemented in population dense areas as a species specific and environmentally friendly means to control vector mosquito populations (Benedict, 2003). Males carrying the dominant sterile allele are introduced into wild populations to compete for mating females. As a result of their mutation, they produce unviable offspring, therefore reducing the population of the subsequent generation (Klassen and Curtis, 2005). Additionally, a flightless adult female phenotype has been developed to restrict the spread of mosquitoes (Fu et al., 2010). The flightless females compete for resources at the larval life stage, when intraspecific competition for resources is at its peak. Consequently, the mutation impedes wing development in the adult life stage, diminishing disease transmission and reproduction (Fu et al., 2010).

Pharmacological mitigation of population density is accomplished through pesticide treatment, such as organophosphates, Dursbant®, malathion, Permanonet®, Abatet®, Scourget®, B.t.i, and Biomistt® (Lines and Kleinschmidt, 2015; Milam et al., 2000). The specificity of pesticides is vitally important to target mosquitoes while leaving negligible

repercussion on the remainder of the ecosystem; however, pesticides demonstrate off-target effects on other wildlife (Pimentel, 1995). Further developments of mutation and pharmacological based control strategies require an understanding of mosquito biology and physiology at multiple stages of their life cycle to increase the potency and specificity of these treatments and restrict the millions of annual cases of disease and deaths that still persist.

1.2 Aquatic Environments of *Aedes aegypti*.

A. aegypti larvae typically reside in stagnant bodies of freshwater including ponds, puddles, temporary water filled containers, marshes, and swamps. Natural phenomena and anthropogenic activities contribute to the salinization of freshwater environments creating brackish water that *A. aegypti* exploit for the proliferation of larval instars (Bradley et al., 1984; Sumner and Belaineh, 2005). The external salinities tolerated by larval mosquitoes vary from species to species. While *Aedes aegypti* and *Culex pipiens* prefer water with an osmolarity less than 300 mOsm, *Culiseta inornata* and *Culex tarsalis* favour water ranging from 300 to 1000 mOsm, and *Aedes taeniorhynchus* and *Aedes togoi* are best adapted to water of 1000 mOsm (Bradley, 1987; Bradley et al., 1984; Garrett and Bradley, 1984). *A. aegypti* are strict osmoregulators, maintaining hemolymph osmolarity within a range of 250-375 mOsm and are able to complete development in external salinity of 300 mOsm (EC₅₀) which is regarded as their survival limit (Bradley, 1987; Edwards, 1982a; Edwards, 1982b; Pannabecker, 1995). When inhabiting freshwater environments, *A. aegypti* larvae face a passive water influx into their hemolymph while ions are lost to the environment via diffusion. In 30% seawater, which is approximately equivalent to an osmolarity of 300 mOsm, the concentration of ions (Na⁺, Cl⁻) is higher than that in the hemolymph and the resulting passive absorption of Na⁺ and Cl⁻ down their concentration gradients necessitates active regulation of homeostatic ion composition to maintain

physiological function (Bradley et al., 1984; Clark et al., 2004; D’Silva et al., 2017; Donini et al., 2006; Donini et al., 2007). Upon the onset of a challenge to hemolymph ion regulation imposed by laboratory exposure to 30% seawater (10.5 gL⁻¹ of Instant Ocean® in distilled water) larval hemolymph Na⁺ and Cl⁻ concentrations increase by ~20 mmolL⁻¹ (Donini et al., 2007). Despite the observed increased concentration of select ions in the hemolymph, to the best of my knowledge, the osmolarity of the hemolymph in response to high salinity has not been measured in *A. aegypti*. However, with the elevation in external salinity, there is an increase in free amino acids in larval hemolymph which is predicted to elevate the overall osmolarity of the hemolymph (Edwards, 1982c). Similarly, the osmoconforming species of mosquitoes, *Culex tarsalis*, elevate hemolymph osmolarity by increasing proline and trehalose concentration in response to external salinity as a way to mitigate the osmotic gradient between the external medium and the hemolymph; however, trehalose, xylose and glucose in larval *A. aegypti* did not change with salinity (Edwards, 1982c; Patrick and Bradley, 2000). Clearly, the variations in aquatic salinity cause the perturbation of hemolymph ions and/or water balance therefore, maintaining osmotic and ionic homeostasis is imperative for physiological function in larvae.

Larvae possess osmoregulatory organs that enable them to maintain ionic and osmotic balance under most conditions and include the gastric caeca, anterior midgut, posterior midgut, hindgut, Malpighian tubules, and the anal papillae (Figure 1) (Bradley, 1987). Physiological plasticity of these osmoregulatory organs has been shown and is essential for survival in the different ionic and osmotic challenges encountered by larvae (Akhter et al., 2017; D’Silva et al., 2017; Donini et al., 2007; Jonusaite et al., 2017a; Jonusaite et al., 2017b; Volkmann and Peters, 1989a). The majority of osmo- and ionoregulatory research in mosquito larvae has focused on ion transporters, channels, and exchangers to understand ion movement across the epithelia of

osmoregulatory organs (Chasiotis et al., 2016; D’Silva et al., 2017; Durant et al., 2017; Kang’ethe et al., 2007; Patrick et al., 2006; Piermarini et al., 2011; Piermarini et al., 2015). However, water is the quintessential molecule for life in all living organisms, therefore a complete understanding of osmoregulatory mechanisms in larval *A. aegypti* must include the study of water transport pathways and their regulation. Cellular membrane permeability to water is facilitated by proteinaceous conduits termed aquaporins (AQPs) that reduce activation energy required for water transport across the hydrophobic lipid bilayer and subsequently across epithelia (Hartridge and Roughton, 1923; Robinson, 1950).

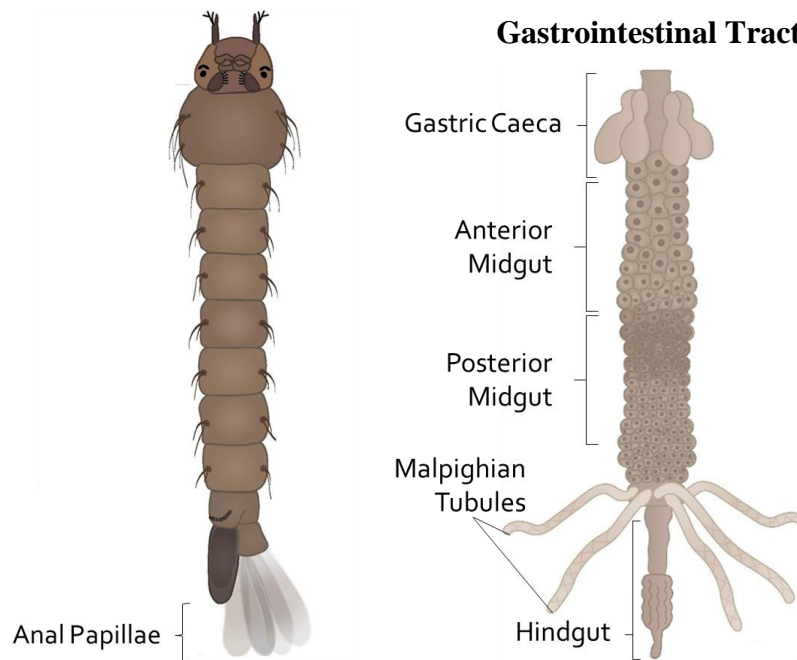


Figure 1: Osmoregulatory organs of larval *Aedes aegypti*.

1.3 Aquaporins

AQPs are ubiquitous integral membrane proteins that have been identified in all taxa studied to date (Agre et al., 1993; Campbell et al., 2008; Finn and Cerdá, 2015; Litman et al., 2009). The majority of research on animal AQPs has been carried out in mammalian models and

it is assumed the major structural characteristics are conserved in other animals (Campbell et al., 2008; Finn and Cerdá, 2015; Preston et al., 1994).

1.3.1 Aquaporin Structure

AQPs are comprised of six transmembrane hydrophobic alpha helical domains (I-VI) with five extra membrane connecting loops (A-E) that emanate intracellularly or extracellularly with both the N-terminus and the C-terminus on the cytosolic side of the membrane (Preston et al., 1994; Verkman and Mitra, 2000). The AQP transmembrane domains fold into an alpha barrel, giving the overall AQP structure an hourglass configuration (Murata et al., 2000). Conserved asparagine-proline-alanine (NPA) motifs located on loops B and E comprise the functional domains which contribute to the characteristic water selectivity of AQPs (Jung et al., 1994). The substantial sequence homology of the two halves of the AQP is predicted to be the product of an ancient gene duplication event (Jung et al., 1994; Pao et al., 1991).

The NPA motif prevents proton leakage via the Grothuss mechanism (process of proton diffusion via hydrogen bond transfer), and allows membranes to maintain the proton electrochemical gradient (Groot et al., 2003). The asparagine amine facilitates hydrogen bonding with the oxygen of the water molecules precluding proton conductance (Fu and Lu, 2007). Hydrogen bonding polarities between water molecules on the extracellular and intracellular halves of the AQP are orientated in opposite directions further precluding proton leakage (Tajkhorshid et al., 2002). Phe56, His180, Cys189, and Arg195 of mammalian AQP1 come together to form a typical AQP extracellular aromatic/arginine constriction of 2.8 Å in diameter enhancing substrate size discrimination (Beitz et al., 2006). The positively charged arginine of the aromatic/arginine constriction weakens hydrogen bonds between water molecules (2.75 Å) expediting water transport through the channel and contributing to proton exclusion (Campbell et

al., 2008; Hub and Groot, 2007). The remainder of the AQP pore is lined with amphipathic residues with outward facing oxygen atoms for hydrogen bonding with water despite the potential for proton interactions (Wu and Beitz, 2007). The aromatic/arginine constriction, NPA motifs, and the oxygen binding amino acids lining the pore combine to give AQPs their water specificity. AQPs are typically arranged in transmembrane homo or hetero tetramers with the same or different AQP homologues, although oligomerization is not imperative for the function of a single AQP channel (Hendriks et al., 2004). The tetramerization may form a putative fifth pore in the centre of four channels which is implicated in gaseous conductance, for example CO₂ in plant AQPs (Roche and Törnroth-Horsefield, 2017).

1.3.2 Aquaporin Regulation

Osmoregulatory challenges faced by the *A. aegypti* mosquitoes that can include adult desiccation in terrestrial environments, adult water load from a blood meal, and varying salinities in larval habitats require tightly regulated water transport which is concomitant with AQP regulation (Bradley, 1987). AQPs allow bidirectional water transport driven by the osmotic gradient that exists across a polarized membrane (Walz et al., 1994). Given the passive nature of water movement through AQPs, regulation of membrane permeability to water is necessary in order to regulate cell volume and extracellular fluid volume (including hemolymph volume). AQP regulation has mainly focused on mammalian models where AQP permeability is modulated through transcription expression, translation, trafficking, and gating (Campbell et al., 2008; Gu et al., 2003; Han et al., 1998; Ishikawa et al., 1998; Kwon et al., 2013; Marrades et al., 2006; Nejsum et al., 2005; Sabolić et al., 1995). The structural conformation of AQPs is also susceptible to changes in pH and calcium concentrations, which can obstruct water transport or lead to post-translational modifications (Virkki et al., 2001). The pH regulation of AQPs was

localized to the pH sensitive external histidine residue in loops A and C (Fischer and Kaldenhoff, 2008; Nemeth-Cahalan et al., 2004). Apart from calcium leading to conformational changes in AQP structure (Reichow et al., 2013), calcium can also trigger translocation of AQPs to the plasma membrane from intracellularly stored vesicular membranes. For example, acetylcholine induced elevation of intracellular Ca^{2+} in the rat parotid gland resulted in the translocation of AQP5 into the cellular membrane (Ishikawa et al., 1998). Similarly, in human salivary glands the translocation of AQPs into the plasma membrane was stimulated by elevated intracellular Ca^{2+} through the activation of type 3 muscarinic receptors and histamine H1 receptors (Ishikawa et al., 1998). Finally, AQP1 translocation in cholangiocytes of the bile duct was stimulated by the hormone secretin (Delporte and Steinfeld, 2006; Kim et al., 2009; Marinelli et al., 1997; Marinelli et al., 1999; Tada et al., 1999). Vesicular translocation as an effective means of regulating AQP function is further supported by occlusion of translocation that results from microtubule inhibition, which prevents vesicular transport towards the cellular membrane (Marinelli et al., 1997; Marinelli et al., 1999; Tada et al., 1999).

Hormonal regulation of AQP2 has also been discerned in detail in the mammalian, kidney and is accomplished by varying the expression and translocation of AQP2 into the renal collecting duct epithelial membrane. AQP2 regulation is mediated by the action of arginine-vasopressin which functions as a hormone on the kidney (Brown et al., 2008; Fushimi et al., 1997; Kwon et al., 2013). Arginine-vasopressin binds to the receptors located on the basolateral surface of principal cells, which activate an intracellular cAMP cascade that in turn activates protein kinase A. The activation of protein kinase A causes the phosphorylation of serine-256 on vesicular AQP2, signaling AQP2 translocation into the apical membrane and leading to greater water reabsorption and urine concentration (Kamsteeg et al., 2000; van Balkom et al., 2002).

When water conservation is no longer necessary, circulating levels of arginine-vasopressin are reduced which allows for the ubiquitination of the membrane bound phosphorylated AQP2 that facilitates endocytosis and degradation of AQP2 (Kamsteeg et al., 2006). AQP regulation has also been demonstrated through the activation of protein kinase C, which causes phosphorylation of serine residues leading to changes in protein permeability (Han et al., 1998; Zelenina et al., 2002).

Despite the significant progress in understanding AQP regulation in mammals the mechanisms underlying invertebrate AQP regulation is in its infancy. The hormonal regulation of *Rhodnius prolixus* Rp-MIP through 5-HT mediated modulation of transcript and protein abundance is, to my knowledge, currently the only study that has deduced a regulatory mechanism of an invertebrate AQP (Martini et al., 2004).

1.3.3 Aquaporin Evolution and Diversification

The importance and diversity of AQPs is apparent from their presence in organisms spanning unicellular eukaryotes, plants and animals with diverse substrate conductance properties including water, polyols, glycerol, ammonia, carbon dioxide, and carbon monoxide (Drake et al., 2015; Endeward et al., 2006; Finn and Cerdá, 2015; Jahn et al., 2004). Despite the technological advancements, *in silico* models, and phylogenetic position, it remains difficult to predict phenotypic function of AQPs due to differences in their primary structures, alternative splicing, post-translational modifications, or the cellular environment in which AQPs are expressed (Campbell et al., 2008; Finn and Cerdá, 2015; Kaufmann et al., 2005). AQPs have been classified into four major groups; aquaporins, aquaammoniaporins, unorthodox aquaporins, and aquaglyceroporins based on their phylogenetic topology and substrate conductance.

The insect AQPs have also been classified into four groups based on phylogeny: entomoglyceroporins, *Drosophila* integral proteins (DRIP), big brain (BIB), and the *Pyrocoelia rufa* integral protein (PRIP); however, despite this classification, a number of identified AQPs from a variety of insects do not fit into these groups (Campbell et al., 2008; Finn et al., 2015).

The holometabolous insects are the most successful terrestrial organisms in part due to their ability to accumulate colligative polyols that protect them from freezing temperatures and desiccation (Adler, 2009; Finn et al., 2015). Polyols are typically transported by members of the aforementioned aquaglyceroporins in the overall general classification of AQPs; however, holometabolous insects do not possess aquaglyceroporins and instead have evolved the apparently insect specific, entomoglyceroporins (Abascal et al., 2014). Neofunctionalized glycerol transport by entomoglyceroporins arose independently of the aquaglyceroporin lineage due to an Ala or Ser substitution of a His residue in the transmembrane domain of the aromatic arginine ring that is present in a water conducting aquaporin (Finn et al., 2015).

Entomoglyceroporins have improved colligative polyol conductance over the lost aquaglyceroporins and therefore have enabled holometabolous insects to possess greater temperature and desiccation tolerance (Finn et al., 2015). The DRIP subfamily consists of aquaporins with high water specificity (Kaufmann et al., 2005). BIB members do not possess transporting capabilities due to the absence of several amino acids upstream of the second NPA motif in *Drosophila melanogaster*, but rather participate in cell to cell adhesion (Hiroaki et al., 2006). BIB was also implicated in divalent cation (Ca^{2+} and Ba^{2+}) transport (Yanochko and Yool, 2004); however, later studies using patch clamp technique demonstrated that BIB was not ion permeable (Tatsumi et al., 2009). PRIP has the capacity to transport water and other solutes,

though it is a preferential water channel (Campbell et al., 2008; Drake et al., 2015; Liu et al., 2016).

1.3.4 *Aedes aegypti* Aquaporins

Six AQP homologues have been identified in the *Aedes aegypti* genome; AaAQP1, AaAQP2, AaAQP3, AaAQP4, AaAQP5, and AaAQP6, following the nomenclature used by Drake et al. with varying molecular masses (Table 1) (Drake et al., 2010; Kambara et al., 2009). Based on mRNA and protein expression analysis, AaAQPs have been identified in various organs in both adult female and larvae of *A. aegypti* (Table 1) (Akhter et al., 2017; Drake et al., 2010; Drake et al., 2015; Duchesne et al., 2003; Marusalin et al., 2012; Misyura et al., 2017). Several AaAQP homologs are expressed within the same organ as well as the same cells, suggesting functional redundancy, independent pathways of regulation, or functional diversity (Akhter et al., 2017; Hendriks et al., 2004; Marusalin et al., 2012). AaAQPs that possess water transport specificity are typically down regulated at the transcript level 3 hours post blood meal (PBM) in adult females, which is approximately when the majority of excess water has been excreted (Drake et al., 2015). In adults, AaAQP1, AaAQP2, AaAQP4 and AaAQP5 are the most abundantly expressed AaAQP transcripts in adult Malpighian tubules (Table 2) (Drake et al., 2010; Drake et al., 2015). A summary of AaAQP properties and expression profiles is provided in Table 2 and larval AaAQPs in osmoregulatory organs are covered in subsequent sections (Section 1.4).

Table 1: *Aedes aegypti* aquaporin predicted molecular mass.

Protein	Accession #	Predicted Monomer Mass (kDa)
AaAQP1	AAF64037.1	26.11
AaAQP2	XP_001656932.1	27.93
AaAQP3	XP_001649747.1	67.5
AaAQP4	XP_001650168.2	31.32
AaAQP5	XP_001650169.2	26.49
AaAQP6	XP_001648319.1	28.66

AaAQP1

The first AQP to be cloned in *A. aegypti* was AaAQP1, which shares the highest sequence homology with *Drosophila* DRIP protein and was demonstrated to preferentially transport water (Drake et al., 2015; Pietrantonio et al., 2000). AaAQP1 transcript abundance changes at various time points following a blood meal in adult female midgut, and Malpighian tubules (Table 2) (Drake et al., 2010; Drake et al., 2015). AaAQP1 has been localized to the tracheolar cells which form the terminal ends of the tracheal system supplying oxygen to the Malpighian tubules (Duchesne et al., 2003; Pietrantonio et al., 2000). Knockdown of AaAQP1 in adult female mosquitoes reduces excretion and improves survival in desiccating conditions suggesting it plays a role in diuresis in adult *A. aegypti* (Drake et al., 2010; Drake et al., 2015).

AaAQP2

AaAQP2 is homologous to the PRIP AQP, which possesses high water conductance based on studies in a heterologous oocyte expression system (Drake et al., 2015). While most AaAQPs are downregulated in the foregut following the consumption of a blood meal, AaAQP2 mRNA abundance remained high with additional elevated transcript abundance in the

Malpighian tubules and downregulated transcript abundance in the hindgut, suggesting its involvement in blood meal dehydration within the adult female (Drake et al., 2010; Drake et al., 2015).

AaAQP3

AaAQP3 is homologous to the BIB, with predicted function in cell to cell adhesion and endosome maturation (Drake et al., 2010; Marusalin et al., 2012). AaAQP3 is highly expressed in larval Malpighian tubules and its expression is not affected in adult osmoregulatory organs upon the consumption of a blood meal; however, transcript abundance in ovaries and fat body is elevated 24 h following a blood meal (Drake et al., 2010; Drake et al., 2015; Marusalin et al., 2012).

AaAQP4

AaAQP4 is an entomoglyceroporin and member of a clade of insect-specific AQPs which have been found in species including *D. melanogaster*, *Anopheles gambiae*, *Pedicus humanus*, *Triboleum castaneum*, *Leishmania major*, *Pichia pastoris* and *A. aegypti* (Kambara et al., 2009). Although AaAQP4 can transport water, it demonstrates much higher affinity for glycerol, urea, erythritol, adonitol, and mannitol (Drake et al., 2015). Glycerol transporting AQPs typically display a cysteine residue situated within the B loop, as well as changes in the aromatic/arginine constriction site, enabling them to have glycerol transport capabilities (Hub and Groot, 2007). Interestingly, AaAQP4 exhibits glycerol transport capabilities despite the absence of the characteristic cysteine amino acid in loop B or changes in the distinctive aromatic/arginine constriction site, though an NPS motif instead of the NPA may give the channel its ability to transport solutes other than water (Drake et al., 2015; Jung et al., 1994). Glycerol, which is a precursor to triacylglycerol and phospholipids, is utilized as an osmolyte in *Culex tarsalis* larval

hemolymph when external salinity is high (Clark et al., 2004; Patrick and Bradley, 2000).

AaAQP4 also possesses high trehalose transport affinity, which is a primary sugar in hemolymph of insects (Thompson and Borchardt, 2003). Trehalose plays a role in energy storage, as well as osmotic regulation in larval hemolymph (Bradley, 1987; Elbein et al., 2003; Garrett and Bradley, 1984; Liu et al., 2013). Therefore, the ability to transport trehalose provides evidence that AaAQP4 is a multifunctional AQP channel important for trehalose, glycerol, and water regulation in hemolymph and cells.

AaAQP5

Despite the lack of glycerol conductance, AaAQP5 is an entomoglyceroporin and member of the same insect-specific AQP clade as AaAQP4 (Drake et al., 2015; Kambara et al., 2009). AaAQP5 transports water and trehalose which may function similarly to AaAQP4 in terms of regulating energy stores as well as osmotic regulation in larval hemolymph. The knockdown of AaAQP5 reduces excretion in adult females and improves survival under desiccation stress (Drake et al., 2010). Conversely, knockdown of AaAQP5 in larvae decreased survival in freshwater, further supporting the role of AaAQP5 in osmoregulation (Drake et al., 2015; Misyura et al., 2017).

AaAQP6

AaAQP6 is closely related to *D. melanogaster* CG12251, vertebrate AQP11 and AQP12 and is characterized as an unorthodox AQP. AaAQP6 transport specificity and properties are unknown though the high mRNA abundance in larval anal papillae may suggest osmoregulatory function (Akhter et al., 2017; Marusalin et al., 2012). AaAQP6 mRNA is also highly abundant in the adult female foregut that is also predicted to participate in the active transepithelial absorption of water after a blood meal (Drake et al., 2010; Drake et al., 2015).

Table 2: *Aedes aegypti* adult and larval aquaporin expression, properties, and phylogeny overview.

MT: Malpighian tubules, MG: midgut, OV: ovaries, TX: thorax, FB: fat body, AP: anal papillae, FG: foregut, R: rectum, C: crop, HG: hindgut, GC: gastric caeca, AQP: aquaporin, PBM: post-blood meal, SG: salivary gland.

Aquaporin	Substrate Permeability	Properties	mRNA abundance	Protein Work	Sources of Information
AaAQP1	Water	<ul style="list-style-type: none"> – H₂O specific transport – homologue of <i>Drosophila</i> DRIP 	<p>Adult</p> <ul style="list-style-type: none"> – highly abundant in MT and MG prior to feeding – downregulated in MT and MG 24 hours PBM – found in MT, MG, OV, TX, FB, SG – MT upregulated 3 hours PBM <p>Larval</p> <ul style="list-style-type: none"> – Highly abundant in MT 	<ul style="list-style-type: none"> – Present in the AP and whole body of larvae – Localization in tracheal cells of MT in larvae – Knockdowns reduce excretion and improve survival in desiccating conditions of adult females 	(Akhter et al., 2017; Drake et al., 2010; Drake et al., 2015; Finn and Cerdá, 2015; Marusalín et al., 2012; Pietrantonio et al., 2000)
AaAQP2	Water	<ul style="list-style-type: none"> – orthologous with AQPs from <i>Drosophila melanogaster</i>, <i>Pediculus humanus</i>, <i>Anopheles gambiae</i>, <i>Tribolium castaneum</i> – homologue of PRIP 	<p>Adult</p> <ul style="list-style-type: none"> – highly abundant in FG, MT, and HG – downregulated in FG, MT and HG 24 hours PBM – found in MT, MG, OV, TX, SG – strongly expressed at all times in MT, MG, and OV – upregulated in MT 3 hours PBM <p>Larval</p> <ul style="list-style-type: none"> – highly abundant in MT and AP 	none	(Akhter et al., 2017; Drake et al., 2010; Drake et al., 2015; Finn and Cerdá, 2015)
AaAQP3	N/A	<ul style="list-style-type: none"> – regulation of cell adhesion – homologue of the <i>Drosophila</i> BIB – does not function as water channel 	<p>Adult</p> <ul style="list-style-type: none"> – no significant expression difference between C, FG, MG, HG, R, MT, OV – found in MT, MG, OV, TX, FB – upregulated in OV and FB 3-24 hours PBM <p>Larval</p> <ul style="list-style-type: none"> – Highly abundant in MT 	none	(Akhter et al., 2017; Drake et al., 2010; Drake et al., 2015; Finn and Cerdá, 2015)

AaAQP4	Water Glycerol Urea Erythritol Adonitol Mannitol Trehalose	<ul style="list-style-type: none"> – high affinity for glycerol, trehalose and other solutes – implicated in AP transepithelial solute transport – characterized as an entemoglyceroporin 	<p>Adult</p> <ul style="list-style-type: none"> – significantly expressed in MT and MG – downregulated in MT 24 hours PBM – found in MT and MG – highly expressed in MT – upregulated in MT 3 hours PBM – downregulated in MG 3-24 hours PBM <p>Larval</p> <ul style="list-style-type: none"> – highly abundant in MT and AP – downregulated in response to brackish water rearing 	<ul style="list-style-type: none"> – Localization in AP apical and basolateral membrane – Down regulate expression in brackish water conditions in larval AP 	(Akhter et al., 2017; Drake et al., 2010; Drake et al., 2015; Finn and Cerdá, 2015)
AaAQP5	Water Trehalose	<ul style="list-style-type: none"> – related to three <i>Drosophila</i> AQPs and four <i>Tribolium</i> AQPs -implicated in regulation of AP cellular volume – implicated in transcellular fluid transport across principal cells of MTs – characterized as an entemoglyceroporin 	<p>Adult</p> <ul style="list-style-type: none"> – significant expression in the MT, downregulated 24 hours PBM – present in the SG – highly expressed in MT, MG, TX, FB – upregulated in MT, TX, FB 24 hours PBM <p>Larval</p> <ul style="list-style-type: none"> – highly abundant in MT – upregulated in response to brackish water rearing 	<ul style="list-style-type: none"> – Localization in AP basolateral membrane – Upregulated abundance in brackish water reared larval AP – Localization in MTs apical and basolateral membranes – Knockdowns reduce larval survival, Malpighian tubule secretion rate, and hemolymph ion concentration 	(Akhter et al., 2017; Drake et al., 2010; Drake et al., 2015; Finn and Cerdá, 2017)
AaAQP6	Unknown	<ul style="list-style-type: none"> – closely related to <i>Drosophila</i> CG12251 and vertebrate AQP11 and AQP12 -characterized as an unorthodox AQP 	<p>Adult</p> <ul style="list-style-type: none"> – no significant expression difference between C, FG, MG, HG, R, MT, OV – found in MT, OV, TX, FB – highly abundant in TX and FG <p>Larval</p> <ul style="list-style-type: none"> – highly abundant in AP – significant transcript downregulation in AP in brackish water reared of larvae 	none	(Akhter et al., 2017; Drake et al., 2010; Drake et al., 2015; Finn and Cerdá, 2015)

1.4 *Aedes aegypti* Larval Osmoregulatory Organs

1.4.1 Midgut

The midgut composes the major portion of the gastrointestinal tract which is subdivided into functionally and morphologically distinct sections, the cardia, gastric caeca, anterior midgut, and posterior midgut (Clark et al., 2005; Volkmann and Peters, 1989b). The different midgut organs participate in ion, fluid, and acid-base balance as well as digestion, water, ion and nutrient absorption (Clark et al., 2005; D'Silva et al., 2017; Onken and Moffett, 2017).

Gastric caeca

The gastric caeca is composed of eight blind-ended diverticula of endodermally-derived epithelia positioned posterior to the cardia and open to the anterior region of the midgut (Volkmann and Peters, 1989b). The gastric caeca are predicted to be responsible for digestion, absorption and storage of nutrients, as well as the maintenance of ion balance (D'Silva et al., 2017; Volkmann and Peters, 1989a; Volkmann and Peters, 1989b). This multifunctional organ is composed of two major cell types; the digestive cells and the ion transporting cells (following the nomenclature proposed by D'Silva *et al.*), and additionally, gastric caeca possess accessory cells that secrete the caecal membrane, as well as imaginal cells (D'Silva et al., 2017; Volkmann and Peters, 1989b). The digestive cells are implicated in the secretion of digestive enzymes and therefore thought to participate in digestion, nutrient absorption and storage (Volkmann and Peters, 1989b; Wigglesworth, 1932). These cells possess numerous apical microvilli with innumerable mitochondria resembling the principal cells of the Malpighian tubules described in a subsequent section (Section 1.4.2) (Volkmann and Peters, 1989b). When larvae are inhabiting FW, the digestive cells are located at the proximal two-thirds of the caeca and express Na⁺/K⁺ ATPase on the basolateral membrane where Na⁺ is transported into the hemolymph and K⁺ into

the cell, establishing the membrane potential. The V-type H⁺ ATPase is expressed on the apical membrane and transports H⁺ into the lumen establishing a proton gradient across the apical membrane of the digestive cells. This proton gradient is used by the apical Na⁺/H⁺ exchanger 8 (AeNHE8) to transport Na⁺ and/or K⁺ out of the cell into the gastric caeca lumen in exchange for H⁺ (Figure 2) (Kang'ethe et al., 2007; Patrick et al., 2006). The ion secreting cells are located at the distal gastric caeca when larvae inhabit FW and these cells possess basolaterally localized V-type H⁺ ATPase which transports H⁺ into the hemolymph while the cation-chloride cotransporter transports Na⁺, K⁺, and Cl⁻ into the cytosol (Figure 2). Basolaterally localized Na⁺/H⁺ exchanger 3 (AeNHE3) is likely to regulate cellular pH balance. Both cell types participate in the formation of the peritrophic membrane which is morphologically analogous to the peritrophic membrane that is found in the midgut (Volkman and Peters, 1989b).

The net movement of water across the gastric caeca is unknown; however, fluxes of major cations have been measured. Concentrations of the major cations are higher in the hemolymph compared to the luminal fluid of gastric caeca and the net flux of these ions across the gastric caeca is luminally directed regardless of whether the larvae are reared in FW or BW (D'Silva and O'Donnell, 2018; D'Silva et al., 2017). Although this information is valuable in understanding the functional role of the gastric caeca in osmoregulation; it does not provide a means to predict water movements since this requires measurement of osmolarity of the hemolymph, cytosol, and luminal fluid as well as elucidation of AaAQP expression. Relatively low transcript abundance of AaAQPs have been demonstrated in the gastric caeca suggesting that water permeability is diminished in this organ (Marusalin et al., 2012). AaAQP protein expression has not been studied in the gastric caeca.

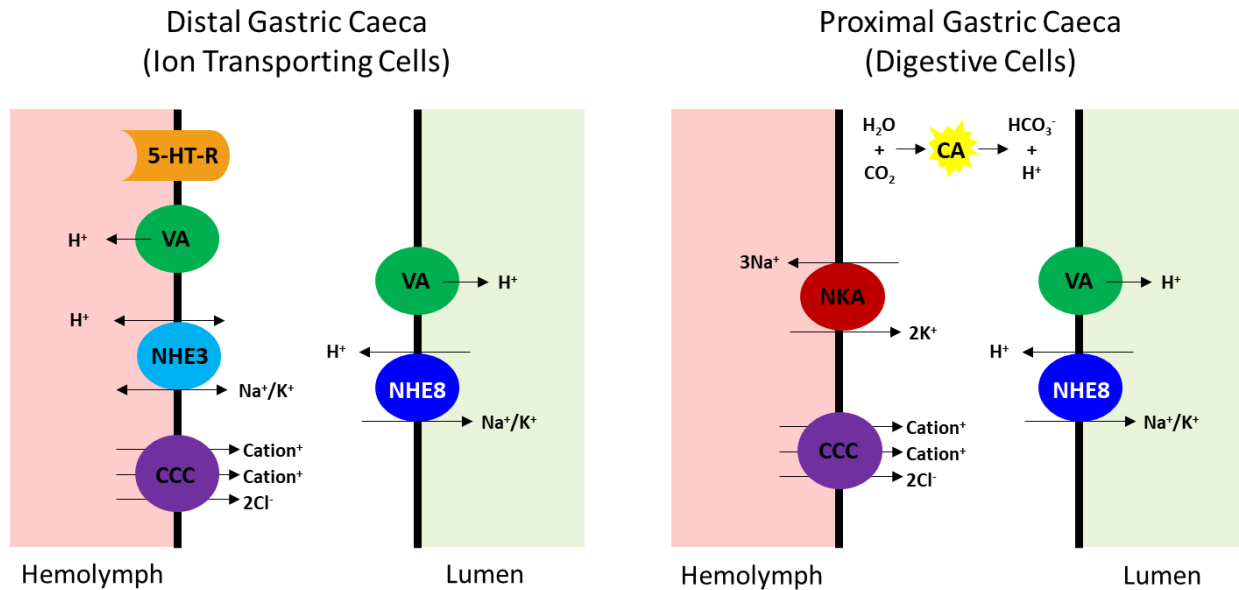


Figure 2: Schematic diagram illustrating membrane transport proteins in the distal and proximal gastric caeca of larval *Aedes aegypti*. 5-HT-R: 5-hydroxytryptamine receptor, VA: V-type H^+ ATPase, NHE: Na^+/H^+ exchanger, CCC: cation-chloride cotransporters, CA: carbonic anhydrase, and NKA: Na^+/K^+ ATPase. Modified from D'Silva and O'Donnell (2018) and D'Silva et. al (2017).

Anterior and Posterior Midgut

The anterior midgut is the segment of the gastrointestinal tract posterior to the gastric caeca. The anterior midgut is involved in ionic and osmotic regulation as well as nutrient digestion and absorption (Corena et al., 2002). The epithelial cells possess sparse short luminal microvilli with mitochondria and a highly infolded basal membrane that altogether is structurally consistent with low absorption (Clark et al., 2005). The intraluminal pH of 10.0 in the anterior midgut is one of the highest recorded in physiological systems (Corena et al., 2002). Luminal alkalisation is established by the active transport of HCl into the hemolymph by basolaterally localized V-type H^+ ATPase and Cl^- channels concomitant with CO_3^{2-} buffering (Figure 3) (Boudko et al., 2001b; Patrick et al., 2006; Zhuang et al., 1999). Inhibition of V-type H^+ ATPase and NHE3 reduced the pH gradient across the anterior midgut epithelium supporting their role in

the contribution to luminal alkalinisation (Figure 3) (Boudko et al., 2001a; Pullikuth et al., 2006). However, additional transporters and pathways that may contribute to alkalinisation remain to be discovered (Onken and Moffett, 2009).

The posterior midgut is proposed to function in nutrient absorption, osmoregulation, as well as acidification of luminal gut contents to compensate for the acid-base imbalance on hemolymph homeostasis caused by the alkalinisation of gut contents at the anterior midgut (Moffett et al., 2012). The epithelial cells possess an apical membrane with long microvilli associated with mitochondria which contains V-type H^+ ATPase, along with basolaterally localized Na^+/K^+ ATPase (Figure 3) (Clark et al., 2005; Patrick et al., 2006). Na^+ transport from the lumen of the posterior midgut occurs through a proposed $Na^+/2H^+$ exchanger and Na^+ -coupled amino acid transporters that is then basolaterally transported into the hemolymph by Na^+/K^+ ATPase (Figure 3) (Jagadeshwaran et al., 2010; Patrick et al., 2006). Unlike the anterior midgut, several isoforms of carbonic anhydrase are expressed in the posterior midgut that potentially contribute H^+ for luminal acidification (Linser et al., 2009). NHE3 is localized on the basolateral membrane and contributes to cellular acid/base balance by transporting protons into the cell and Na^+/K^+ into the hemolymph (Pullikuth et al., 2006). The posterior midgut is also permeable to Cl^- through the paracellular pathway whereby Cl^- enters the hemolymph, driven by cation absorption from the lumen (Clark et al., 1999; Jagadeshwaran et al., 2010).

Low transcript levels of AaAQPs in the anterior midgut and posterior midgut are predicted to attribute to diminished epithelial permeability to water in order to avoid the accumulation of water in the hemolymph driven by the osmotic gradient as well as the active transport of ions and other solutes across the epithelia (Marusalin et al., 2012).

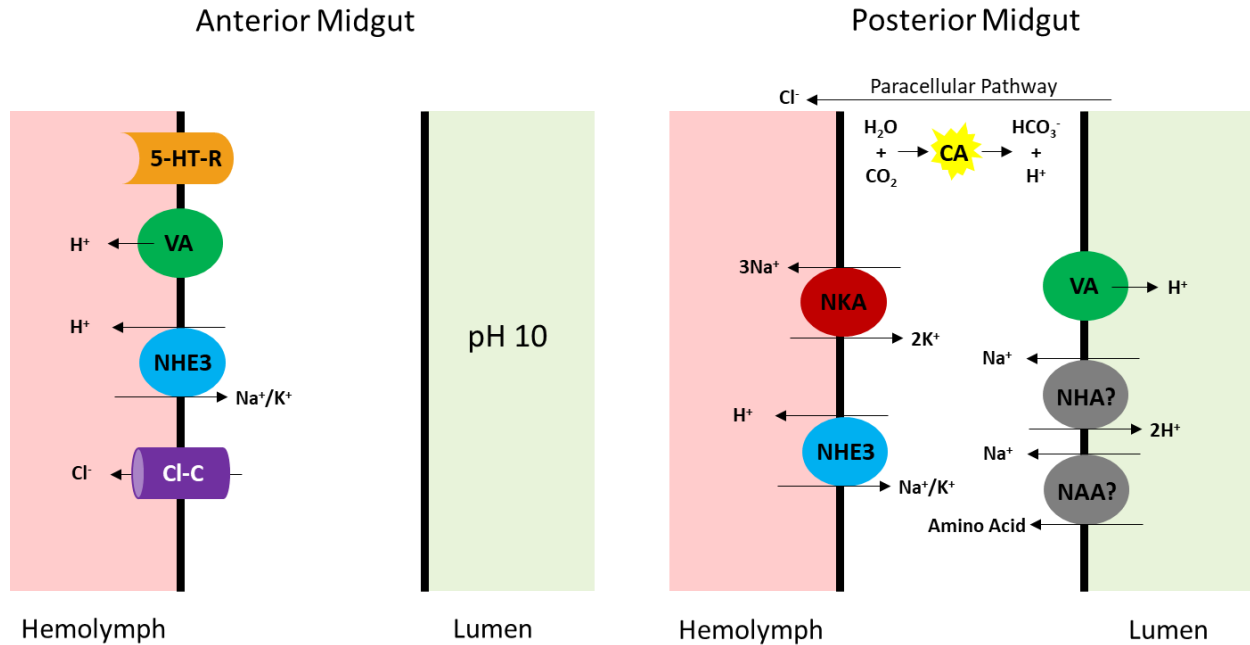


Figure 3: Schematic diagram illustrating membrane transport proteins in the anterior and posterior midgut of larval *Aedes aegypti*. VA: V-type H^+ ATPase, 5-HT-R: 5-hydroxytryptamine receptor, NHE: Na^+/H^+ exchanger, Cl-C: Cl^- channel, CA: carbonic anhydrase, and NKA: Na^+/K^+ ATPase, NHA: $Na^+/2H^+$ exchanger, and NAA: Na^+ /amino acid co-transporter.

1.4.2 Malpighian Tubules

Malpighian tubules are blind ended diverticula of the gastrointestinal tract extending from the junction of the midgut and the hindgut (Beyenbach et al., 2010). Malpighian tubules are secretory organs that participate in waste excretion, osmoregulation and ionoregulation by eliminating nitrogenous waste, excess water, ions, and harmful organic solutes (Beyenbach, 1995; Wright, 1995). Larval *A. aegypti* possess five morphologically and functionally identical Malpighian tubules composed of two cell types; large cuboidal principal cells and squamous stellate cells. The large principal cells predominantly constitute the Malpighian tubule structure with the small stellate cells intercalating between principal cells in the distal two thirds of the Malpighian tubule and comprising 16-18% of the tubule (Satmary and Bradley, 1984). The

principal cells possess apical microvilli and a highly infolded basolateral membrane (Bradley and Snyder, 1989). Smooth septate junctions extend paracellularly, establishing membrane polarity and regulating paracellular transport of water and solutes (Beyenbach, 2003; Jonusaite et al., 2017a; Jonusaite et al., 2017b). Ions from the hemolymph are actively transported against their electrochemical gradients into the cytosol of principal and stellate cells, followed by excretion into the Malpighian tubule lumen at the apical membrane, energized by ionomotive ATPases. *A. aegypti* Malpighian tubules secrete isosmotic fluid at the distal segment of the tubules (Beyenbach et al., 2010). The active ion transport establishes an electroosmotic flow by which water traverses via the transcellular and putative paracellular pathways, however the volume contributions through the individual pathways have not been established (Bradley and Snyder, 1989; Misyura et al., 2017; Pannabecker, 1995).

Basolaterally localized $\text{Na}^+/\text{K}^+/\text{2Cl}^-$ cotransporters allow transmembrane transport of Na^+ , K^+ and Cl^- driven by the Cl^- electrochemical gradient and Na^+ concentration gradient (Scott et al., 2004). Na^+ and K^+ are transported across the apical membrane via NHE8 and NHE3 using the proton electromotive potential established by apically localized V-type H^+ -ATPase (Figure 4) (Beyenbach and Wieczorek, 2006; Beyenbach et al., 2000; Kang'ethe et al., 2007; Lu et al., 2011; Patrick et al., 2006; Piermarini et al., 2009; Weng et al., 2003; Wieczorek et al., 1991). P-type Na^+/K^+ ATPase localization is confined to stellate cells at the distal portion of the Malpighian tubules where transport function is not yet clear (Cabrero et al., 2004; Patrick et al., 2006).

Transepithelial chloride transport is suggested to occur through the transcellular pathway in addition to a proposed paracellular pathway between principal and stellate cells (Beyenbach, 2003). Basolaterally localized $\text{Cl}^-/\text{HCO}_3^-$ exchangers transport Cl^- into the stellate cell cytosol in

exchange for HCO_3^- (Corena et al., 2002; Lu et al., 2011; Piermarini et al., 2010). The cation transport by principal cells creates a lumen positive electrochemical gradient which facilitates passive movement of Cl^- from the stellate cell cytosol through apical Cl^- channels (O'Connor and Beyenbach, 2001).

Ion transport into the tubule lumen drives water transport across the tubule which is essential for osmoregulation and therefore, expression of AaAQPs is important to facilitate transcellular water transport (Misyura et al., 2017). In larvae, AaAQP1, AaAQP4 and AaAQP5 transcript abundance is high in the Malpighian tubules, suggesting that these AQPs partake in transcellular water and solute movement. In fact, the transcellular water transport across the principal cells of larval *A. aegypti* Malpighian tubules was shown to at least in part occur through AaAQP5 localized to both the apical and basolateral membranes (Figure 4) (Misyura et al., 2017).

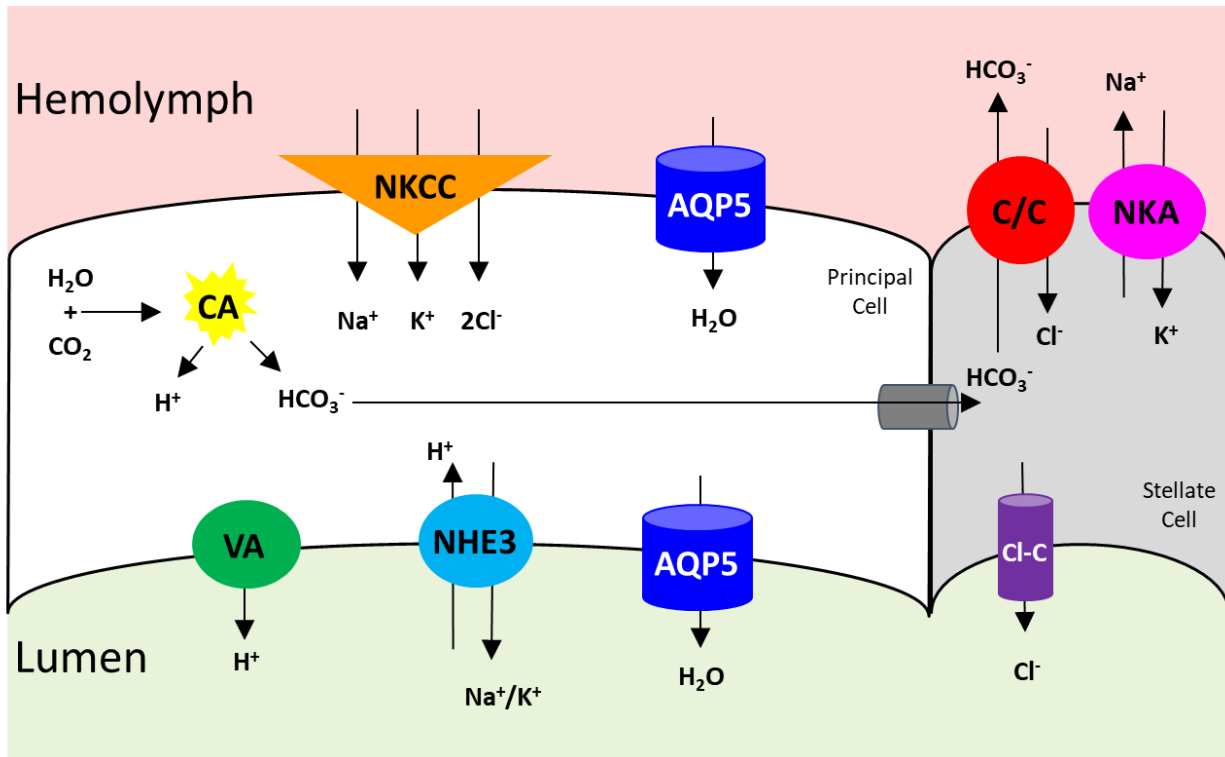


Figure 4: Schematic diagram illustrating membrane transport proteins in the Malpighian tubules of larval *Aedes aegypti*.

VA: V-type H^+ ATPase, NHE3: Na^+/H^+ exchanger 3, Cl-C: Cl^- channel, CA: carbonic anhydrase, and NKCC: $Na^+/K^+/2Cl^-$ co-transporter C/C: Cl^-/HCO_3^- exchanger, AQP5: *Aedes aegypti* aquaporin 5.

1.4.3 Hindgut

The ectodermally derived hindgut in larval *A. aegypti* is composed of the ileum and the rectum that extend posterior from the midgut and function in processing primary urine secreted from the Malpighian tubules for subsequent expulsion into the external environment (Jonusaite et al., 2017a; Larsen et al., 2014; Patrick et al., 2006). The epithelial cells of the ileum do not possess features indicative of transport therefore, this region of the hindgut is implicated in mechanical movement of gut contents towards the rectum (Bradley, 1987; Patrick et al., 2006). The rectal epithelial cells exhibit a highly infolded basolateral membrane which is surrounded by musculature, while the apical membrane has a luminal cuticle (Meredith and Phillips, 1973). In

freshwater environments, excess water elimination and ion accumulation is imperative for larval survival therefore, the rectum is predicted to actively absorb excess ions from the primary urine leaving behind a hypoosmotic urine for expulsion (Ramsay, 1950). In freshwater conditions, basolateral Na^+/K^+ ATPase and apical V-type H^+ ATPase are predicted to facilitate the active absorption of Na^+ , K^+ and Cl^- from the primary urine in the rectum (Figure 5) (Bradley, 1987; Patrick et al., 2006; Ramsay, 1950). Low AaAQP transcript expression in the hindgut is consistent with the purpose of limiting transepithelial water transport due to the high degree of solvent drag generated by active ion absorption of the epithelium (Aly and Dadd, 1989; Marusalin et al., 2012).

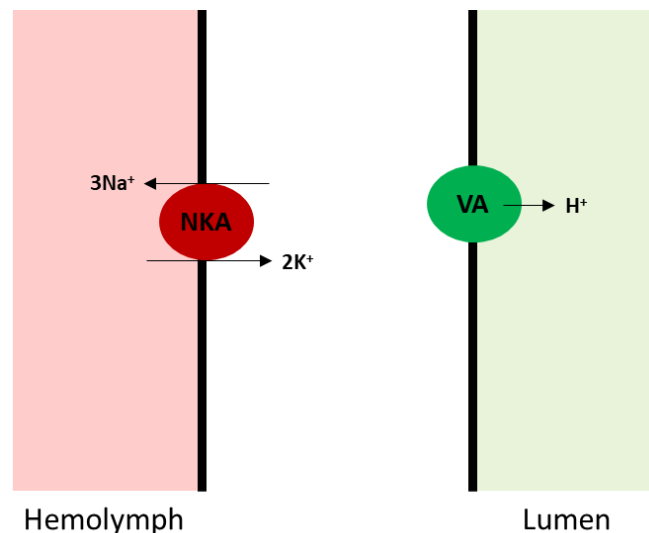


Figure 5: Schematic diagram illustrating the role of membrane transport proteins in the rectum of larval *Aedes aegypti*.

VA: V-type H^+ ATPase, NKA: Na^+/K^+ ATPase.

1.4.4 Anal Papillae

Anal papillae are four externally projecting structures that surround the anus where the lumen is continuous with the hemocoel. The anal papillae participate in osmo- and

ionoregulation in both freshwater and brackish water environments (Del Duca et al., 2011; Donini and O'Donnell, 2005; Larsen et al., 2014; Marusalin et al., 2012). They are composed of a syncytial multinucleated epithelium surrounded by a thin cuticle on the apical membrane (Edwards and Harrison, 1983; Sohal and Copeland, 1966; Wigglesworth, 1932). Apically localized V-type H^+ ATPase and putative Na^+ channels are predicted to facilitate the absorption of Na^+ which is subsequently transported into the hemolymph filled anal papillae lumen using the basolateral Na^+/K^+ ATPase (Figure 6) (Chasiotis et al., 2016; Del Duca et al., 2011; Patrick et al., 2006). Similar to Na^+ absorption, the absorption of K^+ at the apical membrane is proposed to transpire via cation exchangers energized by the proton gradient established by V-type H^+ ATPase, though the pathways have not yet been elucidated (Donini and O'Donnell, 2005). Carbonic anhydrase facilitates the transport of Cl^- by providing HCO_3^- to the putative apically localized Cl^-/HCO_3^- exchangers since pharmacological inhibition of either carbonic anhydrase or Cl^-/HCO_3^- exchangers reduces transapical absorption of Cl^- (Figure 6) (Del Duca et al., 2011; Stobbart, 1971). Anal papillae possess several ammonia/ammonium transporters and Rhesus glycoproteins on both the apical and basolateral membranes that facilitate the removal of ammonia from the hemolymph (Chasiotis et al., 2016; Donini and O'Donnell, 2005; Durant and Donini, 2018; Durant et al., 2017). Anal papillae also possess the presence of septate junction proteins, despite the syncytial epithelium that is void of paracellular junctions suggesting they play a non-junctional role in these organs (Jonusaite et al., 2016; Jonusaite et al., 2017b).

The syncytial epithelium of the anal papillae would preclude the passive absorption of water; however, the anal papillae have been demonstrated to express AaAQPs that create a transepithelial water pathway. The anal papillae express high abundance of AaAQP2, AaAQP4, and AaAQP6 transcripts which would implicate them in passive water and solute transport

across the epithelial membrane (Akhter et al., 2017). AaAQP4 localizes to both the apical and basolateral membrane of the anal papillae proposing osmoregulatory function in the larvae by transporting solutes across the epithelia while AaAQP5 localizes to the basolateral membrane suggesting a potential in cell volume regulation (Figure 6) (Akhter et al., 2017).

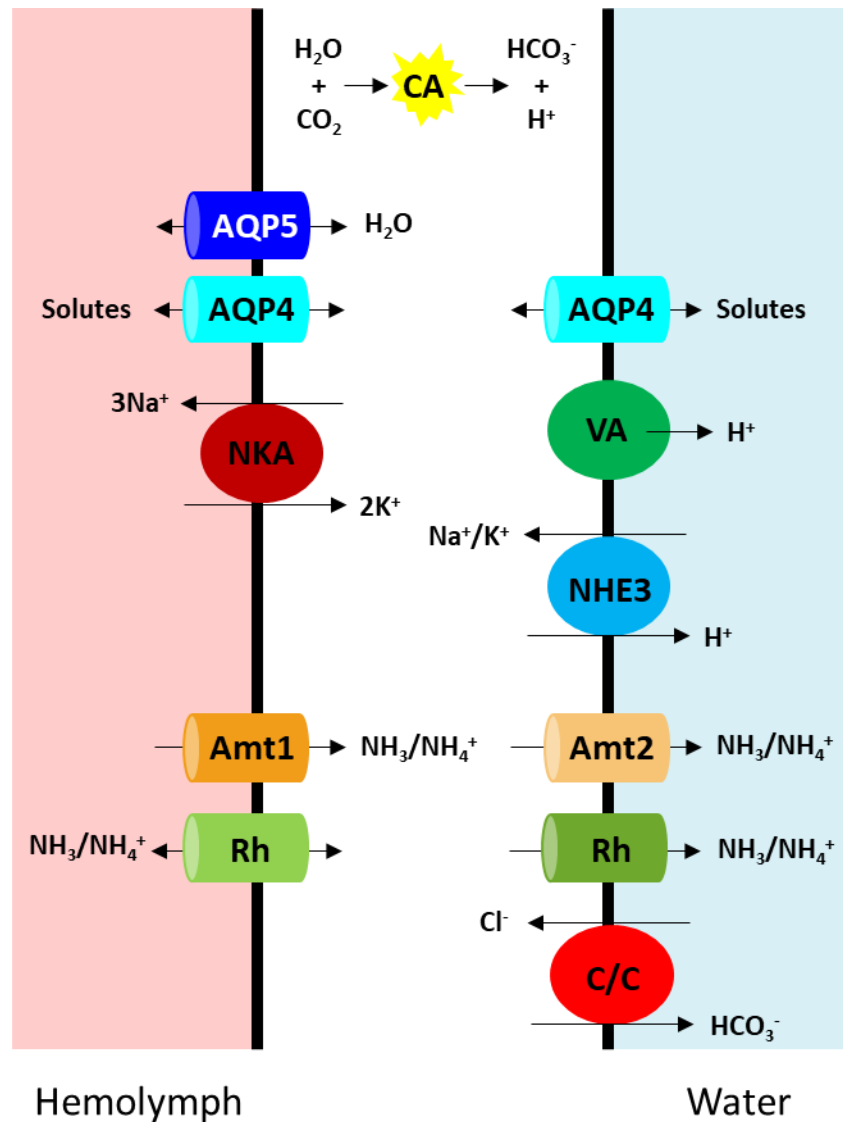


Figure 6: Schematic diagram illustrating membrane transport proteins in the anal papillae of larval *Aedes aegypti*. CA: carbonic anhydrase, AQP5: *Aedes aegypti* aquaporin 5, AQP4: *Aedes aegypti* aquaporin 4, NKA: Na⁺/K⁺ ATPase, VA: V-type H⁺ ATPase, NHE: Na⁺/H⁺ exchanger, Amt: ammonium transporters, Rh: Rhesus glycoproteins, and C/C: Cl⁻/HCO₃⁻ exchanger.

1.5 Objectives and Hypotheses

The objective of this study is to investigate the osmoregulatory organs in larvae of *A. aegypti* in order to identify their role in water transport. Expression of AaAQPs were the focus of this study since these channels are predicted to facilitate water permeability across membranes

that allow for physiological function of *A. aegypti* larvae in the dynamic environmental salinity conditions faced in nature. The gastric caeca (GC), anterior midgut (AMG), posterior midgut (PMG), hindgut (HG), Malpighian tubules (MTs), and anal papillae (AP) are osmoregulatory organs that participate in iono- and osmoregulation. The presence of AaAQP mRNA in these osmoregulatory organs has been detected in distilled water reared larvae (Akhter et al., 2017; Marusalin et al., 2012). It is therefore hypothesized, that the transcripts of AaAQPs in the GC, AMG, PMG, HG, MTs, AP, as well as the whole body will be detected and differentially expressed in larvae reared in freshwater. Additionally, it is hypothesized that AaAQP mRNA will also be detected and differentially expressed in organs of larvae reared in brackish water (30% seawater) since AaAQPs are predicted to be vitally important for physiological function.

Given the diversity in environmental salinities that *A. aegypti* larvae inhabit, it is proposed that the osmoregulatory organs adapt through molecular modifications including the expression of transporters and channels such as the AaAQPs, to accommodate the unique osmoregulatory pressures (Akhter et al., 2017; D'Silva et al., 2017; Jonusaite et al., 2017a). As seen in the anal papillae, the transcript abundance trends observed for AaAQP4 and AaAQP5 were reflected in protein abundance changes when larvae were reared in different salinities (Akhter et al., 2017) Therefore, it is hypothesised that the AaAQP transcript abundance will change in the GC, AMG, PMG, HG, MTs, AP as well as whole body of larval *A. aegypti* in response to brackish water rearing. It is further hypothesized that the patterns of transcript abundance of AaAQPs observed in the osmoregulatory organs will parallel the changes in protein abundance of these AaAQPs in response to brackish water rearing of larval *A. aegypti*. This hypothesis can be tested specifically for AaAQP1, AaAQP4 and AaAQP5 because of the availability of specific antibodies for each of these AaAQPs. Finally, immunohistochemistry will

allow for the localization of AaAQP1, AaAQP4, and AaAQP5 in the various osmoregulatory organs and shed light into the function and regulation of these AaAQPs in larval *A. aegypti* (Akhter et al., 2017; Misyura et al., 2017).

2. MATERIALS AND METHODS

2.1 Animal Care

Aedes aegypti eggs (Linnaeus) were obtained from a colony reared in the Department of Biology, York University, Toronto, Canada. Eggs were hatched in 800 mL of freshwater (FW) or brackish water (BW) with an additional 6 mL of food solution composed of 1.8 g liver powder and 1.8 g inactive yeast in 500 mL of reverse osmosis water. FW was composed of dechlorinated tap water (Toronto municipal tap water) and BW was composed of 10.5 gL⁻¹ Instant Ocean Sea Salt dissolved in double distilled water (approximately equivalent to 144 mmolL⁻¹ NaCl). Larvae were kept at room temperature on a 12 h: 12 h light:dark cycle. Larvae were fed daily with 3 mL of food solution (mentioned above). Rearing water was refreshed every two days until larvae reached the 3rd or 4th instar, upon which point larvae were dissected. The rearing protocol was repeated as described from egg through larva for each biological replicate that was collected.

2.2 Total RNA Extraction and cDNA Synthesis

Larvae were dissected under artificial physiological saline (ingredients outlined in Table 3). 75-80 larvae from a single biological replicate (defined as n = 1) were dissected to isolate their gastric caeca, anterior midgut, posterior midgut, Malpighian tubules, hindgut, and anal papillae and each organ type was kept separate and placed in 350 µL of lysis buffer from the PureLinkTM RNA Mini Kit (Invitrogen, Carlsbad, California, United States) and β-mercaptoethanol (1%). 15-20 whole bodies from a single biological replicate (defined as n = 1) were also collected using the same method for total RNA extraction according to the PureLinkTM RNA Mini Kit instructions. RNA was treated with the TURBO DNAfreeTM Kit (Applied Biosystems, Streetsville, Ontario, Canada) to remove genomic DNA following the manufacturer's instructions. The quality and quantity of RNA was determined using a NanoDrop

2000 spectrophotometer (Thermo Fisher Scientific, Waltham, USA). The quality of RNA was determined based on the ratio between 260:280 nm wavelengths of 2.0 ± 0.4 with the ideal value of 2.0 for RNA, according to manufacturer guidelines. The purified total RNA was utilized in the synthesis of cDNA using the iScript™ cDNA Synthesis Kit (Bio-Rad, Mississauga, Ontario, Canada) according to the manufacturer's instructions. The cDNA was stored at -20°C until subsequent use.

Table 3: Ingredients and their corresponding concentration in larval *A. aegypti* artificial physiological saline, adapted from Clark and Bradley (1996) and Donini et al. (2006).

Solute	Concentration (mmol L ⁻¹)
L-proline	5
L-glutamine	9.1
L-histidine	8.74
L-leucine	14.4
L-arginine-HCl	3.37
glucose	10
succinic acid	5
malic acid	5
citric acid (tri-sodium salt)	10
NaCl	30
KCl	3
NaHCO ₃	5
MgSO ₄	0.6
CaCl ₂	5
HEPES	25

2.3 Quantitative real-time PCR (qRT-PCR)

The relative mRNA abundance of the six AaAQP genes in the various osmoregulatory organs of larval *A. aegypti* reared in FW and BW were quantified using quantitative PCR (qPCR). The primers utilized in the qPCR reactions were designed and described by Marusalin et al., (2012) and listed in Table 3. Each reaction consisted of 10 μl of SsoFast™ Evagreen® Supermix (Bio-Rad), 2 μl of cDNA template, 0.5 μL of 10 μmolL^{-1} forward primer, 0.5 μL of 10

μmolL^{-1} reverse primer, and 7 μl of DNase-free, RNase-free, sterile PCR-grade water (Invitrogen). Reactions were performed in two technical replicates with a no cDNA template control included for each gene in the CFX96™ real-time PCR detection system (Bio-Rad). Reactions ran with the following settings, 2 min of enzyme activation and template denaturation at 95°C, followed by 40 cycles of 5s denaturation at 95°C and 5s of annealing/extension at 58°C. In order to confirm the presence of a single product, a melting curve analysis was performed after each reaction and consisted of holding the product at 95°C for 10s followed by holding the product at 65-95°C in 0.5°C increments, held for 5s each. For each gene and organ assessed, a standard curve was generated to determine primer efficiency. Quantification of transcripts was determined using the Pfaffl method (Pfaffl, 2001). The 18S rRNA gene was used as the reference gene due to its consistent levels of transcript expression under FW and BW treatments. Primers for 18S rRNA were designed and described by Jonusaite et al., (2016) and are included in Table 4.

Table 4: Primers and their characterization utilized in qPCR. Primers for AaAQP1-6 and 18S rRNA were designed and reported previously (Akhter et al., 2017; Jonusaite et al., 2016; Marusalin et al., 2012).

Target	Accession #	Forward Primer	Reverse Primer	Primer Efficiency (%)	Amplicon Size (bp)	Annealing Temperature (°C)
AaAQP1	AF218314.1	ATCGGATTCAGCAGGAGAG	TGATGTGGCAACCACTTAC	102.2	279	58
AaAQP2	XM_001656882	TGGCAAAGTCAGCATTGTTC	ACCCAAAGTAACCGTCATGC	103.8	280	58
AaAQP3	XM_001649697	ATGTTCCGATGCTCATCCTC	TTCTCCCATTTTGCTGTTC	100.8	251	58
AaAQP4	XM_001650118	AAGCAACCAGTCGTTTCTG	GAGCATCGGAACATCAAC	98.1	277	58
AaAQP5	XM_001650119	GGTGTCTCGTTCTGGTGTG	CCAACCCAGTAGACCCAGTG	91.3	206	58
AaAQP6	XM_001647996	ATGCCACTGCTTGTCCTAC	TTCCGAAATGACCTTGGAG	104.7	276	58
18S	U65375	TTGATTCTTGCCGGTACGTG	TATGCAGTTGGGTAGACCA	102.1	194	58

2.4 Immunohistochemistry

Immunohistochemistry of the GC, AMG, PMG, MTs, HG, and AP localizing AaAQP1, AaAQP4, AaAQP5, and V-type H⁺ ATPase was conducted according to a previously published protocol (Chasiotis et al., 2016). FW and BW reared *A. aegypti* larvae were obtained for fixation in Bouin's fixative. Tissues were dehydrated and embedded into paraffin wax. Samples were sectioned on a microtome (Leica Microscopy Inc. RM 2125RT manual rotary, ON, Canada) and placed onto slides for subsequent rehydration and antibody probing. Sections of each organ from FW and BW larvae were placed side by side on the same slide such that they were then treated identically through the immunohistochemical protocol. Anti-AaAQP1 affinity purified primary antibody (1.282 µg mL⁻¹ rabbit polyclonal antibody against CFFKVRKGDDEESYDF, Genscript, NJ, USA), anti-AaAQP4 affinity purified primary antibody (1.044 µg mL⁻¹ rabbit polyclonal antibody against PAEQAPSDVVGKSNQS, Genscript, NJ, USA), or anti-AaAQP5 affinity purified primary antibody (2.568 µg mL⁻¹ rabbit polyclonal antibody against FRREVPEPEYNRELT, Genscript, NJ, USA), in combination with membrane marker guinea pig anti-V-type H⁺ ATPase (kind donation from Dr. Weiczorek, Germany, 1:15000 dilution in ADB) antibodies were used to probe the rehydrated tissue samples. A goat anti-rabbit antibody conjugated to AlexaFluor 594 (Jackson ImmunoResearch) was applied at 1:500 dilution to visualize AaAQP1, AaAQP4, and AaAQP5, while goat anti-guinea pig antibody conjugated to AlexaFluor 488 (Jackson ImmunoResearch) was applied at 1:500 dilution to visualize V-type H⁺ ATPase. Negative control slides were also processed as described above with all primary antibodies omitted. Slides were mounted using ProLong® Gold antifade reagent with DAPI (Life Technologies, Burlington, ON, Canada).

Fluorescent images were captured using an Olympus IX81 inverted fluorescent microscope (Olympus Canada, Richmond Hill, ON, Canada) and CellSense® 1.12 Digital Imaging software (Olympus Canada). AP images were taken on the Zeiss Confocal Microscope using Zeiss Zen LSM Imaging Software. Images were merged using ImageJ 1.49 software (Schneider et al., 2012).

2.5 Protein Processing, Electrophoresis, and Western Blotting

GC, AMG, PMG, HG, MTs, and AP, were isolated under physiological saline from 75-80 *A. aegypti* larvae from each biological replicate reared in FW or BW (defined as $n = 1$) and stored at -80°C after removal of saline, until processing. AP samples were sonicated 3 X 10s at 3.5W using an XL 2000 Ultrasonic Processor (Qsonica, CN, USA) in RIPA homogenization buffer (50 mmolL^{-1} Tris-HCl, pH 7.5, 150 mmolL^{-1} NaCl, 1% sodium deoxycholate, 1% Triton-X-100, 0.1% SDS, 1 mmolL^{-1} PMSF and 1:200 protease inhibitor cocktail (Sigma-Aldrich)). GC, AMG, PMG, HG, and MTs samples were sonicated 3 X 10s at 3.5W using an XL 2000 Ultrasonic Processor (Qsonica) in TRIS homogenization buffer (50 mmolL^{-1} Tris-HCl, pH 7.4 and 1:200 protease inhibitor cocktail; Sigma-Aldrich). RIPA buffer was used for AP samples for optimal extraction and western blot signal of AaAQP1, AaAQP4, and AaAQP5. Homogenates were then centrifuged at 13,000 g for 15 min at 4°C [Sorvall™ Legend™ Micro 21 Centrifuge (ThermoFisher Scientific, USA)]. The protein concentration of the supernatant was measured using the DC protein assay (Bio-Rad) according to the manufacturer's guidelines with bovine serum albumin (BSA) as standards. Measurements were carried out on a Multiskan spectrum spectrophotometer (Thermo Electro Corporation, USA) at 750 nm wavelength.

Samples were prepared for sodium dodecyl sulphate polyacrylamide gel electrophoresis (SDS-PAGE) by heating for 5 min at 100°C with 5× loading buffer [225 mmolL^{-1} Tris-HCl, pH

6.8, 3.5% (w/v) SDS, 35% glycerol, 12.5% (v/v) β -mercaptoethanol and 0.01% (w/v) Bromophenol Blue]. 10 μ g of protein were loaded onto a 4% stacking and 12% resolving SDS-PAGE gel. Electrophoresis was carried out at 110 V for 1.5 h. Proteins were transferred from the gel onto a polyvinyl difluoride (PVDF) membrane using a wet transfer method at 100 V for 1 h in a cold ($\sim 4^{\circ}\text{C}$) transfer buffer (0.225 g Tris, 1.05 g glycine in 20% methanol). The PVDF membrane was then blocked with 5% skimmed milk powder in TBS-T for 1 h at RT and incubated overnight at 4°C with their respective antibodies (Table 5). The PVDF membrane was washed in Tris-buffered saline (TBS-T; 9.9 mmolL^{-1} Tris, 0.15 mmolL^{-1} NaCl, 1 % Tween-20, 0.1 mmolL^{-1} NP-40, pH 7.4) for 15 min and incubated with horseradish peroxidase (HRP)-conjugated goat anti-rabbit antibody (1:5000 in 5 % skim milk in TBS-T) (Bio-rad) for 1 h at RT. PVDF membrane was washed three times for 15 min with TBS-T before carrying out a chemiluminescent reaction using the Clarity™ Western ECL substrate (Bio-Rad). After visualization of detected protein bands, the PVDF membrane was washed with TBS-T for 1 min before probing the membranes for total protein with Coomassie blue as a loading control, described by Welinder and Ekblad (2011). The Image J 1.49 software (USA) was used to quantify the protein abundance of the western blots. All treatment group densitometry ratios were normalized to the total protein density.

Table 5: Antibody concentration used for western blotting. Antibodies were diluted in 5% skimmed milk and TBS-T.

AP: anal papillae, GC: gastric caeca, AMG: anterior midgut, PMG: posterior midgut, HG: hindgut, MT: Malpighian tubules, and WB: whole body.

	AaAQP1 ($\mu\text{g mL}^{-1}$)	AaAQP4 ($\mu\text{g mL}^{-1}$)	AaAQP5 ($\mu\text{g mL}^{-1}$)
AP	0.128	1.044	1.284
GC	0.321	1.044	0.642
AMG	0.321	0.696	1.712
PMG	0.214	1.044	0.642
HG	0.160	1.044	2.568
MT	0.642	0.696	1.284
WB	0.160	1.044	1.284

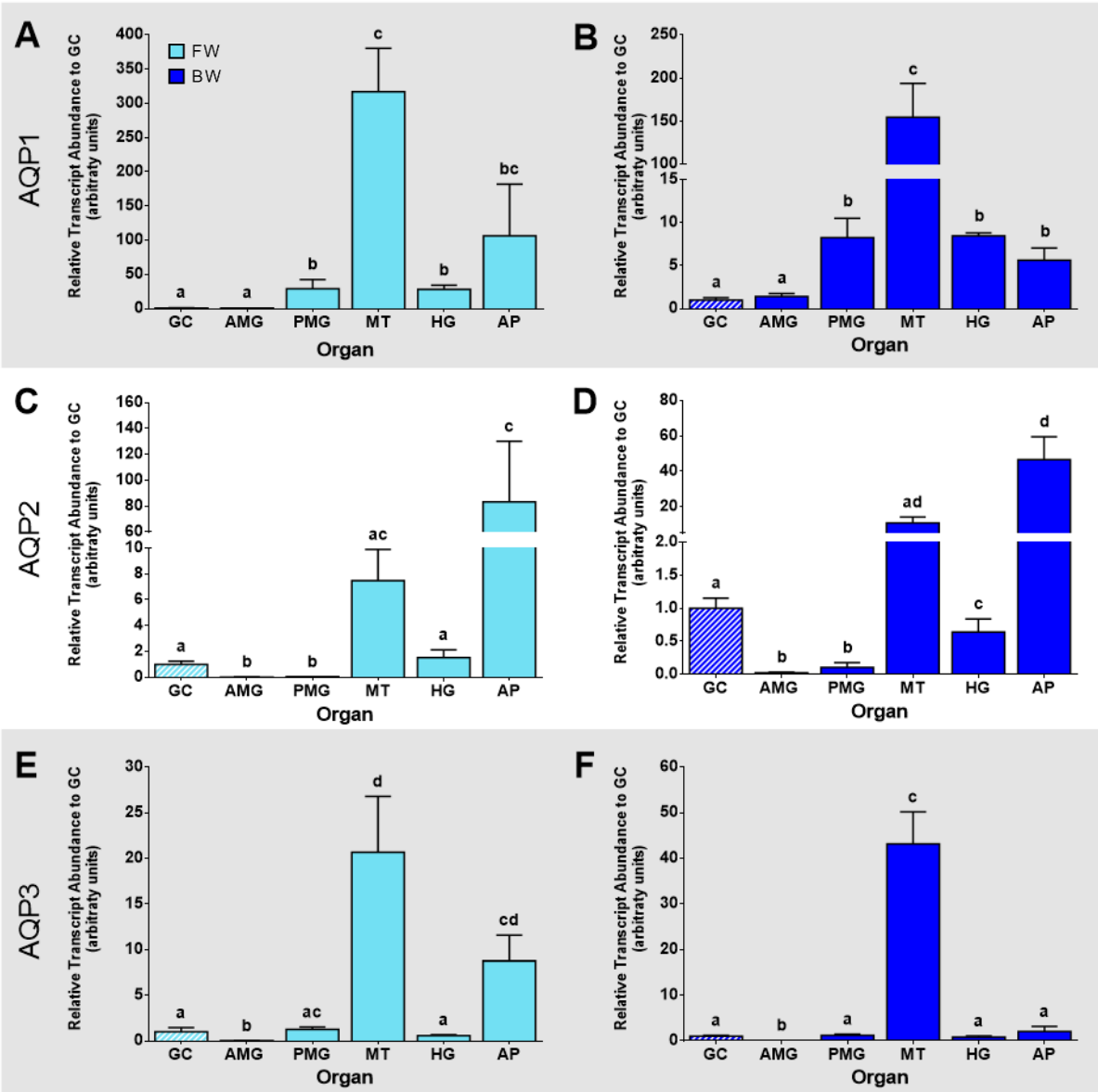
2.6 Statistical Analysis

Data were analyzed using Prism® 5.03 (GraphPad Software Inc., La Jolla, California, USA) and expressed as mean values \pm standard error of the mean (SEM). qPCR and western blot data was log transformed then analyzed using a non-parametric t-test to assess the relative effects of BW treatment. AaAQP and organ specific expression profiles were log transformed before running an ANOVA with Tukey post-hoc test.

3. RESULTS

3.1 AaAQP transcript expression profile in the osmoregulatory organs of FW and BW reared *A. aegypti* larvae

An AaAQP transcript expression profile across osmoregulatory organs is presented with AaAQP mRNA abundance in the various osmoregulatory organs shown relative to the abundance in the GC (Figure 7). The MTs and AP typically contained the greatest AaAQP transcript abundance when compared to the other osmoregulatory organs of FW reared larvae (Figure 7 A, C, E, G, I, and K). AQP transcripts were least abundant in the GC, AMG, and PMG of FW larvae. AaAQP6 was notably abundant in the HG and AP with a 1000-fold difference, when compared to other osmoregulatory organs in FW reared larvae which were the highest fold differences observed between osmoregulatory organs (Figure 7 K). The fold differences of AaAQP6 mRNA abundance in the HG and AP were diminished in BW reared larvae, though the trend remained (Figure 7 L). Larvae reared in BW expressed similar trends of AaAQP transcript abundances in each of the assessed osmoregulatory organs as FW (Figure 7 B, D, F, H, J, and L).



Please find the figure caption on the following page.

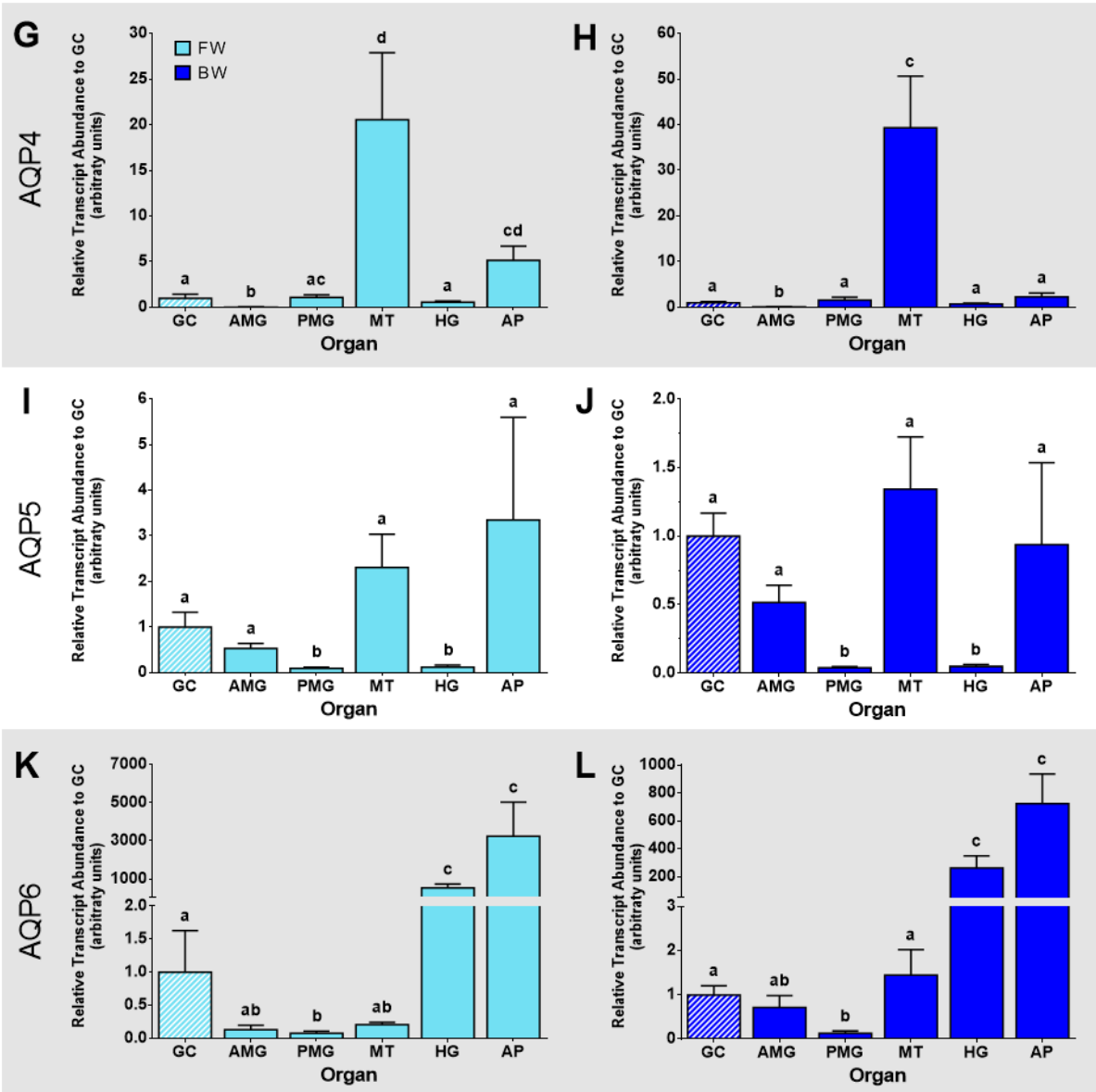
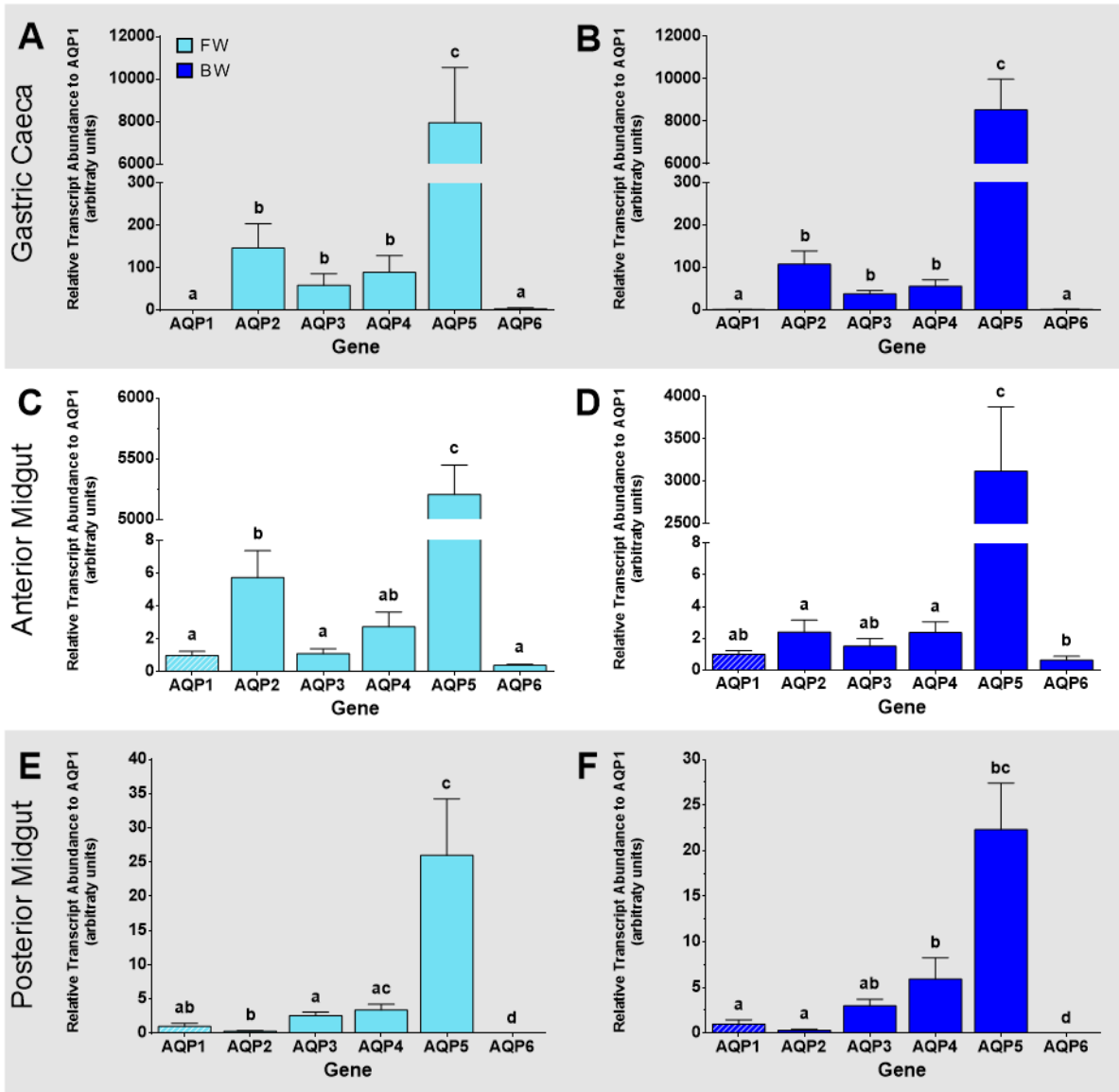


Figure 7: Aquaporin (AQP) mRNA abundance profiles in osmoregulatory organs of freshwater (A,C,E,G,I,K) and brackish water (B,D,F,H,J,L) reared *Aedes aegypti* larvae. Relative AQP1 (A-B), AQP2 (C-D), AQP3 (E-F), AQP4 (G-H), AQP5 (I-J), and AQP6 (K-L) mRNA abundance examined using quantitative-PCR and normalized to 18S ribosomal RNA and expressed as fold change relative to gastric caeca AQP abundance, which was assigned a value of 1.0. Data are expressed as means \pm SEM, ANOVA with Tukey's multiple comparison test and differences were considered significant if $p \leq 0.05$ and significant differences were denoted with different letters above the bars, $n = 4-5$. GC: gastric caeca, AMG: anterior midgut, PMG: posterior midgut, MT: Malpighian tubules, HG: hindgut, and AP: anal papillae.

3.2 Osmoregulatory organ AaAQP transcript expression profile of FW and BW reared *A. aegypti* larvae.

The qPCR data was also analyzed and presented as AaAQP transcript abundance within individual organs relative to the mRNA abundance of AaAQP1 (Figure 8). AaAQP5 transcript abundance was the highest in the GC, AMG, PMG, MTs, and HG of FW reared larvae (Figure 8 A, C, E, G). HG and AP exhibited similar trends of AaAQP transcript abundance, with AaAQP5 and AaAQP6 being the most abundant in FW reared larvae (Figure 8 I and K). AaAQP1, AaAQP3, and AaAQP4 were typically the least abundant AaAQP mRNA observed in the osmoregulatory organs of FW reared larvae (Figure 8). Similar to FW, in BW, AaAQP mRNA abundance in the osmoregulatory organs followed similar trends where AaAQP5 mRNA abundance was the highest in the GC, AMG, PMG, MTs and the HG (Figure 8 B, D, F, H, and J). AaAQP2 abundance was high in the anal papillae in comparison to the abundance of all the other AaAQPs of BW reared larvae (Figure 8 L).



Please find the figure caption on the following page.

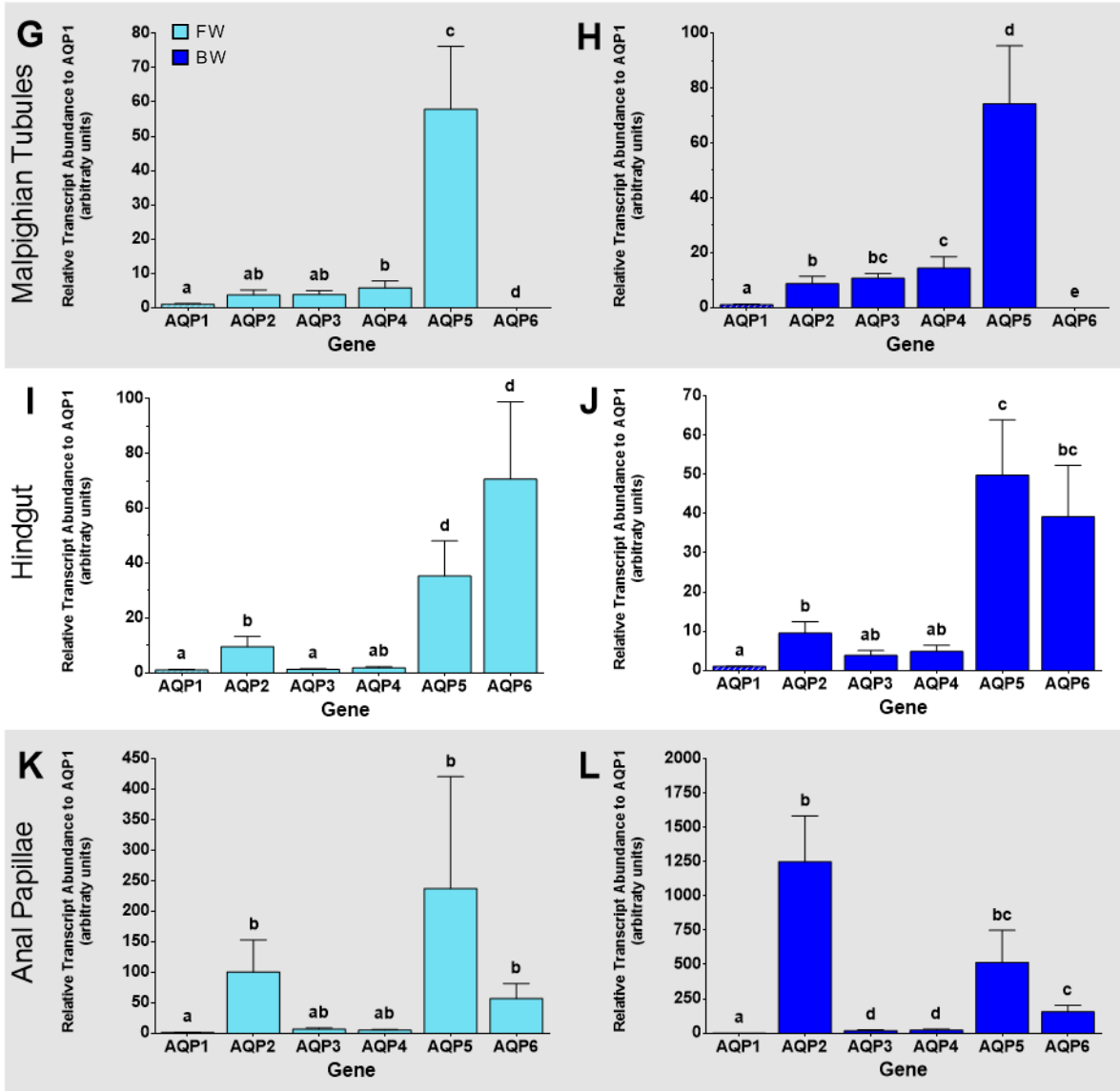


Figure 8: *Aedes aegypti* osmoregulatory organ aquaporin (AaAQP) mRNA abundance of freshwater (A,C,E,G,I,K) and brackish water (B,D,F,H,J,L) reared larvae. AaAQP mRNA abundance in gastric caeca (A-B), anterior midgut (C-D), posterior midgut (E-F), Malpighian tubules (G-H), hindgut (I-J), and anal papillae (K-L) examined using quantitative-PCR and normalized to 18S ribosomal RNA and expressed as fold change relative to AaAQP1 which was assigned a value of 1.0. Data are expressed as means \pm SEM, ANOVA with Tukey's multiple comparison test and differences were considered significant if $p \leq 0.05$ and significant differences were denoted with different letters above the bars, $n = 4-5$.

3.3 AaAQP transcript abundance in response to BW

The qPCR data was also analyzed to directly compare individual AaAQP transcript abundance between FW and BW rearing in osmoregulatory organs (Figure 9). AaAQP2 and AaAQP5 transcript abundance did not change in response to the BW treatment in the organs assessed (Figure 9 B and E). AaAQP1 transcript abundance was two-fold lower in the HG in response to BW treatment, while there was a trend towards a decrease in AP (unpaired t-test; $p = 0.06$; Figure 9 A). AaAQP3 mRNA abundance increased 3-fold in AMG and nearly doubled in the MTs in response to BW, while there was a trend towards a decrease in the AP ($p = 0.06$; Figure 9 C). BW treatment resulted in a two-fold decrease of AaAQP4 mRNA abundance in the AP, while in the other organs analyzed it was consistent between treatments (Figure 9 D). AaAQP6 transcript abundance was lower in the HG and the AP in response to the BW treatment. There was also a decreasing trend in the PMG ($p = 0.07$) and an increasing trend in the AMG ($p = 0.06$; Figure 3 F).

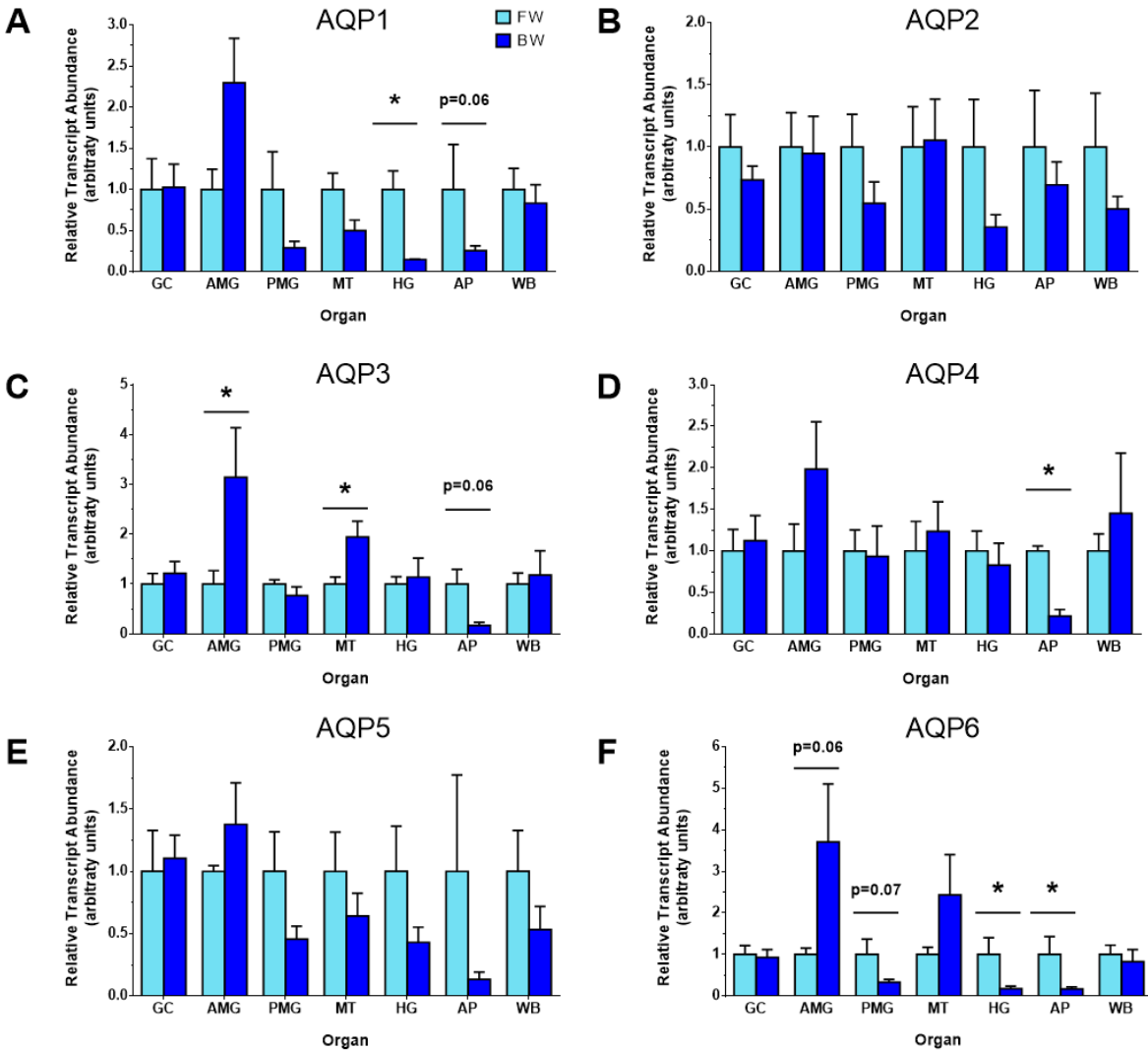


Figure 9: mRNA abundance of aquaporin (AQP) genes in the osmoregulatory organs of larval *Aedes aegypti* in response to brackish water (30% seawater, dark blue bars) relative to freshwater reared larvae (light blue bars). AQP1 (A), AQP2 (B), AQP3 (C), AQP4 (D), AQP5 (E), and AQP6 (F) abundance examined using quantitative-PCR and normalized to 18S ribosomal RNA and expressed as fold change relative to freshwater which was assigned a value of 1.0. Data are expressed as means \pm SEM, statistically analyzed using an unpaired t-tests $p \leq 0.05$ indicated by *, $n = 4-5$. GC: gastric caeca, AMG: anterior midgut, PMG: posterior midgut, MT: Malpighian tubules, HG: hindgut, AP: anal papillae, and WB: whole body.

3.4 AaAQP Protein Abundance in the Osmoregulatory Organs of *A. aegypti* Larvae.

3.4.1 AaAQP1

AaAQP1 protein abundance increased in response to BW in the GC and the AP, while BW rearing did not alter the protein abundance of AaAQP1 in the AMG, PMG, MTs and the HG (Figure 10). GC and AP protein homogenates probed with AaAQP1 antibody displayed a single band at ~60 kDa which was similar in mass to the predicted putative dimer (52.4 kDa) (Figure 10 A and F). Preincubation of AaAQP1 antibody with immunogenic peptide was not successful in GC homogenates, however, in the AP, the band at ~60 kDa was not detected with preincubation, therefore it was assumed that the ~60 kDa band observed in the GC and the AP was AaAQP1 specific (Figure 10 J). AaAQP1 doubled its abundance in the GC in response to BW rearing of the larvae, while the AP demonstrated a 15-fold increase in protein abundance of AaAQP1 in BW reared larvae (Figure 10 A and F). PMG protein homogenates probed with AaAQP1 antibody displayed a single band at ~25 kDa which was similar to the mass of the predicted monomer (26.2 kDa) and was not detected when AaAQP1 antibody was preincubated with peptide, signifying its specificity to AaAQP1 protein which did not change in abundance in BW reared larvae (Figure 10 C and G). Protein homogenates of MTs and the HG displayed a single band at ~23 kDa which was slightly smaller than the predicted monomeric mass of 26.2 kDa (Figure 10 D and E). Immunogenic peptide successfully blocked the band at ~23 kDa in MTs and hindgut samples suggesting that the band was specific to AaAQP1 protein (Figure 10 H). Subsequent quantification of the ~23 kDa band in the MTs and HG samples revealed no change in AaAQP1 protein abundance in response to BW rearing (Figure 10 D and E). AMG protein homogenates incubated with AaAQP1 antibody revealed four bands at ~30 kDa, ~32 kDa, ~34 kDa, and ~65 kDa (Figure 10 B). Preincubation with immunogenic peptide was inconclusive

(data not shown) therefore, it was assumed that the bands observed in anterior midgut samples were all specific to AaAQP1 protein since their specificity could not be disputed by the peptide blocks performed in other organs.

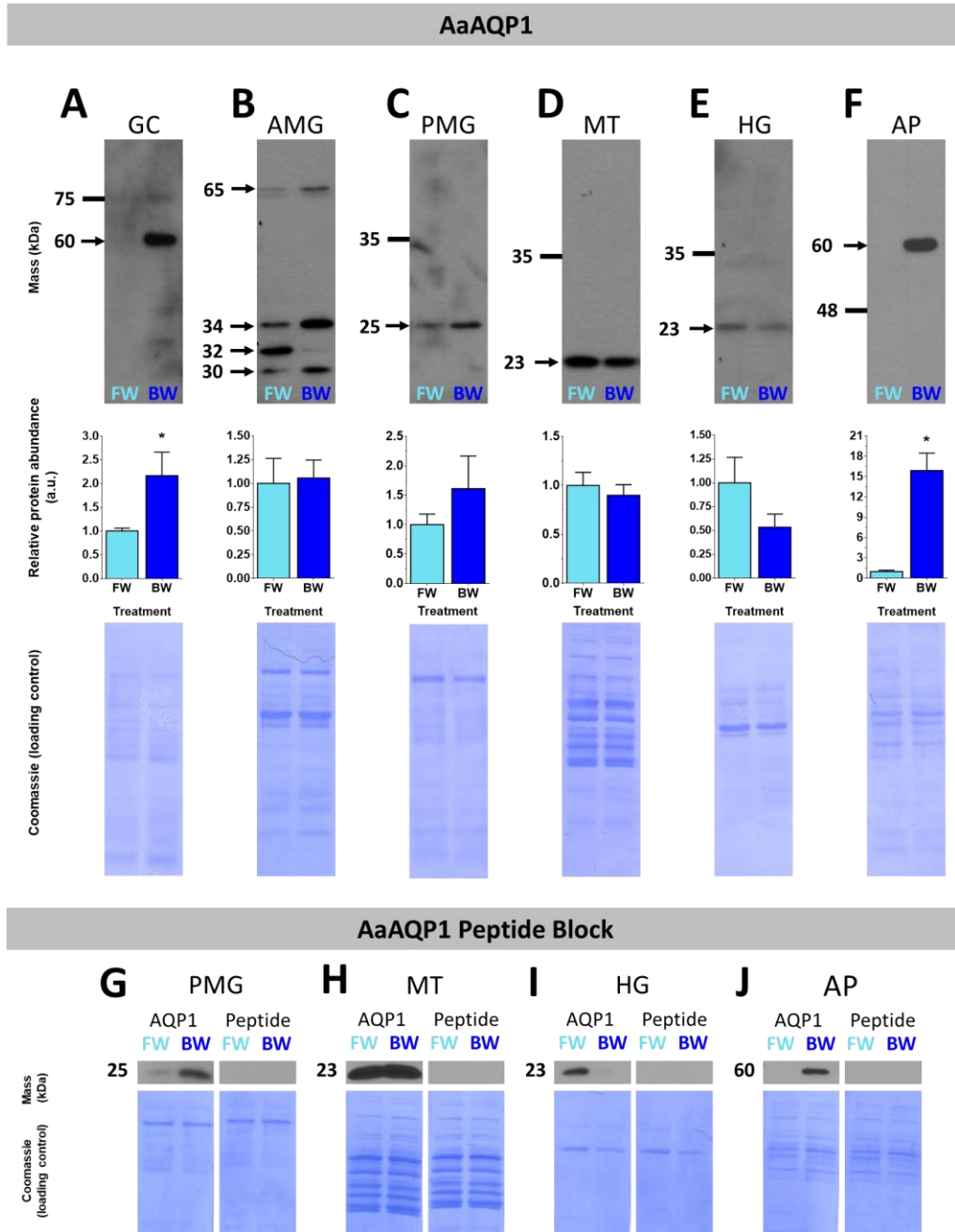


Figure 10: Protein abundance of AaAQP1 in the gastric caeca (A), anterior midgut (B), posterior midgut (C), Malpighian tubules (D), hindgut (E), and anal papillae (F) of freshwater (FW, light blue bars) and brackish water (BW, 30% seawater, dark blue bars) reared larval *Aedes aegypti*. Preincubation of AaAQP1 antibody with immunizing peptide probed for posterior midgut (G), Malpighian tubules (H), hindgut (I), and anal papillae (J). Mean band density were normalized to total protein assessed using Coomassie staining. Brackish water densitometry expressed relative to freshwater which was assigned a value of 1.0. Data are expressed as means \pm SEM. statistically analyzed using an unpaired t-tests $p \leq 0.05$ indicated by *, $n=4-5$. GC: gastric caeca, AMG: anterior midgut, PMG: posterior midgut, MT: Malpighian tubules, HG: hindgut, and AP: anal papillae.

3.4.2 AaAQP4

AaAQP4 protein abundance did not change with BW treatment in the GC, AMG, PMG, MTs, HG and the AP (Figure 11). Western blots of protein homogenates from various osmoregulatory organs that were probed with AaAQP4 antibody displayed varying band patterns in the different organs (Figure 11). Protein homogenates of all the organs observed displayed a common band at ~58 kDa similar in mass to a predicted dimer (63.6 kDa) (Figure 11). The bands at ~57 kDa and ~58 kDa were also shown to be specific for AaAQP4 protein based on the results of the peptide block in the AMG and the MTs samples (Figure 11 G and H). Preincubation of AaAQP4 antibody with immunogenic peptide was inconclusive when probing protein homogenate samples from the GC, PMG, and HG therefore, it was assumed that the observed band at ~58 kDa was specific to AaAQP4 protein and was subsequently quantified. Protein homogenates of AP displayed a band at ~75 kDa and an additional band at ~58 kDa in BW reared AP samples which were both quantified (Figure 11 F). The peptide block for AP revealed an additional band at ~50 kDa which was not observed in experimental samples and was therefore inconclusive (Figure 11 I). In PMG samples, in addition to ~58 kDa, there was an additional band observed at ~25 kDa which was close to the mass of the estimated 31.3 kDa monomer (Figure 11 C). Due to the inconclusive peptide block, the ~25 kDa band was analyzed in the quantification analysis since its specificity could not be ruled out. Similar to the PMG, the MTs also possessed the ~25 kDa band as well as a ~26 kDa band (Figure 11 D). However, the ~26 kDa band was not blocked with immunogenic peptide therefore the bands quantified in the MTs were ~25, ~57, and ~58 kDa (Figure 11 H).

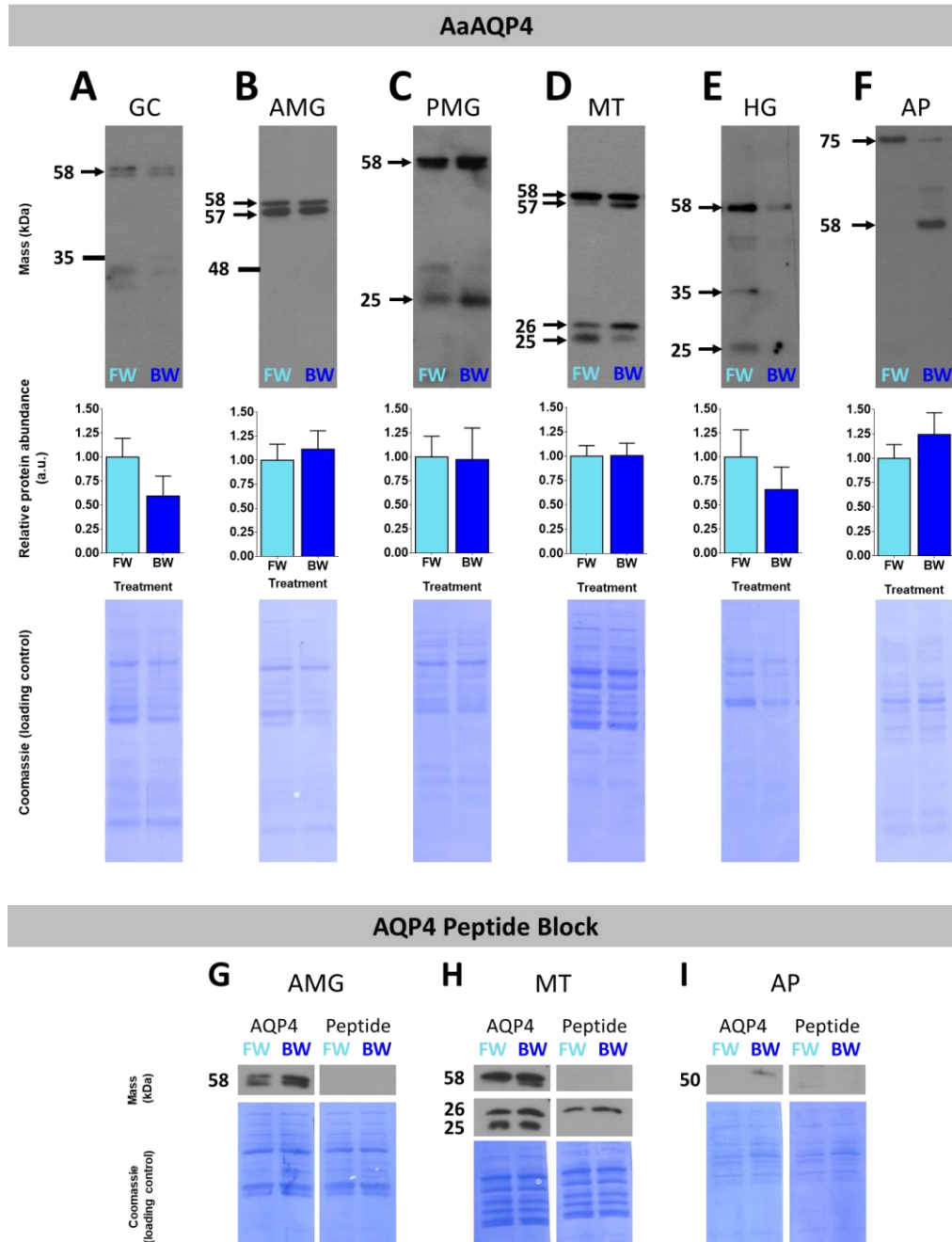


Figure 11: Protein abundance of AaAQP4 in the gastric caeca (A), anterior midgut (B), posterior midgut (C), Malpighian tubules (D), hindgut (E), and anal papillae (F) of freshwater (FW, light blue bars) and brackish water (BW, 30% seawater, dark blue bars) reared larval *Aedes aegypti*. Preincubation of AaAQP4 antibody with immunizing peptide probed for anterior midgut (G), Malpighian tubules (H), and anal papillae (I). Mean band density were normalized to total protein assessed using Coomassie staining. Brackish water densitometry expressed relative to freshwater which was assigned a value of 1.0. Data are expressed as means \pm SEM. statistically analyzed using an unpaired t-tests, n=4-5. GC: gastric caeca, AMG: anterior midgut, PMG: posterior midgut, MT: Malpighian tubules, HG: hindgut, and AP: anal papillae.

3.4.3 AaAQP5

AaAQP5 protein abundance increased in the AP in response to BW, while BW treatment did not alter the protein abundance of AaAQP5 in the GC, AMG, PMG, MTs and the HG (Figure 12). Western blots of protein homogenates from various osmoregulatory organs that were probed with AaAQP5 antibody displayed varying band patterns in the different organs (Figure 12). Protein homogenates from AP probed with AaAQP5 antibody demonstrated a single band at ~26 kDa which was the same mass as the predicted putative monomer and was not detected when AaAQP5 antibody was preincubated with immunogenic peptide (Figure 12 F and K). Quantification of the AaAQP5 monomer in the AP samples demonstrated a 14-fold increase in protein abundance in response to BW rearing of larvae (Figure 12 F). AaAQP5 probed GC protein homogenates showed two bands at ~30 kDa, and ~55 kDa that were both successfully blocked in the peptide block blot therefore, both bands were quantified (Figure 12 A and G). PMG protein homogenate samples displayed two bands at ~26 kDa and ~28 kDa, where both bands were confirmed to be AaAQP5 protein by the peptide block and were therefore quantified (Figure 12 C and H). Three bands were observed in HG protein samples when incubated with AaAQP5 antibody however, the peptide block revealed ~26 kDa was the only specific band to AaAQP5 protein, therefore it alone was used in protein quantification analysis (Figure 12 E and I). AaAQP5 probed membranes for MT protein samples revealed three bands at ~26 kDa, ~60 kDa, and ~75 kDa while the peptide block verified the ~26 kDa band to be specific, which is the mass of the predicted monomer (Figure 12 D and J). Peptide blocks for AMG samples were inconclusive, however based on the peptide block results in the PMG, both the ~28 kDa and ~26 kDa bands were quantified (Figure 12 B, C, and H). In addition, since the heavier band at ~63

kDa in the AMG did not relate to the peptide blocks observed in other organs, it was also quantified since its specificity could not be ruled out (Figure 12 B).

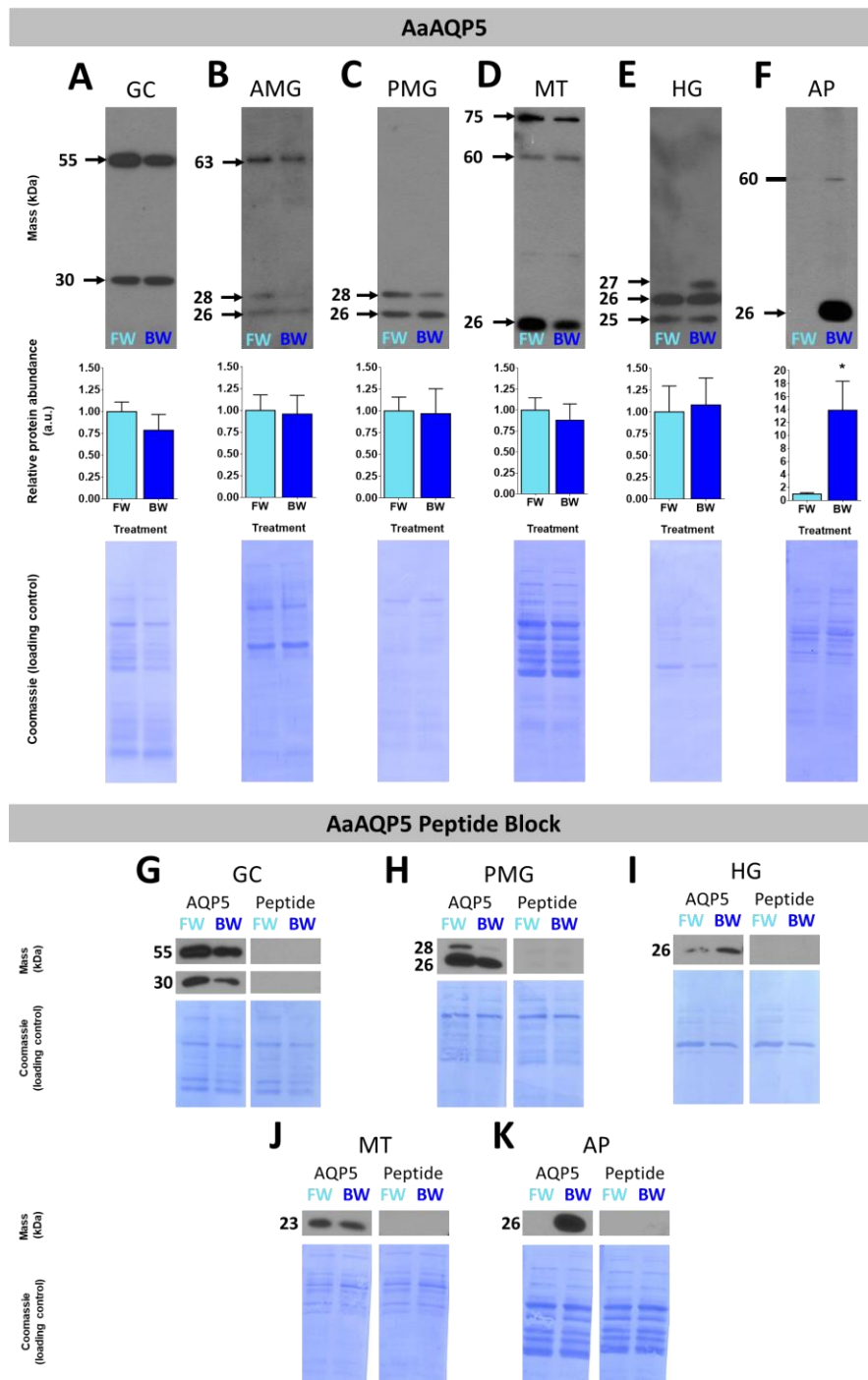


Figure 12: Protein abundance of AaAQP5 in the gastric caeca (A), anterior midgut (B), posterior midgut (C), Malpighian tubules (D), hindgut (E), and anal papillae (F) of freshwater (FW, light blue bars) and brackish water (BW, 30% seawater, dark blue bars) reared larval *Aedes aegypti*. Preincubation of AaAQP5 antibody with immunizing peptide probed for gastric caeca (G), posterior midgut (H), hindgut (I), Malpighian tubules (J), and anal papillae (K). Mean band density were normalized to total protein assessed using Coomassie staining. Brackish water densitometry expressed relative to freshwater which was assigned a value of 1.0. Data are expressed as means \pm SEM. statistically analyzed using an unpaired t-tests $p \leq 0.05$ indicated by *, $n=4-5$. GC: gastric caeca, AMG: anterior midgut, PMG: posterior midgut, MT: Malpighian tubules, HG: hindgut, and AP: anal papillae.

3.5 Immunolocalization of AaAQP1, AaAQP4, and AaAQP5 in the osmoregulatory organs of *Aedes aegypti* larvae

3.5.1 Gastric Caeca

AaAQP1, AaAQP4, AaAQP5, and V-type H⁺-ATPase (VA) immunoreactivity was detected in the gastric caeca of larval *A. aegypti* (Figure 13-15). In FW reared larvae, the VA was notably expressed and localized in the distal portion of the gastric caeca containing ion transporting cells that were facing the hemolymph (Figure 13-15 B and E). The cells at the proximal infolding of the gastric caeca membrane towards the midgut region remained free of immunoreactivity (Figure 13-15 B and E). In BW, VA was also localized to the apical membrane of the digestive cells (Figure 13-15 G and J). In FW reared larvae, AaAQP1 immunoreactivity was intracellular and diffuse in the ion transporting cells of the gastric caeca with select apical localization that co-localized with VA (Figure 13 A and E). In BW, AaAQP1 was also intracellular and diffuse, as well as some basolateral and apical membrane localization in the ion transporting cells (Figure 13 F and J). Immunolocalization of AaAQP4 in the gastric caeca of FW reared larval *A. aegypti* revealed intracellular and diffuse immunoreactivity in the ion transporting cells without specific membrane localization; however, there were some distal regions away from the epithelial infolding where AaAQP4 co-localized with VA on the apical membrane (Figure 14 A and E). In BW, AaAQP4 immunoreactivity remained diffusive with less intensity when compared to FW reared ion transporting cells of the GC (Figure 14 F and J). Immunolocalization of AaAQP5 in the gastric caeca of larvae was localized to the basolateral membrane of ion transporting and digestive cells in FW and BW reared larvae (Figure 15 A, E, F, and J). There was no AaAQP or VA immunoreactivity in control slides where primary

antibody was omitted (Figure 13-15 D and I). DAPI was utilized to visualize nuclei of the gastric caeca (Figures 13-15 C-E, H-J).

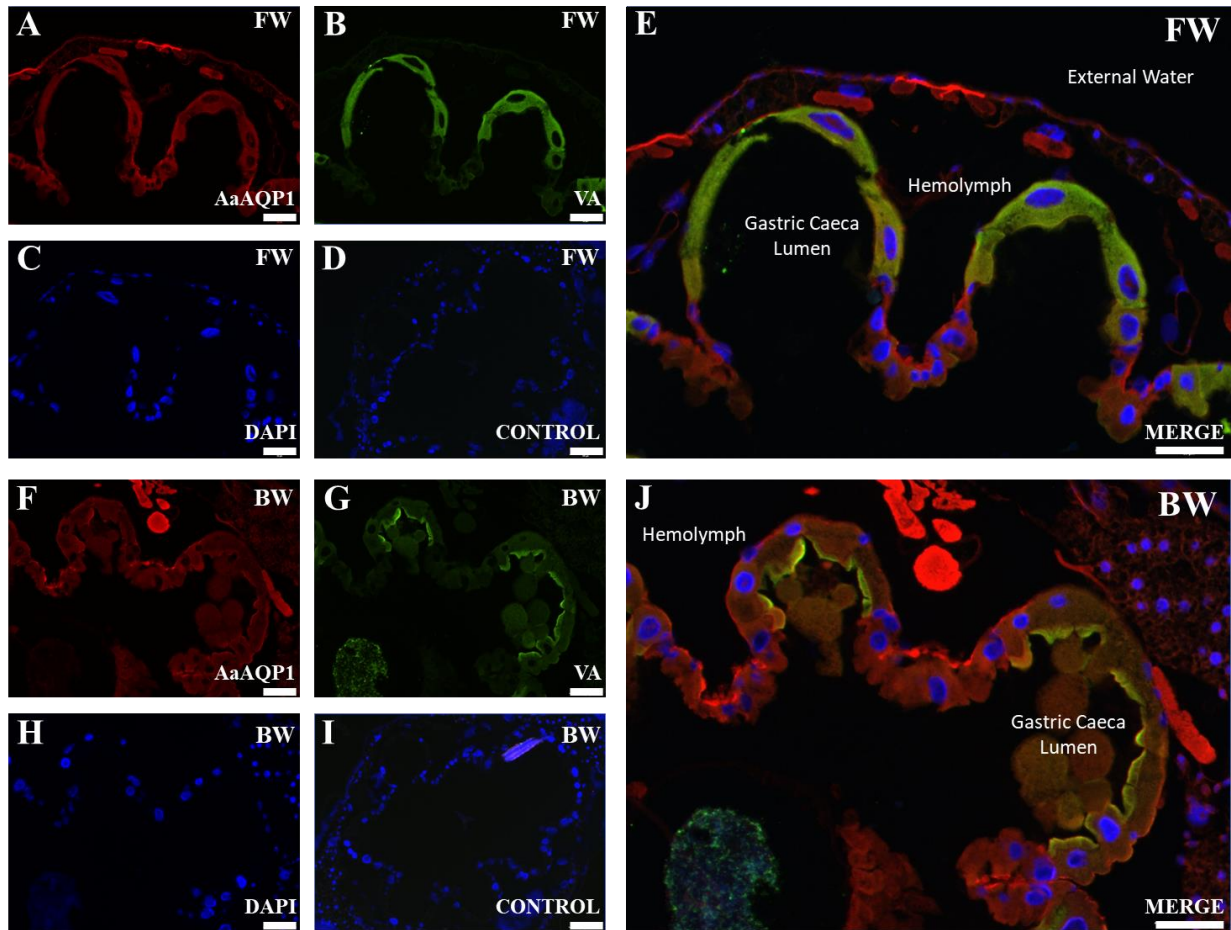


Figure 13: Immunolocalization of AaAQP1 in the gastric caeca of larval *A. aegypti* reared in freshwater (FW) and brackish water (BW) using V-type H^+ -ATPase (VA) as a membrane marker.

Representative paraffin-embedded cross-sections demonstrate AaAQP1 immunoreactivity (red, A, E, F, and J) and V_0 subunit V-type H^+ -ATPase (green, B, E, G, and J). Merged images of A, B, and C (E) and F, G, and H (J) demonstrate any co-localization in yellow. Blue staining indicates nuclei labeled with DAPI (C-E and H-J). Merged image of control cross-sections of gastric caeca (primary antibodies omitted) (D and I). Scale bars: 50 μ m on all experimental images (A-C, E-H, and J); 100 μ m on all control images (D and I).

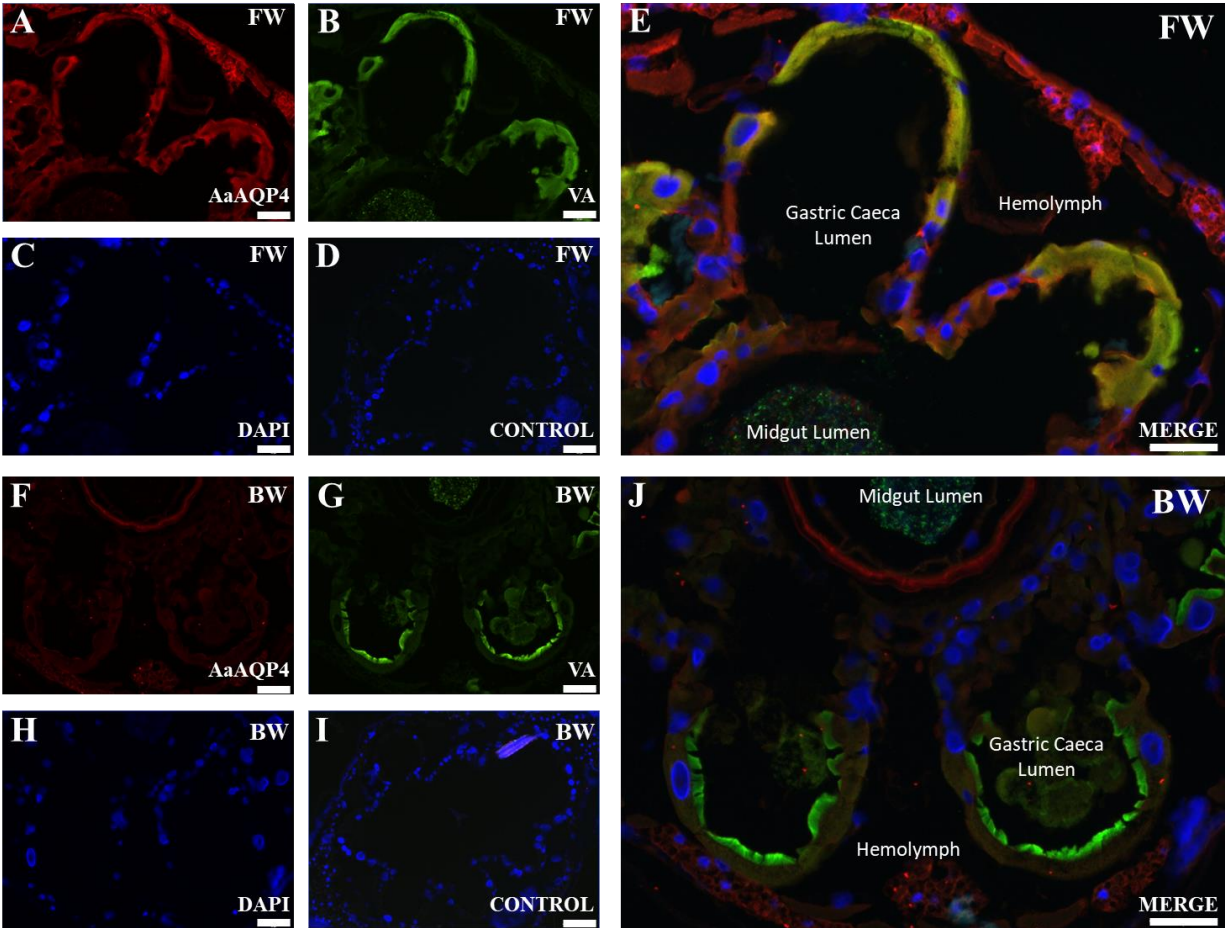


Figure 14: Immunolocalization of AaAQP4 in the gastric caeca of larval *A. aegypti* reared in freshwater (FW) and brackish water (BW) using V-type H⁺-ATPase (VA) as a membrane marker.

Representative paraffin-embedded cross-sections demonstrate AaAQP4 immunoreactivity (red, A, E, F, and J) and V₀ subunit V-type H⁺-ATPase (green, B, E, G, and J). Merged images of A, B, and C (E) and F, G, and H (J) demonstrate any co-localization in yellow. Blue staining indicates nuclei labeled with DAPI (C-E and H-J). Merged image of control cross-sections of gastric caeca (primary antibodies omitted) (D and I). Scale bars: 50 μm on all experimental images (A-C, E-H, and J); 100 μm on all control images (D and I).

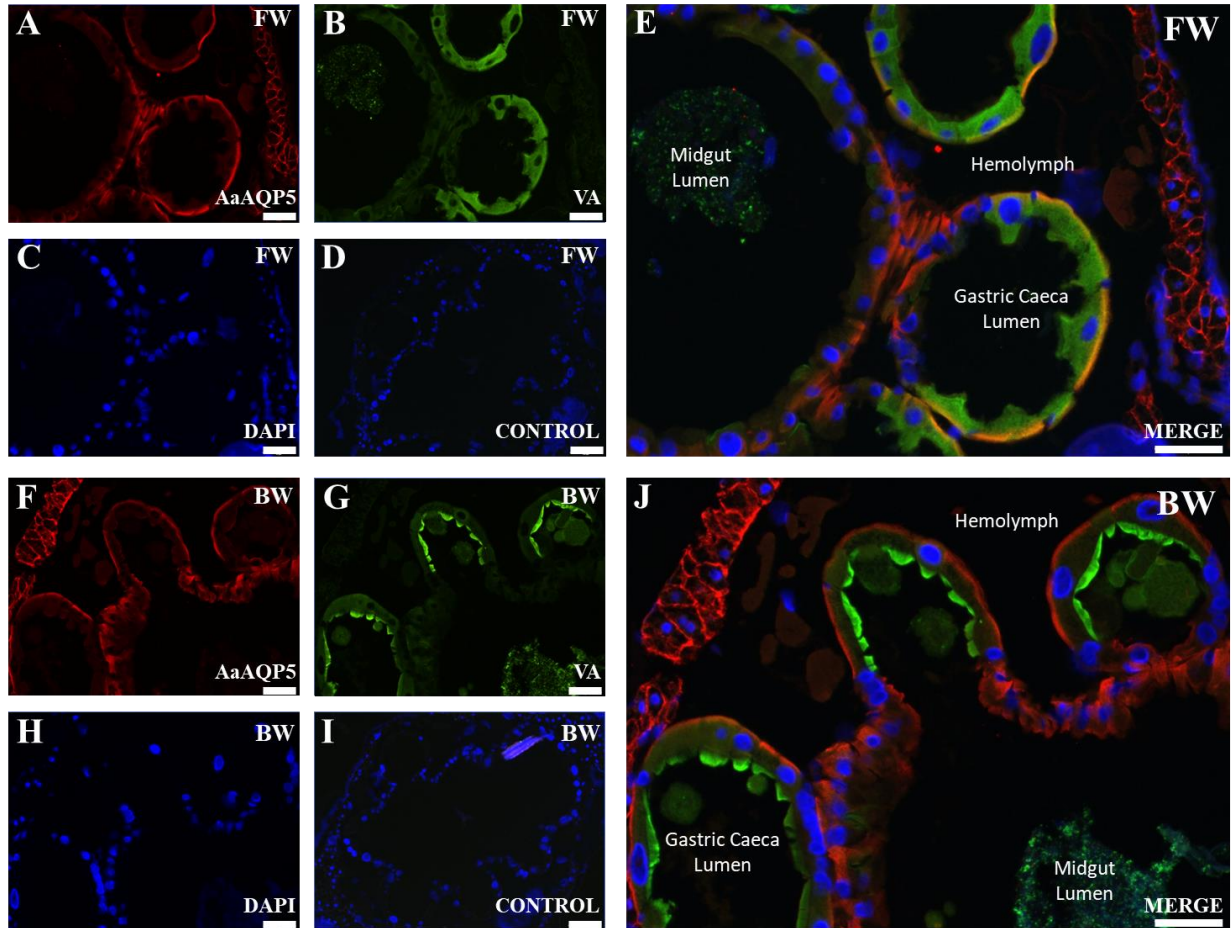


Figure 15: Immunolocalization of AaAQP5 in the gastric caeca of larval *A. aegypti* reared in freshwater (FW) and brackish water (BW) using V-type H⁺-ATPase (VA) as a membrane marker.

Representative paraffin-embedded cross-sections demonstrate AaAQP5 immunoreactivity (red, A, E, F, and J) and V₀ subunit V-type H⁺-ATPase (green, B, E, G, and J). Merged images of A, B, and C (E) and F, G, and H (J) demonstrate any co-localization in yellow. Blue staining indicates nuclei labeled with DAPI (C-E and H-J). Merged image of control cross-sections of gastric caeca (primary antibodies omitted) (D and I). Scale bars: 50 μm on all experimental images (A-C, E-H, and J); 100 μm on all control images (D and I).

3.5.2 Anterior Midgut

AaAQP1, AaAQP4, AaAQP5, and VA demonstrated immunoreactivity detected in the anterior midgut (Figure 16-18). VA immunoreactivity was localized to the basolateral membrane in anterior midgut epithelial cells of FW and BW reared larvae (Figure 16-18 B, E, G and J). Immunolocalization of AaAQP1, AaAQP4 and AaAQP5 in the anterior midgut of FW larvae localized to both the apical and basolateral membranes of epithelial cells with intracellular immunoreactivity that appeared diffuse (Figure 16-18). AaAQP1 and AaAQP4 immunoreactivity in BW reared larval anterior midgut epithelial cells was less pronounced in the membrane while intracellular staining was increased, where it continued to appear diffuse (Figure 16-17 A, E-F and J). AaAQP5 localized to the anterior midgut apical membrane of epithelial cells in BW reared larvae (Figure 18 F and J). There was no AaAQP or VA immunoreactivity in control slides where primary antibody was omitted (Figure 16-18 D and I). DAPI was utilized to visualize nuclei of the anterior midgut (Figures 16-18 D and I).

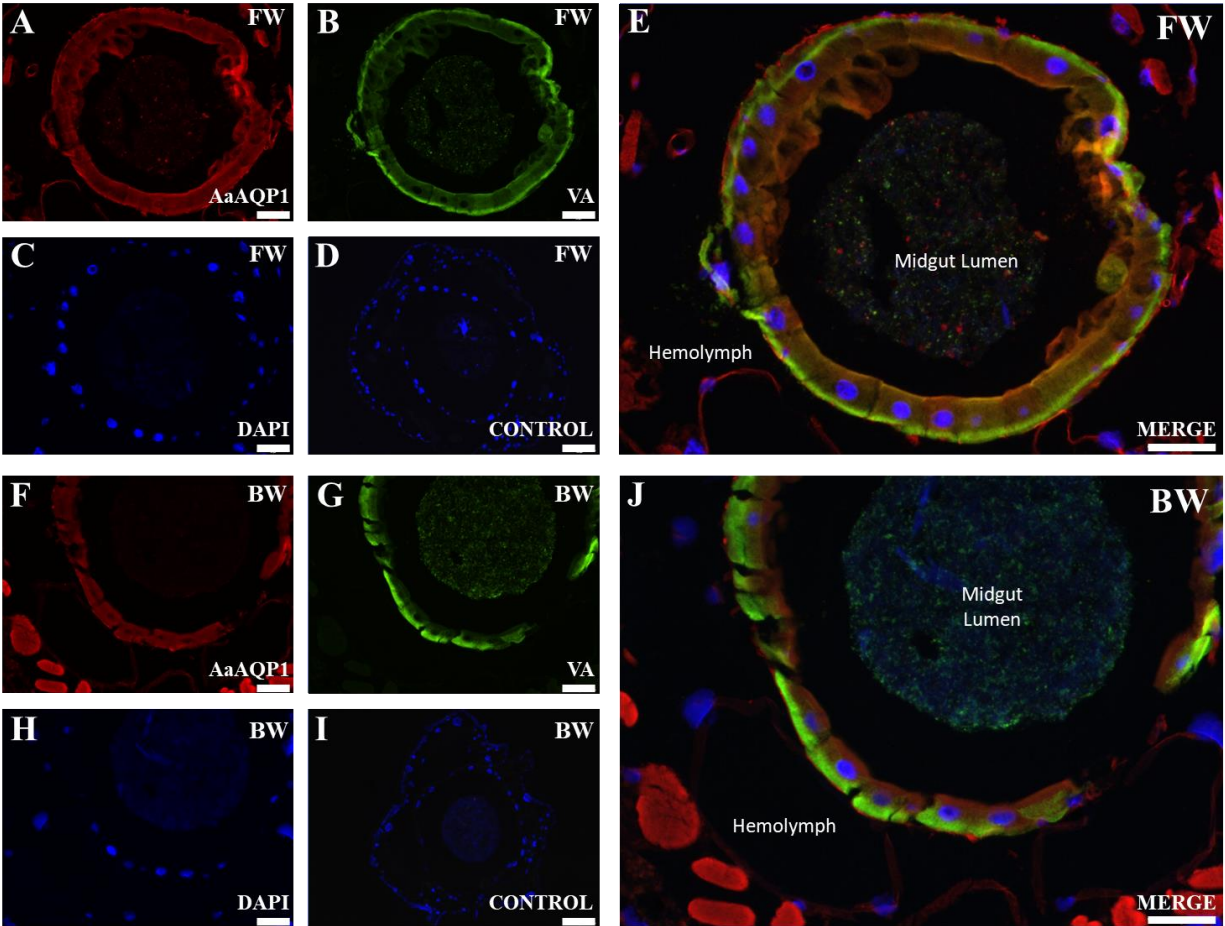


Figure 16: Immunolocalization of AaAQP1 in the anterior midgut of larval *A. aegypti* reared in freshwater (FW) and brackish water (BW) using V-type H^+ -ATPase (VA) as a basolateral membrane marker.

Representative paraffin-embedded cross-sections demonstrate AaAQP1 immunoreactivity (red, A, E, F, and J) and V_0 subunit V-type H^+ -ATPase (green, B, E, G, and J). Merged images of A, B, and C (E) and F, G, and H (J) demonstrate any co-localization in yellow. Blue staining indicates nuclei labeled with DAPI (C-E and H-J). Merged image of control cross-sections of anterior midgut (primary antibodies omitted) (D and I). Scale bars: 50 μm on all experimental images (A-C, E-H, and J); 100 μm on all control images (D and I).

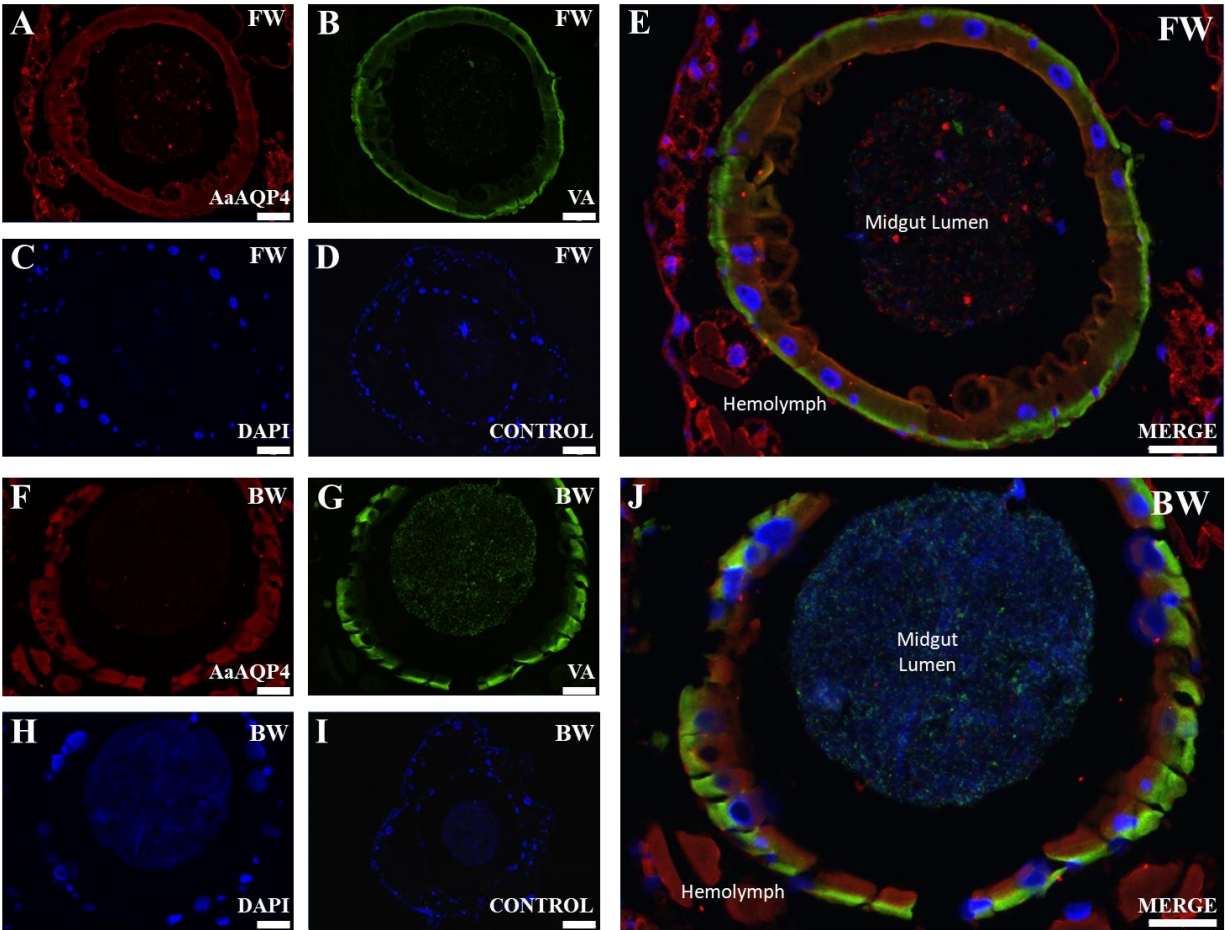


Figure 17: Immunolocalization of AaAQP4 in the anterior midgut of larval *A. aegypti* reared in freshwater (FW) and brackish water (BW) using V-type H^+ -ATPase (VA) as a basolateral membrane marker.

Representative paraffin-embedded cross-sections demonstrate AaAQP4 immunoreactivity (red, A, E, F, and J) and V_0 subunit V-type H^+ -ATPase (green, B, E, G, and J). Merged images of A, B, and C (E) and F, G, and H (J) demonstrate any co-localization in yellow. Blue staining indicates nuclei labeled with DAPI (C-E and H-J). Merged image of control cross-sections of anterior midgut (primary antibodies omitted) (D and I). Scale bars: 50 μ m on all experimental images (A-C, E-H, and J); 100 μ m on all control images (D and I).

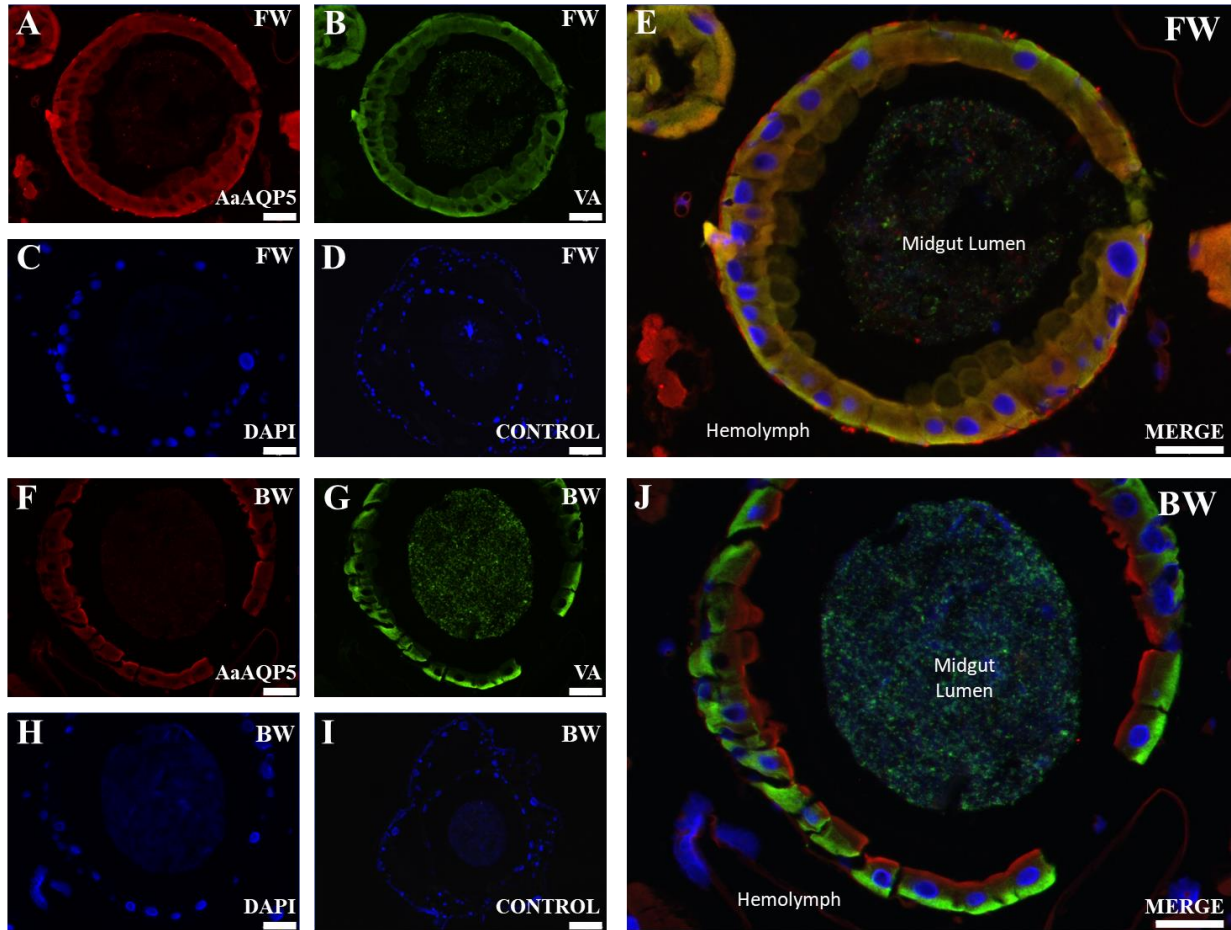


Figure 18: Immunolocalization of AaAQP5 in the anterior midgut of larval *A. aegypti* reared in freshwater (FW) and brackish water (BW) using V-type H^+ -ATPase (VA) as a basolateral membrane marker.

Representative paraffin-embedded cross-sections demonstrate AaAQP5 immunoreactivity (red, A, E, F, and J) and V_0 subunit V-type H^+ -ATPase (green, B, E, G, and J). Merged images of A, B, and C (E) and F, G, and H (J) demonstrate any co-localization in yellow. Blue staining indicates nuclei labeled with DAPI (C-E and H-J). Merged image of control cross-sections of anterior midgut (primary antibodies omitted) (D and I). Scale bars: 50 μ m on all experimental images (A-C, E-H, and J); 100 μ m on all control images (D and I).

3.5.3 Posterior Midgut

AaAQP1, AaAQP4 and VA immunoreactivity was detected in the posterior midgut but not AaAQP5 (Figure 19-21). VA localized to the apical membrane of the posterior midgut epithelial cells as well as intracellularly where it appeared diffuse in both FW and BW reared larvae (Figure 19-21 B, E, G, and J). AaAQP1 demonstrated intracellular immunoreactivity as well as slight localization to the basolateral membrane and partial apical staining at the microvilli of FW posterior midgut epithelial cells which co-localized with VA (Figure 19 A and E). With BW rearing, AaAQP1 intracellular staining increased where it remained diffuse and no staining of the membranes of epithelial cells could be detected (Figure 19 F and J). AaAQP4 immunostaining was localized at the apical and basolateral membrane of the posterior midgut epithelial cells in both FW and BW reared larvae (Figure 20 A, E, F, J). Immunoreactivity of AaAQP5 was negligible in FW and BW reared larval posterior midgut epithelial cells, reflecting what was observed in control preparations where primary antibody was omitted and no AaAQP or VA staining was observed (Figure 21 A, D-F, I, J). DAPI was utilized to visualize nuclei of the posterior midgut (Figures 13-15. C, D, H, I).

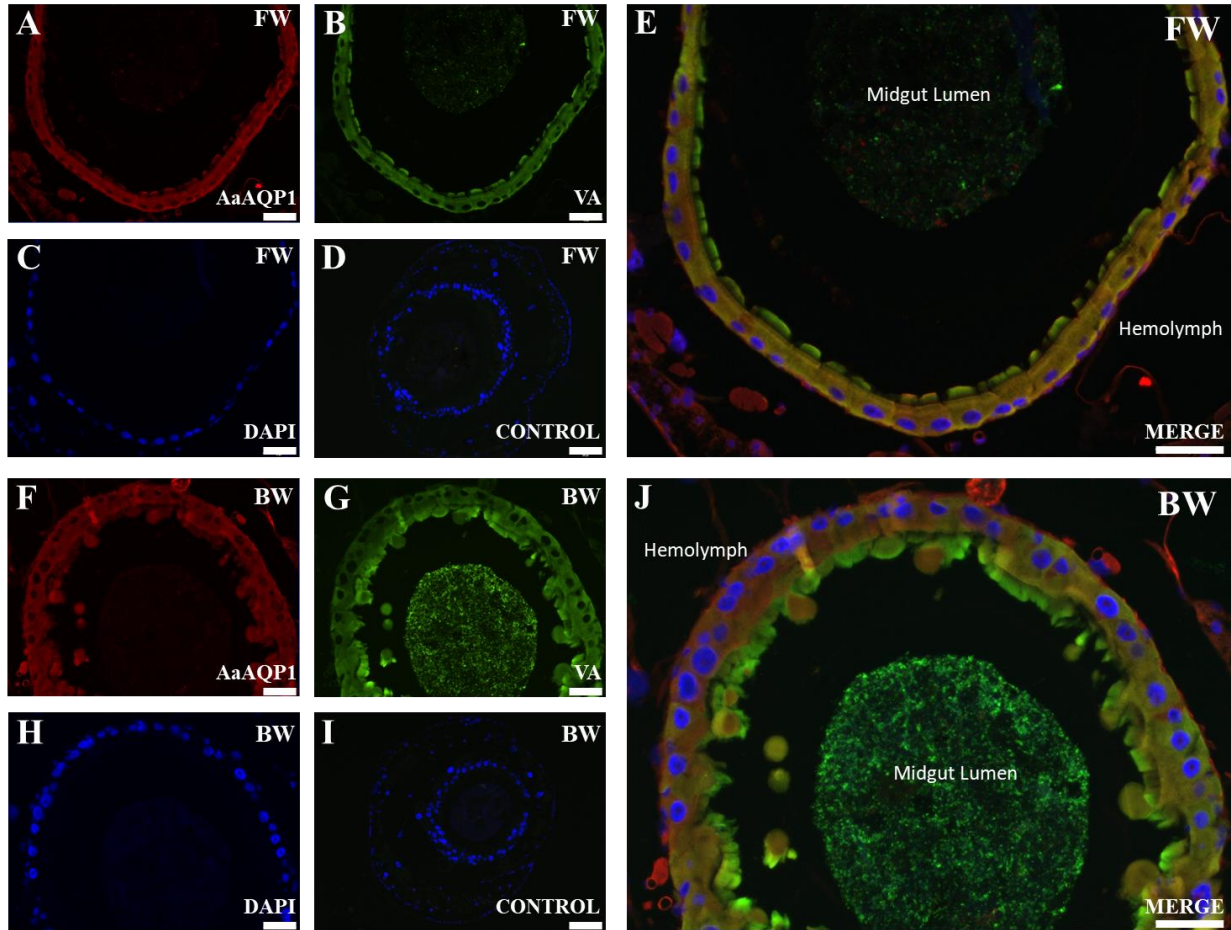


Figure 19: Immunolocalization of AaAQP1 in the posterior midgut of larval *A. aegypti* reared in freshwater (FW) and brackish water (BW) using V-type H⁺-ATPase (VA) as an apical membrane marker.

Representative paraffin-embedded cross-sections demonstrate AaAQP1 immunoreactivity (red, A, E, F, and J) and V₀ subunit V-type H⁺-ATPase (green, B, E, G, and J). Merged images of A, B, and C (E) and F, G, and H (J) demonstrate any co-localization in yellow. Blue staining indicates nuclei labeled with DAPI (C-E and H-J). Merged image of control cross-sections of posterior midgut (primary antibodies omitted) (D and I). Scale bars: 50 μm on all experimental images (A-C, E-H, and J); 100 μm on all control images (D and I).

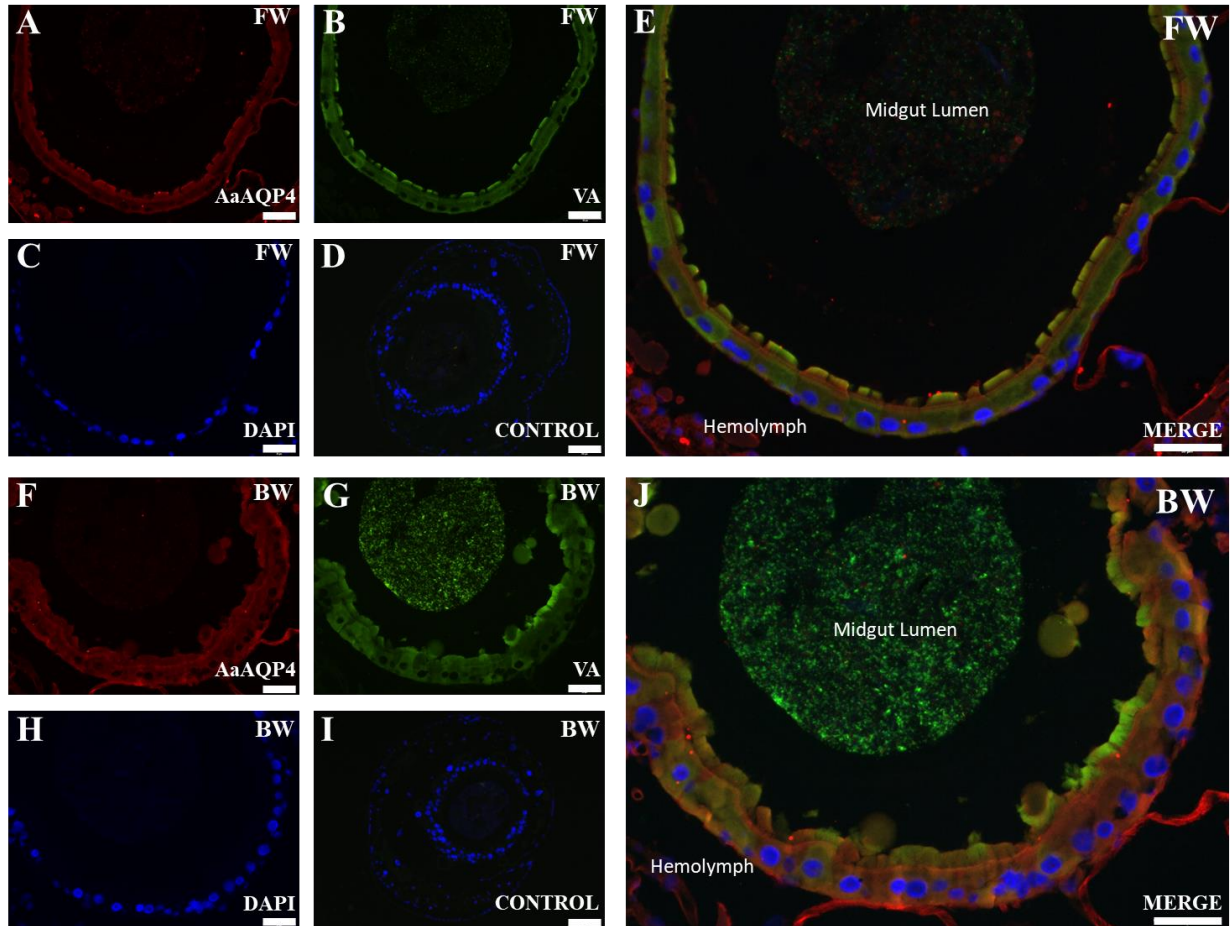


Figure 20: Immunolocalization of AaAQP4 in the posterior midgut of larval *A. aegypti* reared in freshwater (FW) and brackish water (BW) using V-type H^+ -ATPase (VA) as an apical membrane marker.

Representative paraffin-embedded cross-sections demonstrate AaAQP4 immunoreactivity (red, A, E, F, and J) and V_0 subunit V-type H^+ -ATPase (green, B, E, G, and J). Merged images of A, B, and C (E) and F, G, and H (J) demonstrate any co-localization in yellow. Blue staining indicates nuclei labeled with DAPI (C-E and H-J). Merged image of control cross-sections of posterior midgut (primary antibodies omitted) (D and I). Scale bars: 50 μm on all experimental images (A-C, E-H, and J); 100 μm on all control images (D and I).

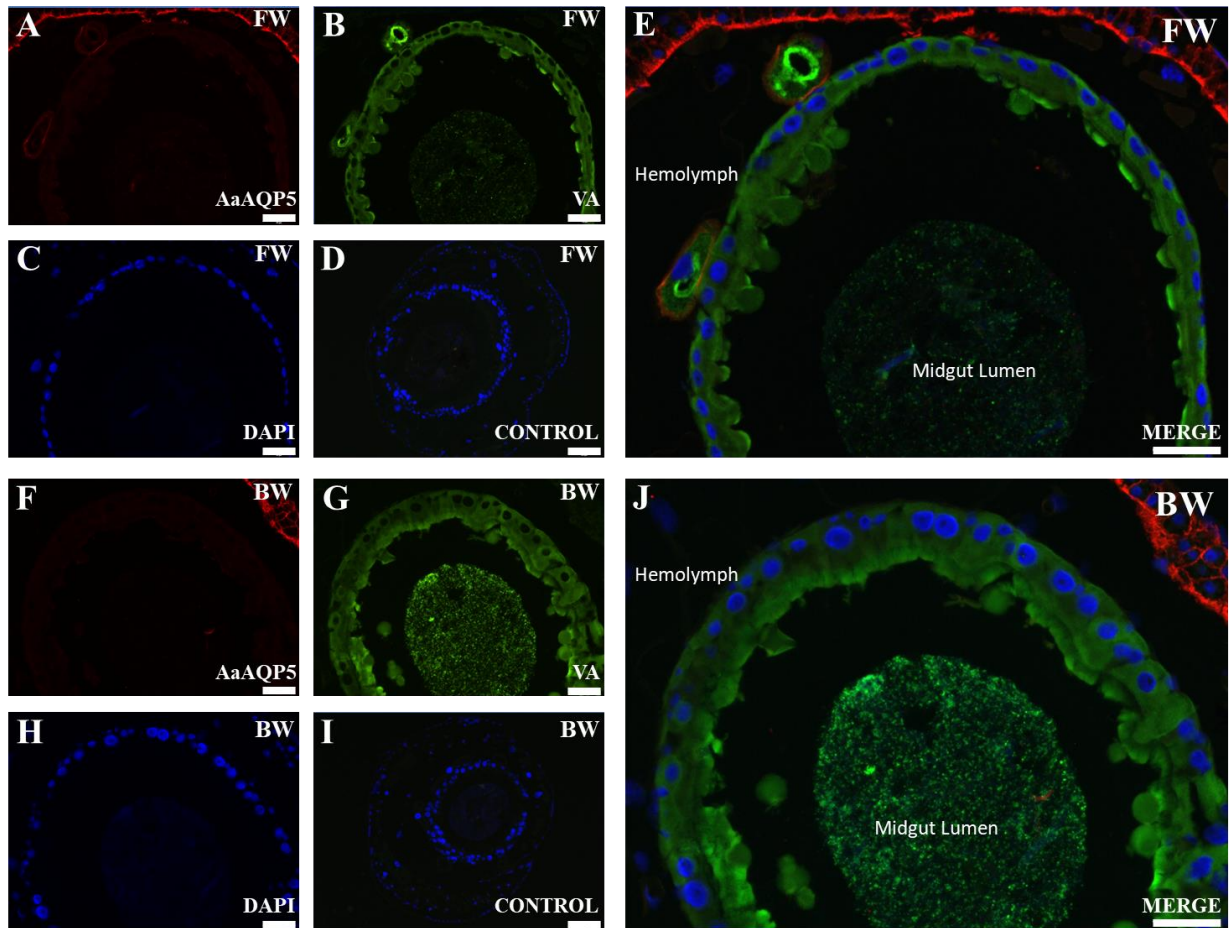


Figure 21: Immunolocalization of AaAQP5 in the posterior midgut of larval *A. aegypti* reared in freshwater (FW) and brackish water (BW) using V-type H^+ -ATPase (VA) as an apical membrane marker.

Representative paraffin-embedded cross-sections demonstrate AaAQP5 immunoreactivity (red, A, E, F, and J) and V_0 subunit V-type H^+ -ATPase (green, B, E, G, and J). Merged images of A, B, and C (E) and F, G, and H (J) demonstrate any co-localization in yellow. Blue staining indicates nuclei labeled with DAPI (C-E and H-J). Merged image of control cross-sections of posterior midgut (primary antibodies omitted) (D and I). Scale bars: 50 μm on all experimental images (A-C, E-H, and J); 100 μm on all control images (D and I).

3.5.4 Hindgut and Malpighian Tubules

AaAQP1, AaAQP4, AaAQP5, and VA immunoreactivity was detected in FW and BW reared larval Malpighian tubules; however only AaAQP4 and VA immunoreactivity was detected in the hindgut (Figure 22-24). VA was apically localized in the HG and the MT epithelial cells (Figure 22-24 B, E, G, and J). AaAQP1 immunoreactivity on the apical membrane of Malpighian tubule principal cells co-localized with VA in both FW and BW reared larvae (Figure 22 A, E-F, J). AaAQP1 was also detected in the stellate cells, where these cells are apparent by the absence of VA immunoreactivity between principal cells and appear red from the AaAQP1 immunoreactivity (arrows, Figure 22 F and J). Specific membrane localization in stellate cells could not be determined due to unavailability of appropriate stellate cell membrane markers at the time of these experiments. Localization of AaAQP4 appeared faintly localized to the apical membrane of Malpighian tubule principal cells in both FW and BW sections (Figure 23 A, E, F, and J). In the hindgut epithelial cells, AaAQP4 staining was intracellular where it appeared diffuse with some apparent staining on the apical and basolateral membranes. The AaAQP4 staining was more intense in FW versus BW (Figure 23 A, E, F, and J). AaAQP5 immunolocalized to the basolateral membrane of Malpighian tubule principal cells of FW and BW reared larvae with less intensity in BW reared larvae (Figure 24. A, E, F, and J). There was no AaAQP or VA immunoreactivity in control slides where primary antibody was omitted (Figure 22-24. D and I). DAPI was utilized to visualize nuclei of the Malpighian tubules and hindgut (Figures 22-24).

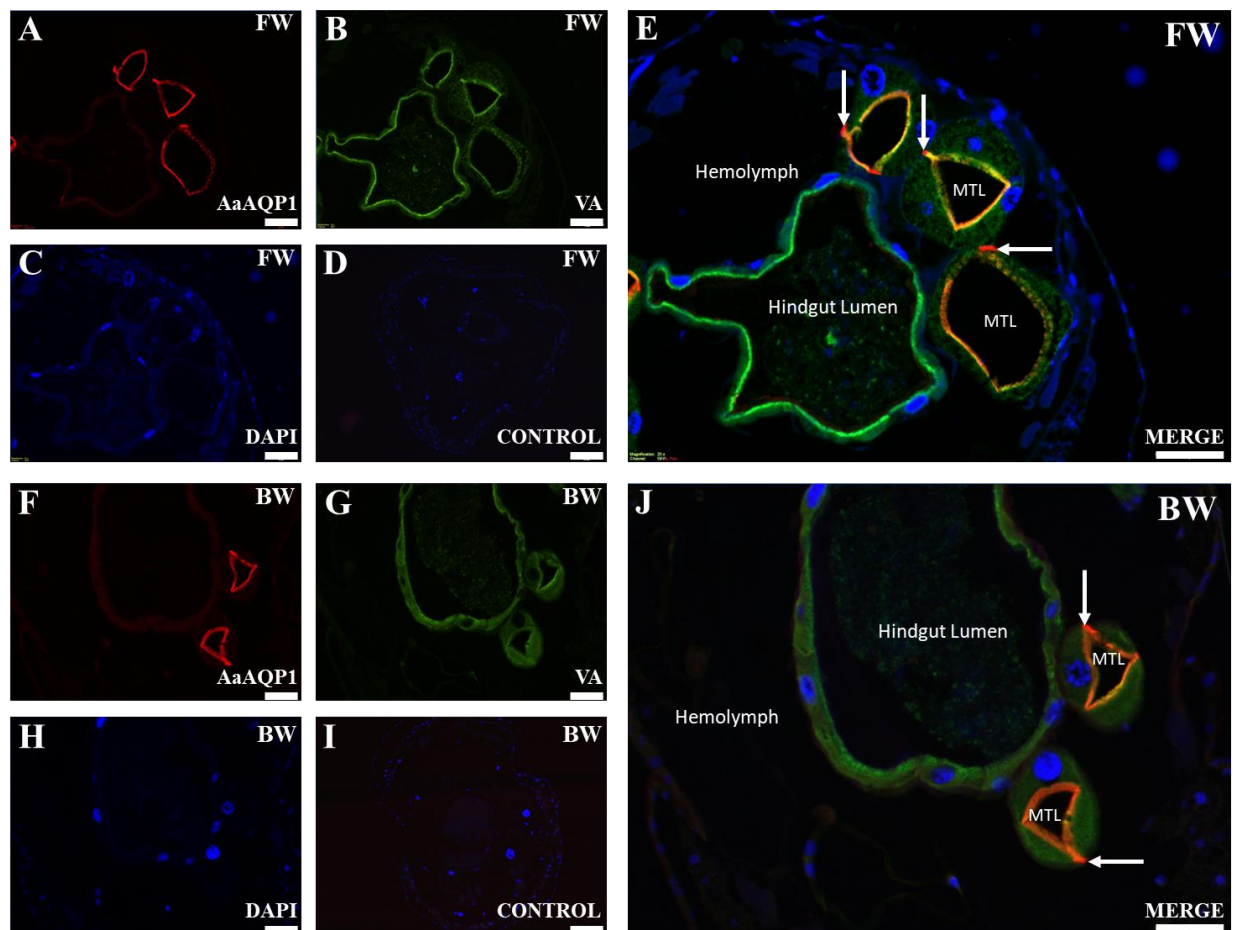


Figure 22: Immunolocalization of AaAQP1 in the Malpighian tubules and hindgut of larval *A. aegypti* reared in freshwater (FW) and brackish water (BW) using V-type H⁺-ATPase (VA) as an apical membrane marker.

Representative paraffin-embedded cross-sections demonstrate AaAQP1 immunoreactivity (red, A, E, F, and J) and V₀ subunit V-type H⁺-ATPase (green, B, E, G, and J). Merged images of A, B, and C (E) and F, G, and H (J) demonstrate any co-localization in yellow. Blue staining indicates nuclei labeled with DAPI (C-E and H-J). Merged image of control cross-sections of Malpighian tubules and hindgut (primary antibodies omitted) (D and I). Arrows point to stellate cells of the Malpighian tubules. Scale bars: 50 μm on all experimental images (A-C, E-H, and J); 100 μm on all control images (D and I). MTL: Malpighian tubule lumen.

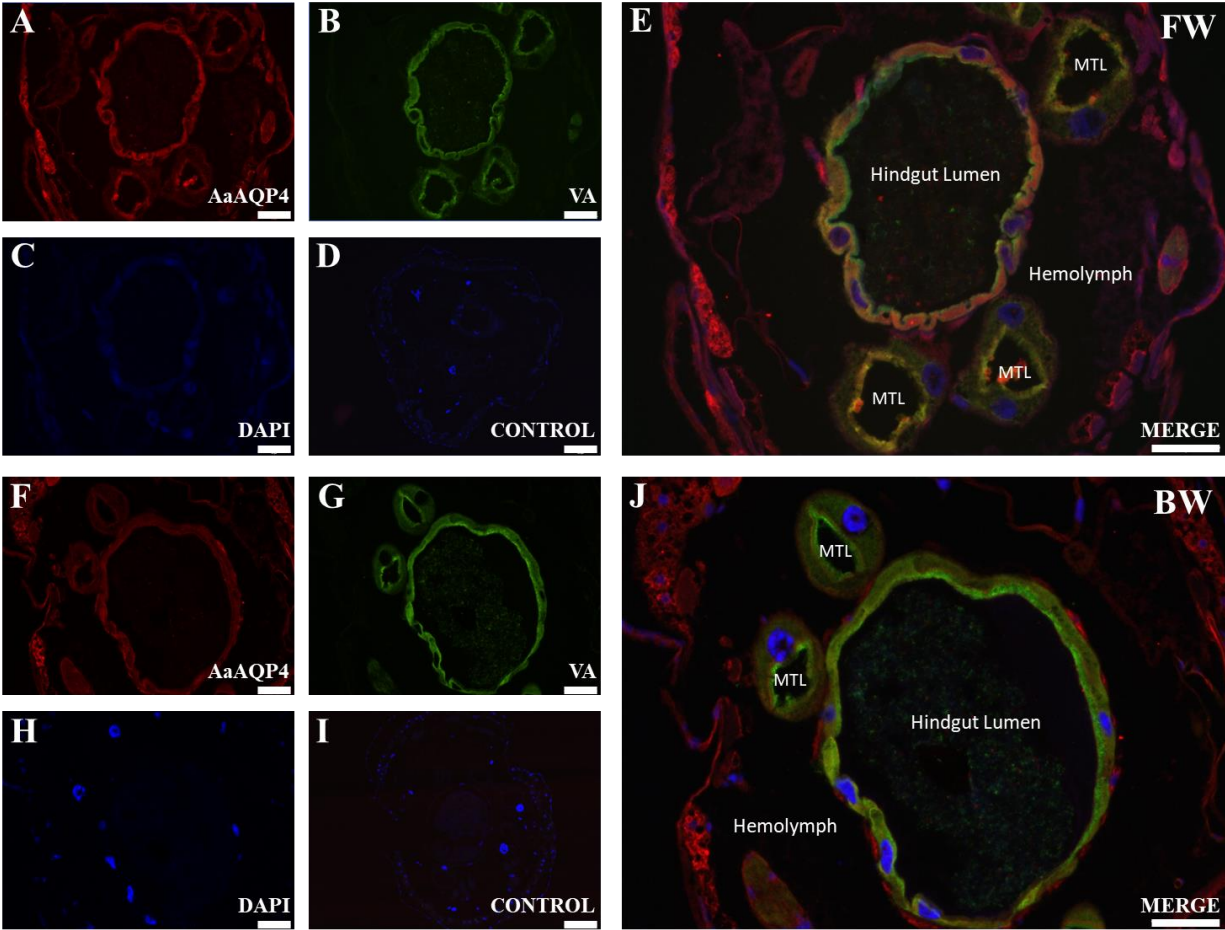


Figure 23: Immunolocalization of AaAQP4 in the Malpighian tubules and hindgut of larval *A. aegypti* reared in freshwater (FW) and brackish water (BW) using V-type H⁺-ATPase (VA) as an apical membrane marker. Representative paraffin-embedded cross-sections demonstrate AaAQP4 immunoreactivity (red, A, E, F, and J) and V₀ subunit V-type H⁺-ATPase (green, B, E, G, and J). Merged images of A, B, and C (E) and F, G, and H (J) demonstrate any co-localization in yellow. Blue staining indicates nuclei labeled with DAPI (C-E and H-J). Merged image of control cross-sections of Malpighian tubules and hindgut (primary antibodies omitted) (D and I). Scale bars: 50 μm on all experimental images (A-C, E-H, and J); 100 μm on all control images (D and I). MTL: Malpighian tubule lumen.

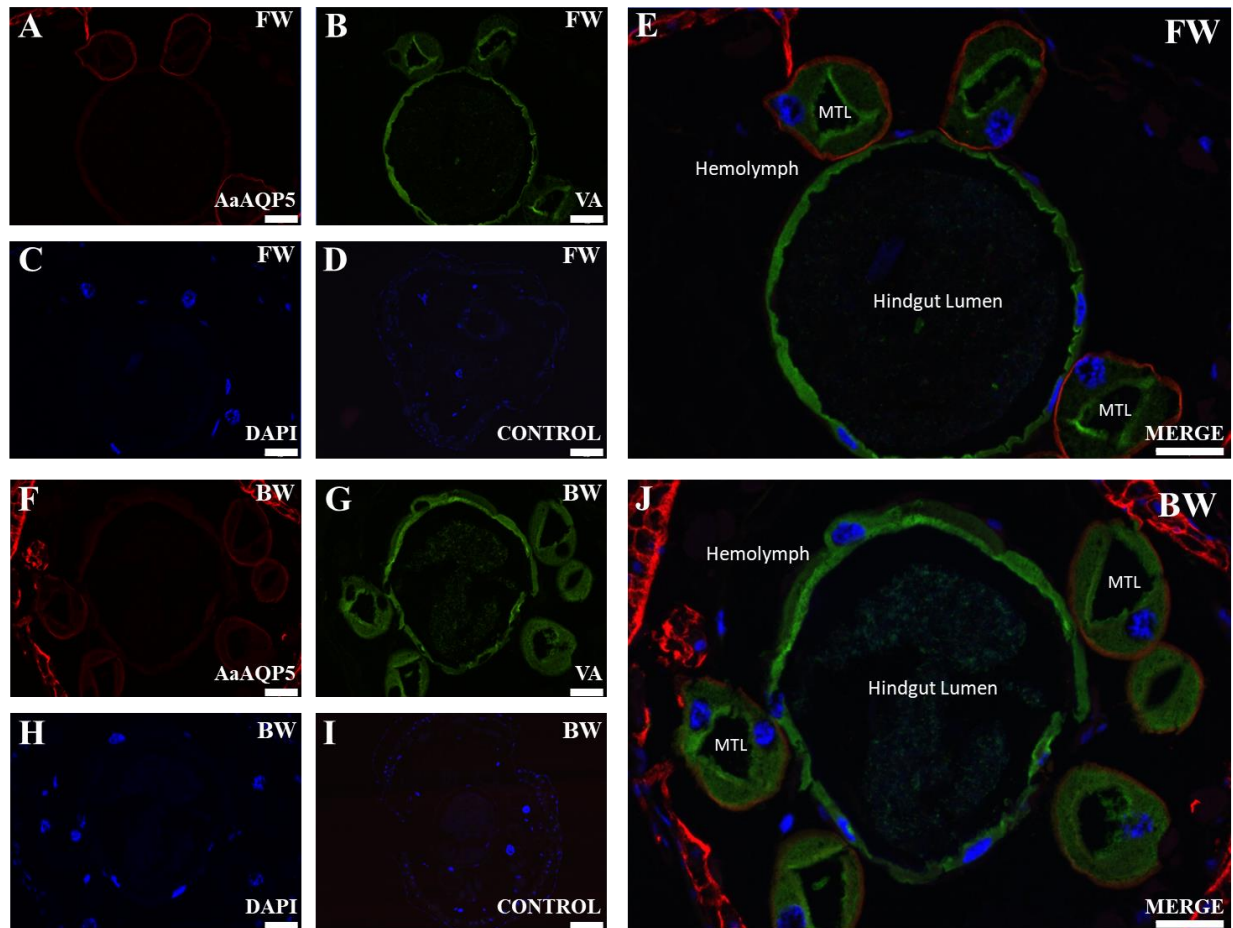


Figure 24: Immunolocalization of AaAQP5 in the Malpighian tubules and hindgut of larval *A. aegypti* reared in freshwater (FW) and brackish water (BW) using V-type H⁺-ATPase (VA) as an apical membrane marker.

Representative paraffin-embedded cross-sections demonstrate AaAQP5 immunoreactivity (red, A, E, F, and J) and V₀ subunit V-type H⁺-ATPase (green, B, E, G, and J). Merged images of A, B, and C (E) and F, G, and H (J) demonstrate any co-localization in yellow. Blue staining indicates nuclei labeled with DAPI (C-E and H-J). Merged image of control cross-sections of Malpighian tubules and hindgut (primary antibodies omitted) (D and I). Scale bars: 50 μm on all experimental images (A-C, E-H, and J); 100 μm on all control images (D and I). MTL: Malpighian tubule lumen.

3.5.5 Anal Papillae

AaAQP1, AaAQP4, AaAQP5 and VA immunoreactivity was detected in the anal papillae of either FW or BW reared larvae. AaAQP staining in the anal papillae was localized to the epithelial membranes and changes with salinity rearing coincided with protein quantification analysis (Figure 25-27). VA was utilized as an apical membrane marker and VA staining displayed no difference between FW and BW reared larvae (Figure 25-27 B, E, G, and J). AaAQP1 immunoreactivity appeared diminished in anal papillae of FW reared larvae compared to BW reared larvae (Figure 25 A, E, F, and J). AaAQP1 appeared to be localized to the apical membrane, but unexpectedly did not appear colocalized with VA (Figure 25 E and J). Consistent with the protein quantification data, AaAQP4 staining was more apparent in FW reared larval anal papillae compared to BW reared larvae (Figure 26 A, E, F, and J). VA staining appeared distinctly apical to the AaAQP4 staining, suggesting that AaAQP4 is located on the basal membrane. There was also additional staining for AaAQP4 in the lumen of the anal papillae (Figure 26 A, E, F, and J). AaAQP5 immunofluorescence was visibly more intense in anal papillae of BW reared larvae when compared to the FW larval samples (Figure 27 A, E, F, and J). AaAQP5 was localized to the basal membrane with slight overlap with VA (Figure 27 E and J). Control slides void of AaAQP and VA primary antibody appeared to possess some immunoreactivity with the secondary antibody incubation (Figure 25-27. D and I). DAPI was utilized to visualize nuclei of the anal papillae however did not appear despite clear indications of nuclei present where membrane was devoid of immunofluorescence with AaAQP and VA incubation (Figures 22-24).

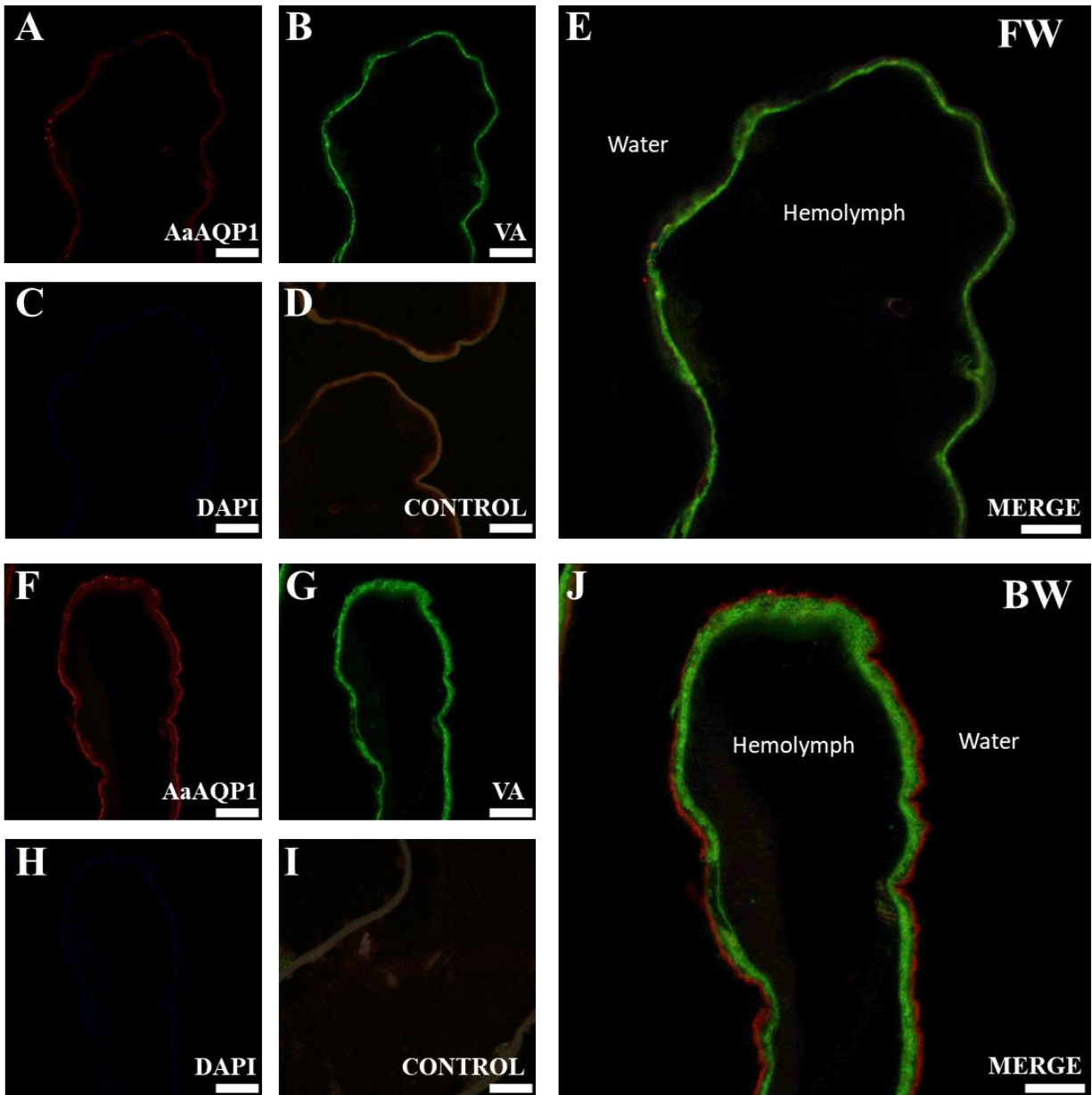


Figure 25: Immunolocalization of AaAQP1 in the anal papillae of larval *A. aegypti* reared in freshwater (FW) and brackish water (BW) using V-type H^+ -ATPase (VA) as an apical membrane marker.

Representative paraffin-embedded cross-sections demonstrate AaAQP1 immunoreactivity (red, A, E, F, and J) and V_0 subunit V-type H^+ -ATPase (green, B, E, G, and J). Merged images of A, B, and C (E) and F, G, and H (J) demonstrate any co-localization in yellow. Blue staining indicates nuclei labeled with DAPI (C-E and H-J). Merged image of control cross-sections of anal papillae (primary antibodies omitted) (D and I). Scale bars: 20 μm on all experimental images (A-C, E-H, and J); 100 μm on all control images (D and I).

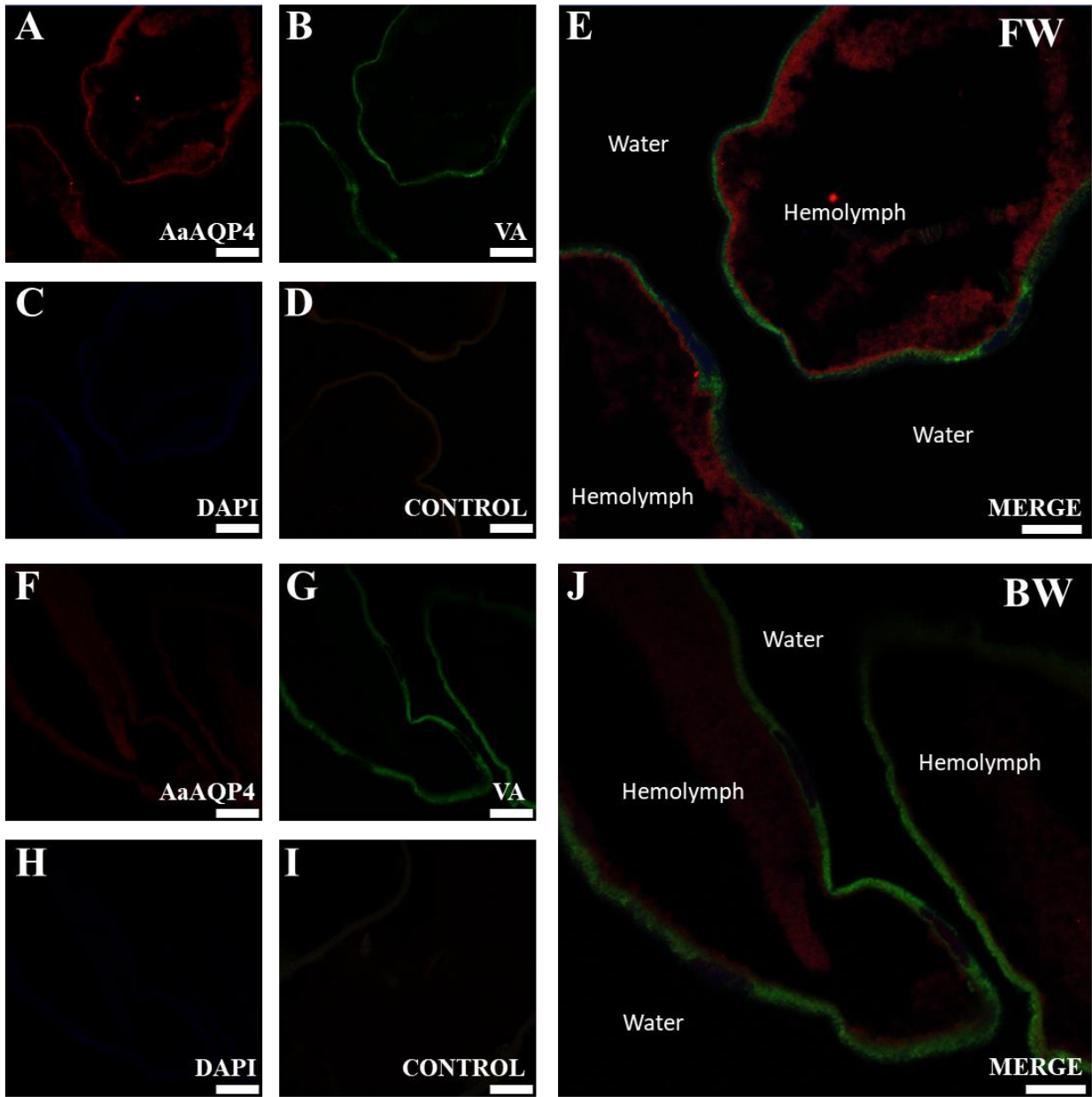


Figure 26: Immunolocalization of AaAQP4 in the anal papillae of larval *A. aegypti* reared in freshwater (FW) and brackish water (BW) using V-type H⁺-ATPase (VA) as an apical membrane marker.

Representative paraffin-embedded cross-sections demonstrate AaAQP4 immunoreactivity (red, A, E, F, and J) and V₀ subunit V-type H⁺-ATPase (green, B, E, G, and J). Merged images of A, B, and C (E) and F, G, and H (J) demonstrate any co-localization in yellow. Blue staining indicates nuclei labeled with DAPI (C-E and H-J). Merged image of control cross-sections of anal papillae (primary antibodies omitted) (D and I). Scale bars: 20 μm on all experimental images (A-C, E-H, and J); 100 μm on all control images (D and I).

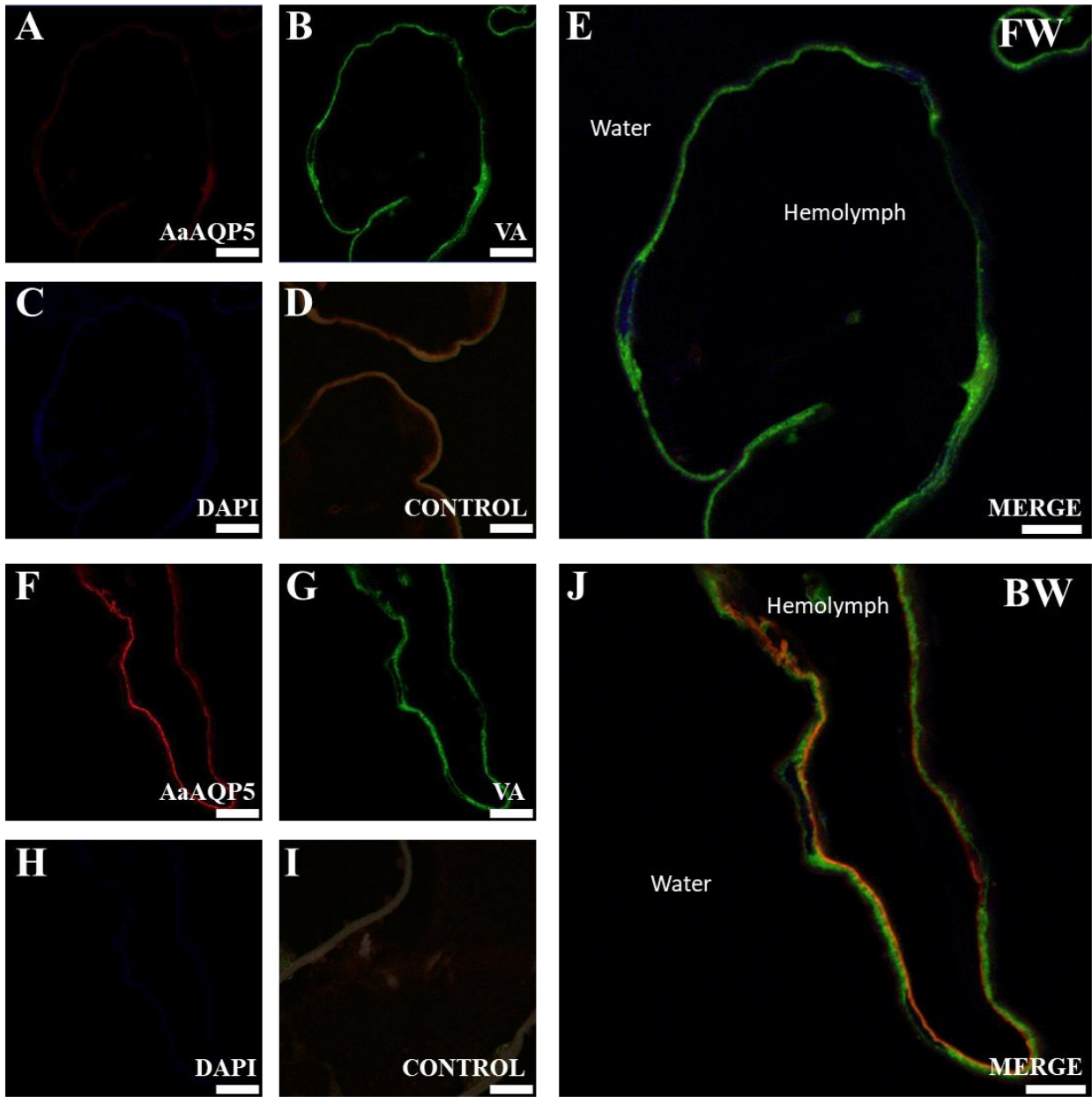


Figure 27: Immunolocalization of AaAQP5 in the anal papillae of larval *A. aegypti* reared in freshwater (FW) and brackish water (BW) using V-type H⁺-ATPase (VA) as an apical membrane marker.

Representative paraffin-embedded cross-sections demonstrate AaAQP5 immunoreactivity (red, A, E, F, and J) and V₀ subunit V-type H⁺-ATPase (green, B, E, G, and J). Merged images of A, B, and C (E) and F, G, and H (J) demonstrate any co-localization in yellow. Blue staining indicates nuclei labeled with DAPI (C-E and H-J). Merged image of control cross-sections of anal papillae (primary antibodies omitted) (D and I). Scale bars: 20 μm on all experimental images (A-C, E-H, and J); 100 μm on all control images (D and I).

4. DISCUSSION

4.1 Overview

This study provides a comprehensive expression profile of *Aedes aegypti* aquaporins AaAQP1, AaAQP4 and AaAQP5 in the osmoregulatory organs of larvae. Furthermore, the transcript expression of the remaining three *A. aegypti* aquaporins (AaAQP2, AaAQP3 and AaAQP6) is also provided. The transcripts of all six AaAQPs were detected in the osmoregulatory organs of larvae therefore the first hypothesis can be accepted. Results show that the transcript abundance of some of the AaAQPs changes when larvae are reared in BW when compared to FW reared larvae; therefore, the second hypothesis can also be accepted. These changes in transcript abundance were organ and AaAQP specific and, in the case of AaAQP1, AaAQP4 and AaAQP5, did not always reflect the observed changes in protein abundance therefore, the third hypothesis must be rejected.

The observed patterns of AaAQP expression in the osmoregulatory organs and, in the case of AaAQP1, AaAQP4 and AaAQP5, the localization of these AaAQPs to epithelial cells and their membranes, strongly indicates that these transporters are of primary importance in mediating water and solute transport in epithelia of larvae. Furthermore, the observed changes in transcript and/or protein abundance of select AaAQPs in select osmoregulatory organs, as well as observed differences in AaAQP cellular localization in epithelia when larvae are reared in BW, strongly suggests that AaAQP regulation is important for osmoregulation in larvae. This is particularly significant since larvae inhabit water with different salinities that impose different osmoregulatory challenges.

4.2 AaAQPs in the Gastric Caeca

The gastric caeca is one of the first osmoregulatory organs that encounters imbibed water therefore, it would be one of the first organs to handle the osmotic pressures that accompany the diverse environmental salinities in which the larvae reside. The gastric caeca of FW and BW reared larvae exhibit similar rates of transepithelial Na^+ and H^+ transport into the lumen at the proximal region which is composed primarily of the digestive cells (D'Silva et al., 2017). This suggests that the digestive cells may carry out nutrient absorption in exchange for ions, which would be readily available in the hemolymph in BW conditions (Boudko, 2012; Boudko et al., 2015; D'Silva et al., 2017). What remains unclear is the direction of water flux, if any, that occurs across the gastric caeca epithelium. The results of this study clearly illustrate the expression and localization of AaAQPs in ion transporting and digestive cells, suggesting that water and solute flux is possible through the transcellular pathways. In FW it has been postulated that the osmotic gradient across the gastric caeca favours the absorption of water from the lumen into the hemolymph because the imbibed water is clearly hypoosmotic to the hemolymph (D'Silva et al., 2017). However, as indicated above, there is secretion of ions into the lumen of the gastric caeca in FW and BW reared *A. aegypti* larvae, therefore it has alternatively been postulated water may be secreted into the lumen if this ion secretion is sufficient to establish an inward directed electroosmotic flow (D'Silva and O'Donnell, 2018). In BW of up to 30% seawater it may be assumed that the imbibed water is isosmotic to the hemolymph which suggests there would be no net flux of water across the gastric caeca; however the ionic concentration of intralumenal Na^+ , K^+ , and H^+ are actually lower than the 30% seawater rearing medium, therefore it was proposed that the osmotic gradient may be similar to that of FW reared larvae where absorption of water into the hemolymph is favoured. If this is the case, then this

may explain the lack of differences in AaAQP transcript abundance in the gastric caeca of FW and BW reared larvae, since this would suggest that the direction of water fluxes is unchanged between the salinity treatments. On the other hand, secretion of digestive enzymes into the gastric caeca lumen may contribute to luminal osmolarity to a greater extent than the ion contribution, therefore potentially eliminating the osmotic gradient between the lumen and the hemolymph in both FW and BW treatments (D'Silva et al., 2017; Dadd, 1975; Volkmann and Peters, 1989b). Enzyme secretion has been demonstrated in the gastric caeca of the fly, *Rhynchosciara americana*, which suggests that *A. aegypti* larvae may also have the capability for enzymatic secretion by the digestive cells that contribute to osmolarity of the gastric caecal content (Terra et al., 1979). Given the possible scenarios for the osmotic gradient across the gastric caeca epithelium, the movement of water and the role of AaAQP expression can only be speculated at this time since water movement is passive and predominantly dependent on the osmotic gradient. What is clear is that AaAQPs are expressed in the gastric caecal cells where they can mediate water and solute transport.

4.2.1 Transcript Abundance

Of the AaAQPs that are expressed by gastric caeca cells, AaAQP5 transcript abundance is the highest compared to other AaAQPs regardless of whether larvae are reared in FW or BW. This suggests that AaAQP5 is the major contributor to transcellular water transport in the gastric caeca although this assumption is based solely on transcript levels at this stage (Drake et al., 2015; Misyura et al., 2017). The results of this study are consistent with previous work that showed that AaAQP5 transcript abundance tended to be highest compared to other AaAQPs albeit this difference was not statistically significant (Marusalin et al., 2012). A notable difference between the current study and the study conducted by Marusalin et al. (2012) was the

distilled water (Na^+ : $2 \mu\text{molL}^{-1}$ and Cl^- : $4 \mu\text{molL}^{-1}$) rearing conditions as opposed to the dechlorinated tap water rearing conditions (Na^+ : $800 \mu\text{molL}^{-1}$ and Cl^- : $705 \mu\text{molL}^{-1}$) in the current study which may have influenced the changes in transcript abundances observed; however based on the trends observed in the current study, there may be other factors that contribute to the discrepancy. AaAQP1 and AaAQP2 transcript abundance was the next highest observed in the gastric caeca, which are predicted to play a similar role in water transport across the gastric caeca epithelium given the high water conductance of AaAQP1 and AaAQP2. However, little is known about AaAQP2 protein expression or localization in the gastric caeca therefore its water transport function can only be inferred and the potential role of AaAQP1 based on protein expression and localization is discussed below (Drake et al., 2015). AaAQP4 transcript abundance in the gastric caeca is predicted to mediate solute transport and is discussed below. AaAQP3 transcript abundance in the gastric caeca was comparable to AaAQP1 and AaAQP2 abundance. Since this aquaporin is related to a *D. melanogaster* aquaporin BIB that does not transport water, but is rather involved in cellular adhesion, it is likely that AaAQP3 plays a similar role to maintain epithelial integrity and polarity in larval gastric caeca (Campbell et al., 2008; Drake et al., 2010; Drake et al., 2015; Marusalin et al., 2012; Tatsumi et al., 2009; Yanochko and Yool, 2004). AaAQP6 transcript abundance in the gastric caeca was low suggesting that it may not play an important role in water or solute transport in the gastric caeca. Finally, when considering AaAQP transcript abundance in the osmoregulatory organs, the gastric caeca generally showed low levels of AaAQP transcript abundance and therefore relative to other organs, water flux may not be as prominent at this organ as in other organs that are mainly involved in osmoregulation.

4.2.2 Protein Expression

The availability of custom antibodies against AaAQP1, AaAQP4 and AaAQP5 allowed for the analysis of protein expression for these three AaAQPs in the osmoregulatory organs. Western blot analysis of gastric caeca protein homogenates probed with these custom antibodies revealed AaAQP monomers and also putative oligomerization of AaAQPs. In the gastric caeca, AaAQP5 resolved at ~30 kDa which is the predicted molecular mass of the AaAQP5 monomer and was blocked with preincubation of AaAQP5 antibody with the immunogenic peptide. The bands observed at ~60 kDa, ~58 kDa, and ~60 kDa for AaAQP1, AaAQP4, and AaAQP5 respectively, were similar to the predicted mass of the putative dimers. AQPs aggregate into tetramers in cell membranes, therefore the observed putative dimers may possess sustained intrinsic multimerization interactions despite chemical and heat induced protein denaturation for western blotting as was previously shown with other membrane proteins (Chasiotis et al., 2016; Durant and Donini, 2018; Jonusaite et al., 2017a; Jonusaite et al., 2017b; Mahmood and Yang, 2012; Misyura et al., 2017; Smith and Agre, 1991). Despite the predicted dogma of transcript abundance reflecting protein abundance in accordance with consistent translation rate, this was not observed in the present study. AaAQP1 transcript abundance was unaltered in response to BW rearing in contrast to the elevated AaAQP1 protein abundance in the gastric caeca of BW reared larvae. Protein and mRNA degradation rates could be asynchronous and therefore the abundance patterns for transcript and protein may not be equivalent. For example, in BW reared larvae the AaAQP1 protein may not be catabolised as quickly as it may be in FW gastric caeca while the rate of mRNA translation remains consistent, leading to the observed discrepancy between transcript and protein abundances. AaAQP1 was shown to be specific for water transport and therefore the results suggest that water flux may be increased across the GC cells in

BW conditions (D'Silva and O'Donnell, 2018; D'Silva et al., 2017; Drake et al., 2015; Marusalin et al., 2012). Furthermore, changes in AaAQP1 localization from primarily intracellular to both apical and basolateral membranes in the gastric caeca cells with BW treatment supports this notion (Figure 28). The mechanism behind this apparent translocation of AaAQP1 to the membrane is not known but perhaps is regulated hormonally as observed with mammalian AQP2 via vasopressin (Brown et al., 2008; Kwon et al., 2013; Nielsen et al., 1995; Sabolić et al., 1995). AaAQP1 mass did not change between FW and BW reared larvae supporting the possibility of regulation through phosphorylation which would have negligible mass modifications on a western blot and would only be detectable using phosphorylation-specific antibodies (Bonenfant et al., 2003; Dephoure et al., 2013; Mandell, 2003).

AaAQP5 is expressed on the basolateral membrane of the gastric caeca cells. Here AaAQP5 may function in mediating water exchange between the cell and hemolymph. AgAQP1A and AgAQP1B splice variants were identified in the mosquito, *Anopheles gambiae* gastric caeca at the basolateral membrane, similarly to AaAQP5 localization in the *A. aegypti* gastric caeca (Tsujimoto et al., 2013). Because of the high water permeability of AgAQP1A and AgAQP1B it was speculated that their function includes water transport across the gastric caeca epithelium similar to the predicted function of AaAQP5. On the other hand, AaAQP5 is a competent trehalose transporter and its expression on the basolateral membrane may function to permit trehalose, the major sugar in insect hemolymph, to enter the gastric caecal cells to sustain metabolic activity of the cells (Elbein et al., 2003; Liu et al., 2013).

Although the AaAQP4 immunoreactivity appears to be diminished in the gastric caeca of BW reared larvae, the protein abundance was no different between FW and BW treatment in western blotting studies. AaAQP4 has a high affinity for solutes like glycerol and very low

affinity for water (Drake et al., 2015). This discrepancy could be a result of sectioning through regions of the gastric caeca with diminished AaAQP4 expression. Osmolytes such as glycerol in the hemolymph may be elevated in animals reared in higher salinity. For example the osmoconforming species of mosquitoes, *Culex tarsalis*, elevate hemolymph osmolarity by increasing proline and trehalose concentration in response to high external salinity as a way to mitigate the osmotic gradient between the external medium and the hemolymph (Patrick and Bradley, 2000). Therefore, if there is a decrease in AaAQP4 protein expression as suggested by the immunohistochemistry results, this may indicate a response to limit loss of accumulating osmolytes in the hemolymph to the lumen of the gastric caeca, provided the solute gradient favours luminal fluxes (D'Silva and O'Donnell, 2018; D'Silva et al., 2017). Since AaAQP4 is an entomoglyceroporin responsible for the transport of solutes such as trehalose and glycerol, it would be beneficial for *A. aegypti* larvae to mitigate osmolyte loss by downregulating AaAQP4 in the gastric caeca in BW conditions, though this was not confirmed based on protein quantification analysis.

4.2.3 What AaAQP Expression May Indicate About Gastric Caeca Functions

Rearing of larvae in 10-30% seawater alters the morphology and function of the gastric caeca (D'Silva and O'Donnell, 2018; D'Silva et al., 2017; Volkmann and Peters, 1989b; Volkmann and Peters, 1989a). First, the regionalization of ion transporting cells at the distal third of the gastric caeca of FW reared larvae is lost with 30% seawater rearing (D'Silva et al., 2017). Second, the number of mitochondria and the length of the apical microvilli in the digestive and ion transporting cells are both reduced with BW rearing and these changes are concomitant with reduced V-type H⁺ ATPase activity and decreased transepithelial H⁺ transport (D'Silva et al., 2017; Volkmann and Peters, 1989a). Furthermore, V-type H⁺ ATPase also appeared to localize

at both membranes in FW reared larvae, however became apically localized in response to BW rearing which may contribute to the diminished H^+ transport into the lumen under BW conditions. Activity of Na^+/K^+ ATPase is also diminished which may contribute to the overall decreased rate of transepithelial movement of Na^+ and K^+ (D'Silva et al., 2017). The persistence of Na^+ and H^+ secretion at the proximal gastric caeca with BW rearing implicates ion secretion in digestion rather than osmoregulation and this is further supported by the increased AaAQP1 expression which is possibly allowing for passive water movement to enable digestion, nutrient diffusion, and mechanical gut content mixing (D'Silva et al., 2017). Interestingly, the pH of the gastric caeca lumen remains consistent between FW and BW reared larvae despite the decreased magnitude of H^+ secretion and this may be a mechanism to maintain AaAQP function by precluding possible AaAQP morphological changes upon exposure to different pH as shown in the killifish, *Fundulus heteroclitus* AQP0 (Virkki et al., 2001).

To conclude on the observations of AaAQP expression in the gastric caeca, AaAQP1 is most likely to mediate water flux across the gastric caeca, AaAQP4 is likely to mediate osmolyte fluxes across the gastric caeca and finally, AaAQP5 is most likely to mediate the uptake of trehalose by gastric caecal cells in order to sustain their metabolic activity. Furthermore, based on the increased expression of AaAQP1 in gastric caeca of BW reared larvae, it is proposed that in BW the gastric caeca are more permeable to water which may aid with digestion or serve to dilute the luminal contents of the gastric caeca. The gastric caeca epithelial transport model is presented with additional findings from this study in Figure 28.

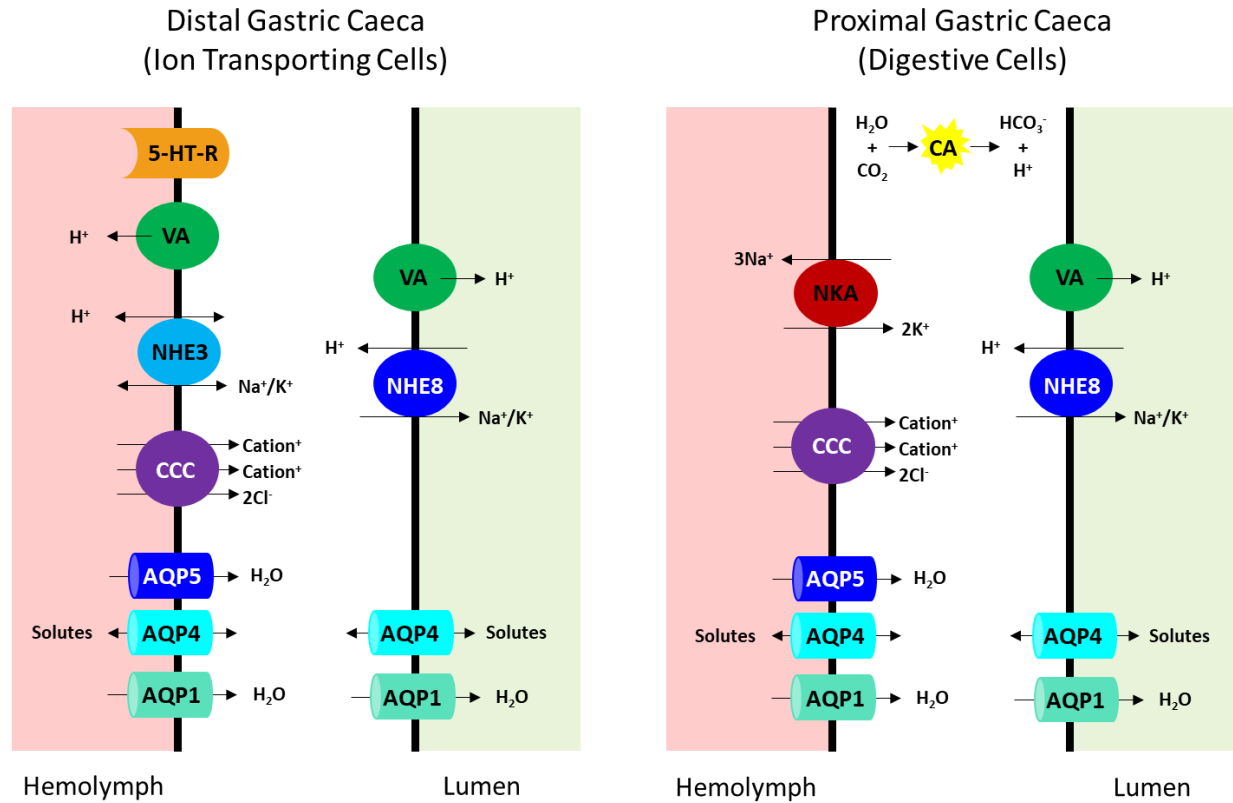


Figure 28: Updated schematic diagram illustrating membrane transport proteins in the distal and proximal gastric caeca of larval *Aedes aegypti*. 5-HT-R: 5-hydroxytryptamine receptor, VA: V-type H^+ ATPase, NHE: Na^+/H^+ exchanger, CCC: cation-chloride cotransporters, CA: carbonic anhydrase, NKA: Na^+/K^+ ATPase. AQP1: *Aedes aegypti* aquaporin 1, AQP4: *Aedes aegypti* aquaporin 4, and AQP5: *Aedes aegypti* aquaporin 5. Modified from D'Silva and O'Donnell (2018) and D'Silva et. al (2017).

4.3 AaAQPs in the Anterior Midgut.

4.3.1 Transcript Abundance

The anterior midgut functions in digestion and possibly nutrient and ion absorption, processes which require water. The osmotic gradient across the anterior midgut epithelium is predicted to be dependent on the external rearing medium due to the relatively passive conveyance of imbibed water and nutrients, in addition to the compartmentalization of the gastric caeca allowing for isolated luminal environments between these two organs. In this respect, in FW the osmotic gradient should favour water absorption into the hemolymph whereas in BW

there may be a negligible osmotic gradient across the epithelium. Transport of ions, solutes, and amino acids across the anterior midgut epithelium has been proposed; however, apically localized transporters have yet to be identified (Figure 29) (Bradley, 1987; Clark et al., 1999). In comparison to other osmoregulatory organs, the overall abundance of AaAQP mRNA is low suggesting that epithelial permeability is diminished perhaps to attenuate the passive absorption of water, particularly in FW environments where the gradient favours absorption of water into the hemolymph. Similar to the gastric caeca, AaAQP5 transcript was high relative to transcripts of other AaAQPs suggesting, at least based on mRNA abundance, that it plays a predominant role in transcellular water and perhaps trehalose flux across the anterior midgut epithelium (Drake et al., 2015; Misyura et al., 2017). AaAQP1 (a DRIP homologue), AaAQP4, and AaAQP6 demonstrated low mRNA abundances in the anterior midgut supporting the prediction that overall transcellular water transport is predominantly mediated by AaAQP5 but may also perhaps occur through AaAQP2 (a PRIP homologue) which shows considerable transcript abundance in the anterior midgut. A previous study reported the highest transcript abundance of AaAQP4 and AaAQP1 in the midgut of larval *A. aegypti* (Marusalin et al., 2012). The discrepancy between the previous study and the current study may be due to further subdivision of the midgut into the anterior and posterior regions in the current study that was not performed previously (Marusalin et al., 2012). Additionally, different water rearing conditions could have also driven the differences in AaAQP abundance as described in the previous section (Section 4.2.1). In the Antarctic midge, *Belgica antarctica*, AQP2 and DRIP-AQP (homologues to AaAQP1) have been identified in the midgut and shown to mediate water transport along the midgut epithelium in terrestrial insects where water absorption is necessary for survival. Since AQP2 and DRIP-AQP elevate water absorption with their expression in the midgut epithelium, it

would be expected that downregulating expression would mitigate water absorption into the hemolymph (Yi et al., 2011). Since DRIP-AQP of *B. antarctica* is a homolog of AaAQP1, it may be postulated that DRIP-AQP and AaAQP1 mediate comparable functions in these two organisms. Therefore, the low AaAQP1 transcript abundance in *A. aegypti* anterior midgut may be indicative of diminished water absorption. In adult female mosquitoes, AaAQP transcript abundance changed in response to blood feeding, indicating that in adult mosquitoes AaAQPs play a role in digestion through blood meal dehydration and osmoregulation (Drake et al., 2010; Drake et al., 2015). BW treatment demonstrated a trend towards elevated AaAQP6 transcript abundance, perhaps acting in a similar manner by increasing water absorption into the hemolymph across the anterior midgut, though more studies need to be performed to elucidate substrate conductance of AaAQP6. The anterior midgut also displays relatively high AaAQP3 mRNA abundance in BW environmental conditions, proposing it plays a role in increasing cellular adhesion in an attempt to modulate paracellular epithelial integrity as observed with septate junction proteins (Jonusaite et al., 2017a; Jonusaite et al., 2017b).

4.3.2 Protein Expression and Localization

Western blots of anterior midgut protein homogenates that were probed with AaAQP1 antibody resulted in bands at ~30 kDa, ~32 kDa, ~34 kDa, and ~65 kDa. The predicted mass of the AaAQP1 monomer is 26.2 kDa which is lighter than the bands observed. AQPs can undergo post-translational modification which includes glycosylation and may have contributed to the higher mass of the AaAQP1 bands observed (Brown et al., 2008; Hendriks et al., 2004; Kwon et al., 2013; Öberg et al., 2011; van Balkom et al., 2002). Several invertebrate AQPs have been shown to possess glycosylation sites for example, *Rhodnius prolixus*, *Caenorhabditis elegans*, and specifically AaAQP1, AaAQP3, AaAQP4, and AaAQP6 of *Aedes aegypti* (Figure 30)

(Tomkowiak and Pienkowska, 2010). The degree of glycosylation and possible additional phosphorylation may account for the putative AaAQP1 bands observed at ~30 kDa, ~32 kDa, and ~34 kDa. Since preincubation of the AaAQP1 antibody with its respective immunization peptide was inconclusive, specificity could not be concluded with confidence. The band at ~65 kDa could be a dimer of AaAQP1 with some degree of glycosylation. Alternatively, perhaps the band at ~65 kDa was a heterodimer with another AaAQP homologue expressed in the anterior midgut.

Western blots of anterior midgut protein homogenates probed with AaAQP4 antibody resolved in a double band at ~57 kDa and ~58 kDa which could be a heterodimer of AaAQP4 with another AaAQP such as AaAQP1 or AaAQP5, or an AaAQP4 monomer with a relatively high degree of post-translational modifications (Table 1). Both bands were successfully blocked by preincubation of the AaAQP4 antibody with immunogenic peptide suggesting that these bands are indeed AaAQP4 in the anterior midgut homogenates.

Anterior midgut protein homogenates showed ~26 kDa, ~28 kDa, and ~63 kDa bands on western blots probed with AaAQP5 antibody. These bands were assumed to be AaAQP5 protein despite the fact that peptide blocks for this antibody on anterior midgut homogenates were inconclusive due to a high degree of protein-peptide-antibody interactions between non-specific proteins and the immunogenic peptide. The ~26 kDa band corresponds with the predicted mass of the AaAQP5 monomer and the ~28 kDa band may represent a monomer with post-translational modifications. The band at ~63 kDa is suspected to be either a homodimer or a heterodimer of AaAQP5 and another AaAQP with post-translational modifications (Table 1). The protein abundances of AaAQP1, AaAQP4, and AaAQP5 in the anterior midgut were the same in FW and BW reared larvae. This suggests that transcellular water and select solute

permeability across the anterior midgut of larvae is consistent in FW and BW despite variations in osmotic gradients encountered by this organ.

Immunolocalization of AaAQP1, AaAQP4, and AaAQP5 changed with BW rearing in the anterior midgut. Unaltered protein abundance with changes in localization of AaAQP1, AaAQP4, and AaAQP5 may suggest that these AaAQPs are regulated through membrane trafficking rather than changes in expression and, if so, this might be achieved through hormonally stimulated pathways (Campbell et al., 2008; Kwon et al., 2013). AaAQP1, AaAQP4 and AaAQP5 were localized to the apical and basolateral membranes of epithelial cells of the FW anterior midgut where they can mediate the passive absorption of water and solutes across the midgut. In BW AaAQP1 and AaAQP4 were predominantly intracellular, indicating that membrane permeability to water and select solutes (examples: glycerol, trehalose) through these AaAQPs is likely to be decreased, though it should be stated that AaAQP proteins that were not assessed at the protein level in this study may also contribute to water and solute permeability. In this case, AaAQP2 requires further study at the protein level because the anterior midgut has considerable levels of AaAQP2 mRNA. AaAQP5 was localized to both the apical and basolateral membranes of anterior midgut epithelial cells in FW larvae but became predominantly apical in BW larvae (Figure 29). Vesicular AQP8 stimulation with Bt2cAMP resulted in the translocation of vesicular AQP8 into the plasma membrane, increasing membrane water permeability (García et al., 2001). A similar mechanism utilized by *A. aegypti* may be possible, where modulation of membrane permeability is facilitated by translocation of intracellularly stored AaAQP5. The translocation of AaAQP5 to the apical membrane may suggest that exchange of water between the anterior midgut lumen and the epithelial cells is of particular importance when larvae are inhabiting BW. Apically localized AQP1 in the Japanese

eel, *Anguilla japonica*, allows for the absorption of water from the intestinal lumen into the intestinal epithelial cells, where the intestine demonstrated elevated water absorption in eels reared in seawater environments (Aoki et al., 2003). This is thought to be a mechanism for coping with osmotic loss of water to the environment by increasing the uptake of water at the intestine (Aoki et al., 2003). AaAQP5 translocation to the apical membrane of anterior midgut in BW reared larvae may serve a similar purpose.

Apart from water, both AaAQP4 and AaAQP5 are entomoglyceroporins that transport solutes like trehalose and glycerol. In particular, AaAQP4 has enhanced glycerol transport capabilities, despite the absence of the typical cysteine residue that permit other AQPs to transport glycerol (Drake et al., 2015). The glycosylation of human AQP10 increases the pore affinity to glycerol and thus AaAQP4 glycosylation may be a mechanism to regulate glycerol transport through this transporter without the glycerol specific cysteine residue (Öberg et al., 2011). Based on the band patterns shown in the western blots in this study (see section 3.4.2) and the predicted glycosylation sites on AaAQP4 (Figure 30 D), it is predicted that glycosylation contributes to AaAQP4's glycerol specific transport conformation demonstrated by Drake *et al.* (2015).

The highly alkaline environment of the anterior midgut could alter the function of AaAQPs (Fischer and Kaldenhoff, 2008; Nemeth-Cahalan et al., 2004; Németh-Cahalan and Hall, 2000). There is evidence that the histidine amino acid in loops A and C of AQPs is pH sensitive responding by increasing or decreasing AQP permeability in response to varying extracellular pH (Nemeth-Cahalan et al., 2004). Bovine and killifish AQP0 are functionally affected by the extracellular pH, specifically modulating permeability through pH dependent histidines in loops A and C (Nemeth-Cahalan et al., 2004). Killifish AQP0 loop A histidine conferred higher permeability to water in alkaline environments (Nemeth-Cahalan et al., 2004). Based on putative AaAQP protein folding analysis, AaAQP2, AaAQP3, AaAQP4, AaAQP5, and

AaAQP6 possess histidine residues on extracellularly exposed loops A or C and therefore, possess the potential for pH regulation through the histidine residues (Figure 30). Specifically, AaAQP4 and AaAQP5 are localized to the apical membrane where loops A and C would be in direct contact with the alkaline environments. However, at this point it is difficult to predict whether the high alkaline environment of the anterior midgut lumen would increase or decrease AaAQP permeability, therefore further studies are required to elucidate pH response in these AaAQPs.

To conclude on the AaAQP expression in the anterior midgut, AaAQP1, AaAQP4 and AaAQP5 were localized to both the apical and basolateral membranes of epithelial cells in FW reared larvae where water and solute absorption through these aquaporins is likely to occur. The results provide compelling evidence that AaAQP regulation at the anterior midgut is accomplished by shuttling AaAQP proteins between the cytosol and the plasma membranes of the epithelial cells rather than altering expression. This may permit for quick alterations in water and solute permeability as conditions dictate. In BW the majority of AaAQP1 and AaAQP4 are apparently removed from the plasma membrane and sequestered in the cytosol while AaAQP5 congregates on the apical side of the epithelial cells. Together this suggests that overall permeability to water and solutes like glycerol and trehalose may be diminished in BW conditions but that water flux across the apical membrane may be enhanced.

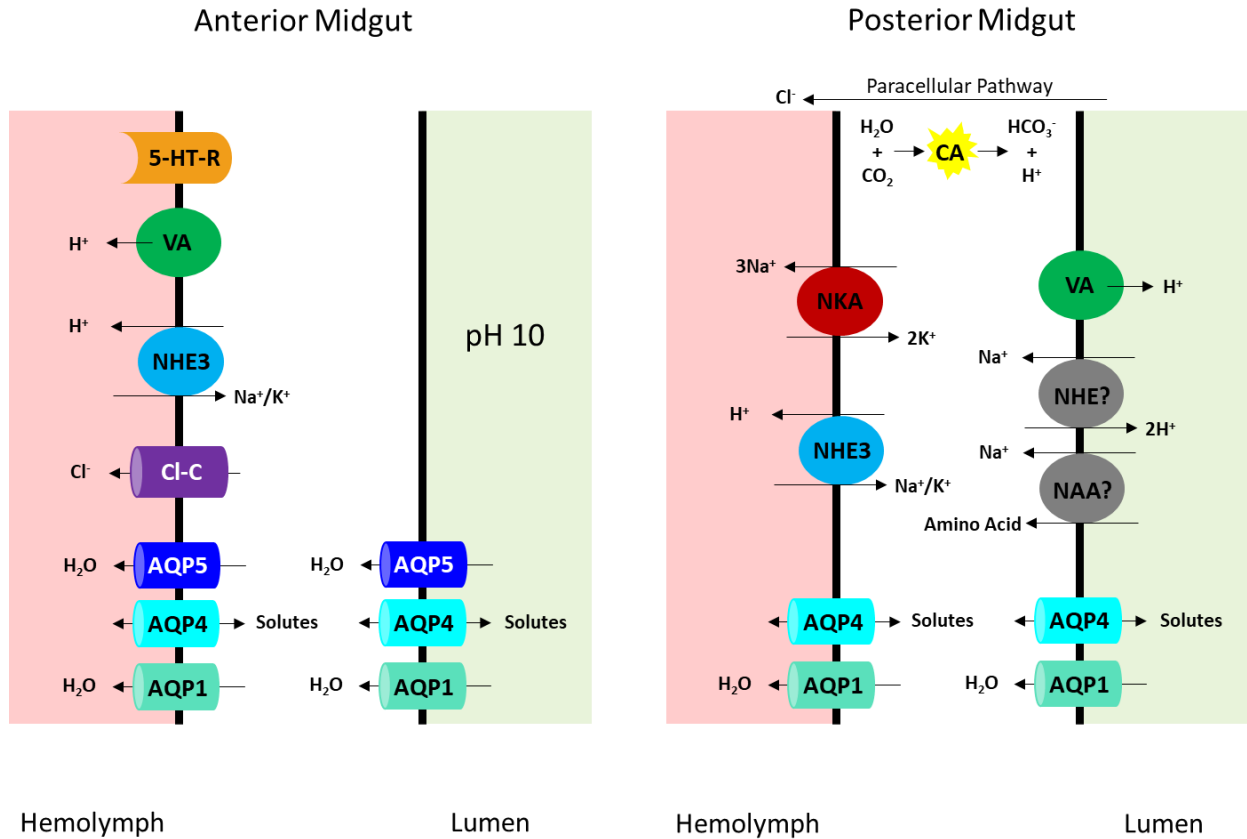
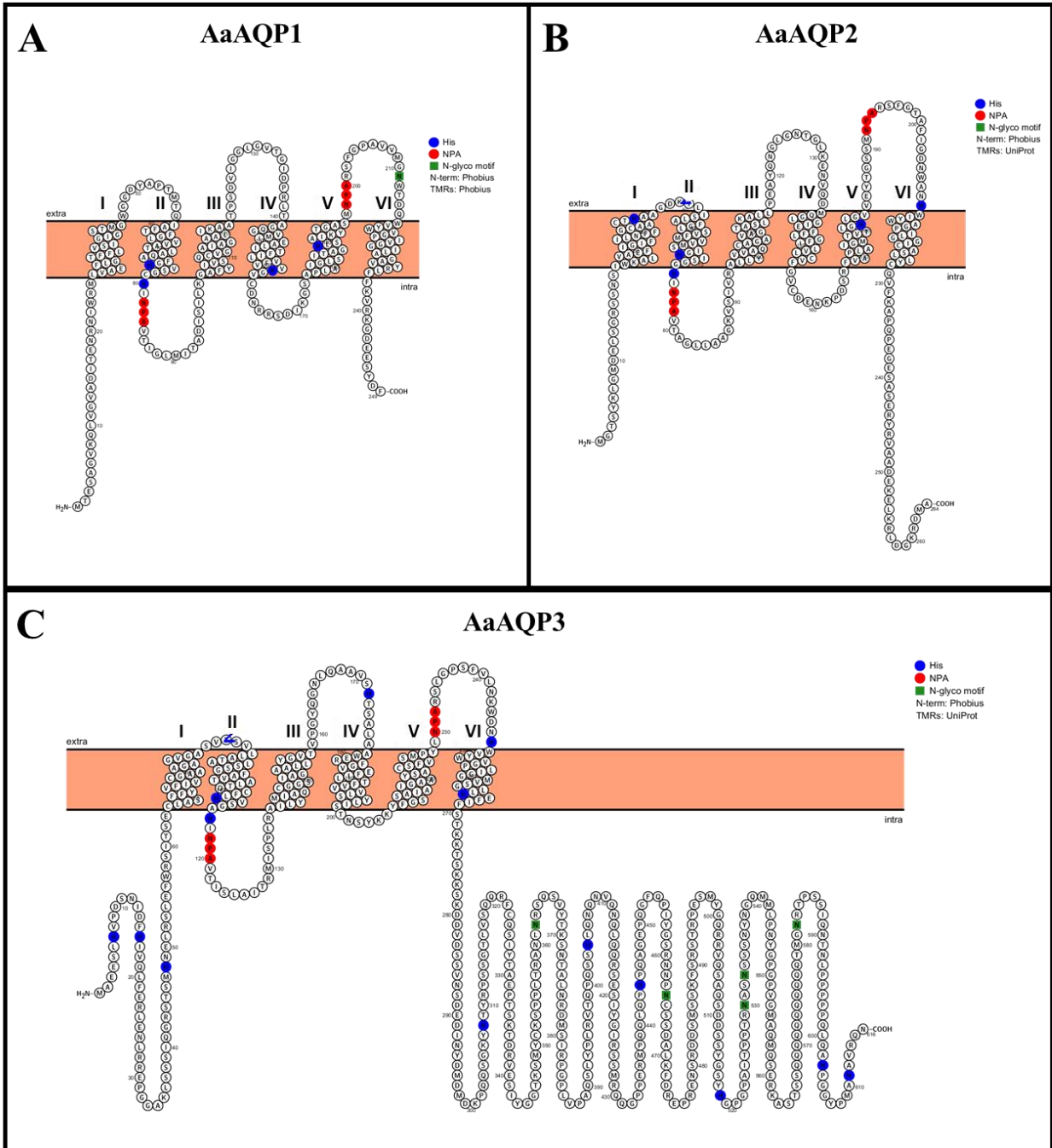


Figure 29: Updated schematic diagram illustrating membrane transport proteins in the anterior and posterior midgut of larval *Aedes aegypti* in freshwater habitat. VA: V-type H^+ ATPase, 5-HT-R: 5-hydroxytryptamine receptor, NHE: Na^+/H^+ exchanger, Cl-C: Cl^- channel, CA: carbonic anhydrase, and NKA: Na^+/K^+ ATPase, NAA: Na^+ /amino acid co-transporter, and *Aedes aegypti* aquaporin 1, AQP4: *Aedes aegypti* aquaporin 4, and AQP5: *Aedes aegypti* aquaporin 5.



Please find the figure caption on the following page.

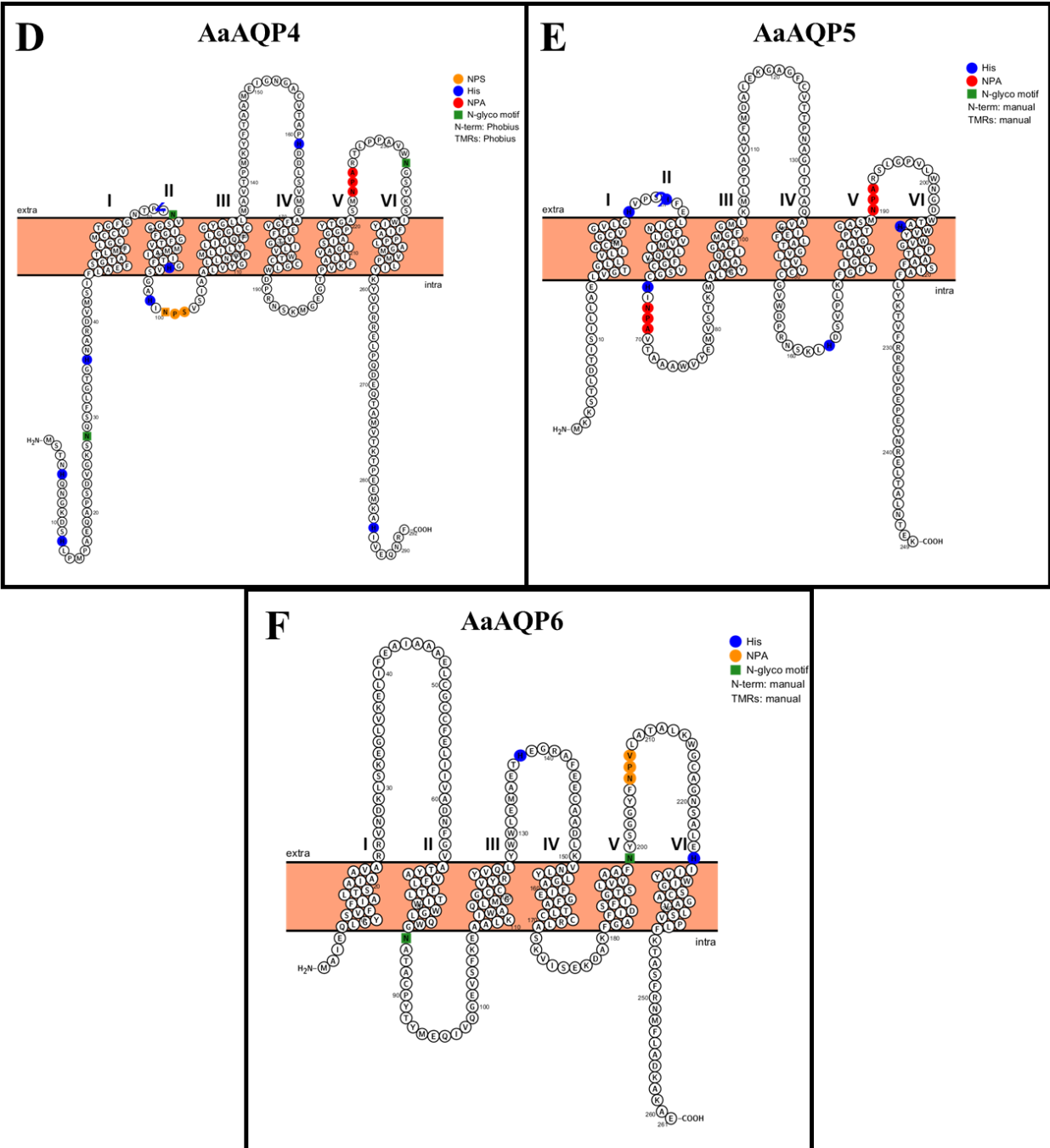


Figure 30: Topology predictions of unfolded putative AaAQPs in the plasma membrane using TMPred and Protter software (Hofmann, 1993; Omasits et al., 2014). The transmembrane regions are labelled I–VI. NPA domain, histidine residues, and N-glycosylation sites identified. AaAQP1 (A), AaAQP2 (B), AaAQP3 (C), AaAQP4 (D), AaAQP5 (E), and AaAQP6 (F).

4.4 AaAQPs in the Posterior Midgut

4.4.1 Transcript Abundance

At the posterior midgut the absorption of amino acids, ions, and minerals generates an osmotic drag that is predicted to drive water absorption into the hemolymph. With the exception of AaAQP2 and AaAQP6, the transcript abundance profile of AaAQPs in posterior midgut largely mirrored those found in the anterior midgut (see section above). The transcript abundance of AaAQP5 was the highest and there was moderate transcript abundance of AaAQP1, AaAQP3 and AaAQP4. Interestingly the anterior midgut contained a considerable level of AaAQP2 transcript, but this was almost undetectable in the posterior midgut relative to other AaAQP transcripts. Similarly, AaAQP6 transcript abundance was low in the posterior midgut, but clearly detectable in the anterior midgut. Similar to the anterior midgut, the posterior midgut generally contains low levels of AaAQP transcripts. This may be a method for limiting the passive absorption of water at the posterior midgut such that it does not become excessive. AaAQP transcript abundance in the posterior midgut was similar between FW and BW reared larvae suggesting that AaAQP regulation may not be driven by changes in mRNA expression.

4.4.2 Protein Expression and Localization

Western blots of posterior midgut protein homogenates probed with AaAQP1 antibody revealed a single band at ~25 kDa which is similar to the predicted mass of the AaAQP1 monomer. Furthermore, this band was no longer detected if the AaAQP1 antibody was preincubated with immunogenic peptide confirming its identity as AaAQP1 protein. AaAQP1 abundance in the posterior midgut was no different between FW and BW reared larvae indicating that AaAQP1 is important for posterior midgut function regardless of the external salinity. It is

likely that AaAQP1 serves to transport water across the epithelium since AaAQP1 localized to the apical and basolateral membrane of epithelial cells, as well as intracellularly. The intracellular immunoreactivity is suggestive of intracellular storage of AaAQP1 which may be utilized based on the water transport needs of the posterior midgut. The cellular localization of AaAQP1 did not change under different rearing conditions further supporting the importance of this AaAQP to the function of the posterior midgut regardless of the external salinity.

Western blots of posterior midgut protein homogenates probed with AaAQP4 antibody, revealed bands at ~25 kDa and ~58 kDa which are likely to represent the monomer and dimer of AaAQP4, respectively. The predicted molecular mass of the monomer is 31.3 kDa which is heavier than the bands observed. At this time the reason for this remains unclear; however, the bands detected may represent truncated AaAQP4 monomers that have undergone protein processing resulting in amino acid cleavage. The ~58 kDa band may also represent heterodimers with other AaAQP homologues expressed in the posterior midgut. AaAQP4 localized to the apical and basolateral membranes of the posterior midgut epithelium, suggesting that AaAQP4 allows for transepithelial transport of polyols such as trehalose and glycerol at the posterior midgut (Figure 29). Apical localization of AaAQP4 in the posterior midgut epithelium is consistent with apical localization of aquaglyceroporins (entomoglyceroporins) in the midguts of *Bombyx mori* and *Anomala cuprea* that preferentially transport solutes such as glycerol and urea at the apical membranes (Nagae et al., 2013). Similar to AaAQP1, the AaAQP4 protein abundance and localization did not change in response to BW rearing conditions suggesting that the role of AaAQP4 in posterior midgut function is important regardless of external salinity.

Western blots of posterior midgut protein homogenates probed with AaAQP5 antibody displayed two bands at ~26 kDa and ~28 kDa corresponding to the predicted mass of the

AaAQP5 monomer and potentially a monomer that has undergone post-translational modification. Unexpectedly, AaAQP5 could not be detected using the same antibody in immunohistochemical sections of the posterior midgut. At this time it is reasonable to conclude that AaAQP5 is expressed in the posterior midgut given the qPCR and western blot data however a better understanding of its function requires further work to localize the protein in this organ.

In conclusion, AaAQP1, AaAQP4, and AaAQP5 western blot data implicate protein expression despite the absence of immunoreactivity to AaAQP5 in the posterior midgut. AaAQP1 and AaAQP4 are predicted to facilitate transcellular transport of water and solutes across the epithelial membrane driven by the electroosmotic flow generated by ion and nutrient absorption in both FW and BW.

4.5 AaAQPs in the Hindgut

In FW larvae, the hindgut was demonstrated to be an ion reabsorption organ that creates dilute urine for expulsion, therefore, it could be predicted that AaAQP expression would be downregulated in the hindgut of FW larvae in order to avoid passive water absorption into the hemolymph (Ramsay, 1950). In BW, the luminal hindgut fluid osmolarity is predicted to be equivalent to that of the rearing media or perhaps even higher such that excess ions that are passively accumulated remain in the urine for expulsion. The exact mechanism for how this occurs is not entirely clear; however, the hindgut absorption of ions could be downregulated in BW reared larvae as was observed in the *Chironomus riparius* larval hindgut where decreased Na⁺/K⁺ ATPase and V-type H⁺ ATPase activity reduced K⁺ absorption (Donini et al., 2006; Donini et al., 2007; Jonusaite et al., 2013).

In seawater dwelling larvae, the urine that is expelled from the larvae is hyperosmotic to the hemolymph in order to preclude the excessive absorption of ions in an effort to maintain

hemolymph ionic homeostasis (Asakura, 1980; Meredith and Phillips, 1973). However, in contrast to freshwater *A. aegypti* larvae, the rectum (a salt secreting gland) of seawater larvae possess a specialized segment to their rectum that actively secretes ions into the rectal lumen (Asakura, 1980; Bradley and Phillips, 1975; Larsen et al., 2014). In saline reared larval mosquitoes of *Ochlerotatus taeniorhynchus* (formerly *Aedes taeniorhynchus*) increasing external salinity leads to an increase in the ionic composition of excreted fluid from the rectum (Bradley and Phillips, 1975). Despite the absence of the salt secreting gland in the *A. aegypti* larvae, they may keep the ions removed from the hemolymph by the Malpighian tubules in the rectal lumen therefore leading to the concentration of luminal contents by reducing absorption of ions at the rectum in BW habitats.

In the current study, the hindgut of *A. aegypti* contained the greatest abundance of AaAQP6 compared to other organs and AaAQP6 transcript abundance was the greatest compared to the other AaAQPs in the hindgut. These data are consistent with previous studies of distilled water reared larvae which also showed that AaAQP6 transcript abundance in the hindgut was high (Marusalin et al., 2012). The transport specificity of AaAQP6 is unknown although it is most similar to the unorthodox mammalian AQPs which may not transport water. Interestingly, AaAQP6 transcript abundance was downregulated in response to BW rearing. Based on these results, AaAQP6 may possess ion conductance because, in freshwater, the hindgut reabsorbs ions while in BW ion reabsorption must be limited (Donini et al., 2006; Jonusaite et al., 2011; Jonusaite et al., 2013). AQP ion conductance has been shown in mammalian AQPs, such as in the rat AQP1 where Na⁺ conductance was shown when AQP1 was expressed in oocytes (Boassa et al., 2006; Yasui et al., 1999).

AaAQP2 is a competent water transporter and its transcript was detected in the hindgut implicating its involvement in transcellular water transport across the hindgut epithelium in both FW and BW rearing conditions since the transcript abundance did not change. In adult *A. aegypti* females, AaAQP2 transcript abundance decreased 24 h following a blood meal, supporting AaAQP2's role in osmoregulation in the hindgut. However, it should be noted that the osmoregulatory challenges faced by larvae and adults are idiosyncratic to the life stage when there is an absence of a water load from a blood meal (Drake et al., 2015).

4.5.1 AaAQP1

The observed relatively low AaAQP1 transcript abundance in relation to other AaAQP genes in the hindgut in this study has been previously demonstrated in distilled water reared larvae (Marusalin et al., 2012). Furthermore, AaAQP1 transcript abundance was downregulated in the hindgut in response to BW rearing and, since AaAQP1 is a water transporting AQP, this implies that water permeability in the hindgut is downregulated via the transcellular pathway to perhaps decrease water loss from the hemolymph into the hindgut lumen if luminal contents are concentrated (see above). However, the AaAQP1 protein abundance in the hindgut was no different between FW and BW reared larvae, therefore transcript abundance of AaAQP1 does not necessarily reflect protein abundance in the hindgut. Western blots of hindgut protein homogenates probed with AaAQP1 antibody displayed a single band at ~23 kDa which is lighter than the predicted mass of the monomer at 26.2 kDa. To further complicate our understanding of AaAQP1 function in the hindgut, AaAQP1 immunolocalization could not be detected. Anacu AQP1 was localised to the apical plasma membrane of rectal epithelial cells in the shining leaf beetle, *Anomala cuprea*. *A. cuprea* are terrestrial therefore require the active absorption and retention of water from their environment and expression of water specific AQPs on the apical

membrane allows for water absorption from the rectal lumen into the epithelial cells for absorption across the basolateral membrane into the hemolymph (Nagae et al., 2013). This supports that the absence of AaAQP1 in the hindgut of *A. aegypti* would diminish water absorption in these FW larvae.

The pea aphid *Acyrtosiphon pisum*, consumes highly concentrated plant phloem sap, which stimulates water loss from the hemolymph into the gut lumen because of the osmotic gradient. ApAQP1 was identified in the stomach and the posterior intestine, and shown to be involved in a homeostatic water cycling mechanism that transfers water from the distal intestine to the stomach, preventing water loss driven by the osmotic gradient between the gut contents and the hemolymph (Shakesby et al., 2009). The water cycling mechanisms may be present in the *A. aegypti* larvae if AaAQP1 permits water absorption into the hemolymph where water that is absorbed across the hindgut epithelium is cycled back into the Malpighian tubule lumen which is possible because the Malpighian tubules are arranged in close proximity to the hindgut.

4.5.2 AaAQP4

AaAQP4 transcript abundance was one of the lowest when compared to other AaAQP transcripts in the hindgut, suggesting there is reduced solute transport across this epithelium. AaAQP4 transcript abundance did not change in response to BW environmental conditions proposing that solute transport is not particularly important for hindgut function or simply indicating that other solute transporters are utilized at the hindgut. Western blotting of hindgut protein homogenates probed with AaAQP4 antibody displayed several bands at ~25 kDa, ~35 kDa, and ~58 kDa. The band at ~25 kDa is predicted to be the putative monomer which was confirmed to be AaAQP4 protein based on a similar band observed in Malpighian tubule which was successfully blocked with preincubation of the antibody with immunogenic peptide. The

band at ~35 kDa is anticipated to be the monomer with post-translational modifications which may signal translocation of AaAQP4 to the cellular membrane (Hendriks et al., 2004). Finally, the band at ~58 kDa is predicted to be the dimer with post-translational modifications. AaAQP4 protein abundance did not change in response to BW rearing, which indicates that its role in the hindgut is similar in both FW and BW environmental conditions. AaAQP4 modestly localized to the apical and basolateral membrane, however, the majority of AaAQP4 signal was intracellular, perhaps indicating vesicular storage (Figure 31). Membrane bound AaAQP4 in the hindgut would mediate polyol transport across the epithelial membrane in the hindgut of the larvae such as trehalose for sustained metabolic activity. However, in FW, AaAQP4 is predicted to result in glycerol and trehalose loss into the hindgut lumen due to the concentration gradient of dilute hindgut contents. Apically localized AaAQP4 would possibly modulate intracellular glycerol and trehalose that would enable cellular osmoregulation, cellular functions, or energy synthesis.

4.5.3 AaAQP5

In the hindgut, AaAQP5 transcript was highly abundant when compared to other AaAQP genes expressed and predicted to mediate trehalose and water transport across the hindgut epithelium via the transcellular pathway. AaAQP5 transcript did not change with BW rearing suggesting that AaAQP5 function is required in both environmental rearing conditions. Western blotting of hindgut protein homogenates probed with AaAQP5 antibody resolved three bands at ~25 kDa, 26 kDa, and ~27 kDa. The band at ~25 kDa is the predicted monomer while the rest are likely to be monomers with varying degrees of post-translational modifications. AaAQP5 protein abundance did not change in response to BW rearing which corresponds with the transcript abundance data further indicating that AaAQP5 is required under both rearing conditions. In the silkworm, *Bombyx mori*, AQP-Bom1 and AQP-Bom3, which are homologs of

DRIP and PRIP AQPs, respectively, have been identified in the hindgut of the larvae (Azuma et al., 2012). Given that *B. mori* are terrestrial they require the conservation of water in order to avoid desiccation, therefore apically localized AQP-Bom1 and basolaterally localized AQP-Bom3 in the hindgut may permit water absorption from the hindgut. Similarly, AQP2, AQP3 and DRIP-AQP of the Antarctic midge, *Belgica antarctica*, were localized in the epithelium of the hindgut where water reabsorption would be favourable in the desert-like conditions (Yi et al., 2011). Therefore, the lack of AaAQP5 immunofluorescence in the hindgut membrane may suggest a possible downregulation of AaAQP5 expression in the hindgut to avoid passive water absorption as seen in terrestrial insects.

In conclusion, AaAQP1 and AaAQP5 expressed in the hindgut may perhaps participate in promoting cellular function opposed to osmoregulation. The absence of immunoreactivity of AaAQP1 and AaAQP5 indicate that the epitope for antibody binding may be inaccessible in immunohistochemical sectioning, therefore immunostaining was not observed. Additionally, AaAQP4 expression in the hindgut may facilitate solute transport into the cell as well as allow for transcellular transport of these solutes for osmoregulation. Further assessment of AaAQP6 transport conductance of ions would also further our understanding of AaAQP function in the hindgut.

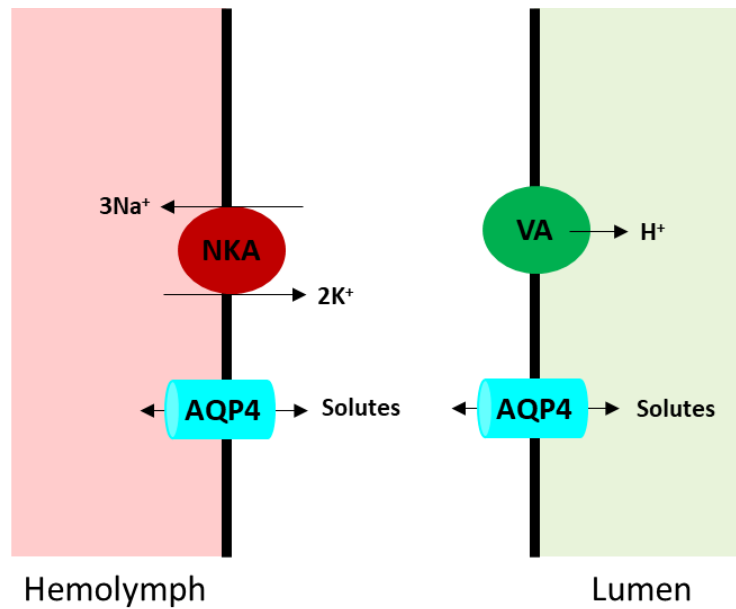


Figure 31: Updated schematic diagram illustrating the role of membrane transport proteins in the hindgut of larval *Aedes aegypti*.

VA: V-type H⁺, ATPase, NKA: Na⁺/K⁺, and AQP4: *Aedes aegypti* aquaporin 4.

4.6 AaAQPs in the Malpighian Tubules

The Malpighian tubules are the main secretory organs that rid the hemolymph of excess water which is passively absorbed into the body in FW environments. In BW-reared larvae this organ appears to function in a similar manner, where the fluid secretion rate is comparable to FW reared larvae but with reduced transepithelial K⁺ secretion, despite the different challenges on water balance under these conditions (Donini et al., 2006). The reduced K⁺ secretion is thought to allow for increased secretion of Na⁺ thereby helping to alleviate the elevated concentration of hemolymph Na⁺ observed in BW reared larvae (Donini et al., 2006). The Malpighian tubules had the greatest abundance of AaAQP transcript expression out of all the organs assessed in this study, and it is predicted that the AQPs facilitate the transport of water and polyols through the transcellular pathway of the tubules. This was directly demonstrated for AaAQP5 which is expressed in the principal cells (Misyura et al., 2017). In this study, AaAQP5 had the highest

transcript abundance compared with other AaAQPs in the Malpighian tubules and this result differs from a previous study that demonstrated equivalent AaAQP1, AaAQP3, AaAQP4 and AaAQP5 transcript abundance when larvae were reared in distilled water (Marusalin et al., 2012). The difference in abundance of AaAQP transcript between studies may be driven by the discrepancy between rearing conditions; however, the stable secretion rate measured from the distal portion of the Malpighian tubules of distilled water and BW reared larvae may suggest that transcript levels would remain stable to maintain the capacity for consistent secretion rates (Donini et al., 2006; Marusalin et al., 2012). In fact, this notion is consistent with the results which showed no differences in transcript abundance of AaAQPs that transport water in Malpighian tubules of FW and BW reared larvae. AaAQP3 that is predicted to participate in promoting cellular adhesion and is suspected to have no transporting function was salinity responsive displaying higher transcript abundance in Malpighian tubules with BW rearing. Greater AaAQP3 transcript abundance in Malpighian tubules may indicate greater cellular adhesion between the cells. However, it should be noted that the evidence of AaAQP3 participation in cellular adhesion is solely based on studies with *D. melanogaster* BIB, and therefore assessment of AaAQP3 transport capabilities is required through heterologous expression assays in oocytes to extrapolate possible AaAQP3 function (Tatsumi et al., 2009; Yanocho and Yool, 2002; Yanocho and Yool, 2004). The modulation of expression of septate junction protein snakeskin, mesh, and gliotactin resulting from BW rearing was shown to decrease the paracellular permeability of Malpighian tubules epithelium (Jonusaite et al., 2017a; Jonusaite et al., 2017b). If one considers that in Malpighian tubules of BW reared larvae there is (1) diminished paracellular permeability, (2) consistent expression abundance of water transporting AaAQPs as found in FW reared larvae and (3) no differences in fluid secretion rates

of Malpighian tubules. This together leads to the conclusion that an additional pathway for water exists in the tubules of BW reared larvae. Since AaAQP3 transcript abundance is higher in BW tubules this suggests that AaAQP3 may transport water and that this may be the basis for the additional water transporting pathway in tubules of BW reared larvae. In adult *A. aegypti* Malpighian tubules, AaAQP1, AaAQP4, and AaAQP5 have been implicated in removal of accumulated excess fluid in the hemolymph that accompanies the consumption of a blood meal and this conclusion was based on knockdown studies that demonstrate bloating of mosquitoes injected with excess fluids into the hemolymph in accordance with the water load that would be experienced during blood feeding (Drake et al., 2010; Drake et al., 2015). However, the contribution of transcellular transport through AaAQP1, AaAQP4 and AaAQP5 in the adult Malpighian tubules have only been speculated since contribution of excretion in adult mosquitoes encompasses the cumulative function of several osmoregulatory organs.

4.6.1 AaAQP1

AaAQP1 transcript abundance was relatively low in the Malpighian tubules suggesting that this AaAQP is not a major contributor to water flux across the Malpighian tubules. Water-specific aquaporin transcripts have been identified in other organisms, implicating their function in water transport such as the kissing bug, *Rhodnius prolixus*. RhoprAQP1 (DRIP homologues) transcript in the *R. prolixus* Malpighian tubules changed over the course of 24 h following the consumption of a blood meal which reflected the need for water secretion by the Malpighian tubules, whereby RhoprAQP1 transcript abundance was reciprocal to the time following blood meal consumption (Echevarría et al., 2001; Staniscuaski et al., 2013). Similar trends were shown with AaAQP1 transcript abundance in adult female Malpighian tubules following the consumption of a blood meal (Drake et al., 2010).

Western blotting of Malpighian tubule protein homogenates probed with AaAQP1 antibody revealed a single band at ~23 kDa that is predicted to be the monomer, and was demonstrated to be specific binding to AaAQP1 protein based on the peptide block. Larvae reared in BW did not show changes in AaAQP1 protein abundance compared with FW reared larvae, suggesting that water transport across the Malpighian tubules through AaAQP1 is maintained in both rearing conditions. This was also supported by the sustained Malpighian tubules secretion rate in distilled water and BW reared larvae, however based on mRNA abundance may still be a minor contributor to water transport when compared to other AaAQPs (Donini et al., 2006). AaAQP1 localized to the apical membrane of principal cells and was also proposed to localize in the stellate cells, however membrane specific localization in stellate cells could not be discerned (Figure 32). Since AaAQP1 localization does not change with salinity, this suggests that AaAQP1 is necessary for Malpighian tubule function in the different rearing conditions; however, there may be instances where AaAQP1 expression or localization is regulated which requires further analysis. Cellular and membrane discrimination of AQP expression has been noted in various animal models, demonstrating that AQP expression and localization are highly diverse. For instance, the expression of Aqp4019 and AQP17664 in *D. melanogaster* was demonstrated in the principal cells of the Malpighian tubules using *in situ* hybridization (Kaufmann et al., 2005); and the mammalian AQP2 which is expressed in the principal cells of the renal tubules (Sabolić et al., 1995). Within the adult *Anopheles gambiae*, AgAQP1 was shown to be expressed by stellate cells in the distal portion of the MTs and in the principal cells at the proximal end (Liu et al., 2011; Tsujimoto et al., 2013), while the DRIP water channel in *D. melanogaster* is restricted to stellate cells of both larval and adult life stages

(Kaufmann et al., 2005), supporting possible AaAQP1 localization in the stellate cells of *A. aegypti*.

AaAQP1 function in water transport was further assessed in adult *A. aegypti* demonstrating its contribution to survival and to excretion pathways (Drake et al., 2010; Drake et al., 2015). Global knockdown of AaAQP1 in the organism allowed for greater survival in desiccating environments indicating greater retention of water within the body as well as reduced total excreted fluid, which together implicates AaAQP1 in water removal from the hemolymph under nominal conditions (Drake et al., 2010; Drake et al., 2015).

4.6.2 AaAQP4

The transcript abundance of the entomoglyceroporin AaAQP4 was also relatively high in the Malpighian tubules relative to other AaAQPs indicating solute transport across the Malpighian tubule epithelium through the transcellular pathway is inherent for Malpighian tubule function in both FW and BW conditions. Blood feeding by adult *A. aegypti* alters the transcript abundance of AaAQP4 in the Malpighian tubules throughout the process of blood meal digestion, exhibiting elevated transcript levels 3 h following a blood meal which are then downregulated over the course of 24 h. Similarly, the *R. prolixus* putative aquaglyceroporin, RhoprMIP-A transcript abundance diminishes over the course of 48 h following blood meal consumption (Staniscuaski et al., 2013). The changes in aquaglyceroporin and entomoglyceroporin transcript abundance in the various organisms indicate the transport of solutes by the Malpighian tubules that may accumulate from the consumption of a blood meal. AaAQP4 transcript abundance did not change in response to BW rearing in the Malpighian tubules which also reflected the stable AaAQP4 protein abundance in both FW and BW, further

supporting the consistent fluid secretion rate by the Malpighian tubules with different external salinities (Donini et al., 2006).

Western blotting of Malpighian tubules protein homogenates probed with AaAQP4 antibody revealed several resolved bands at ~25 kDa, ~26 kDa, ~57 kDa, and ~58 kDa. The band at ~25 kDa is predicted to be the resolved monomer which was suggested to be AaAQP4 protein by the peptide block. The ~26 kDa band was deemed to be non-specific binding since it remained detectable after preincubation of the antibody with immunogenic peptide. The ~57 kDa and ~58 kDa bands were specific for AaAQP4 and predicted to be a dimer or alternatively, those bands would represent heterodimers with other AaAQPs such as AaAQP1 or AaAQP5 that would result in a lighter protein mass (Table 1) (Neely et al., 1999).

AaAQP4 localized to the apical membrane of the Malpighian tubule principal cells suggests solute transport across the apical membrane. Glycerol transporting AQPs have been localized in the Malpighian tubules at the apical membrane previously, such as an aquaglyceroporin in *Anomala cuprea* (Nagae et al., 2013). Various AQPs have membrane specific localization, such as mammalian AQP2 at the apical membrane of colon epithelial cells and mammalian AQP4 localized to the kidney basolateral membrane (Gallardo et al., 2001; Tamma et al., 2001; Terris et al., 1995). AaAQP4 immunoreactivity appeared diminished in the membrane in BW larvae, indicating that solutes may accumulate in the hemolymph or the cytosol and could be used to overcome the osmotic challenge of BW may favourably be precluded from secretion out of the hemolymph by downregulating membrane bound AaAQP4.

The AaAQP4 NPA-NPS motif within the pore is analogous to the mammalian AQP7 motif (Figure 30) (Ishibashi et al., 1997). Transport of urea and water were demonstrated through the AQP7 NPA-NPS pore, which indicate the potential likelihood for AaAQP4 to possess similar

transport properties in addition to the identified conductance of AaAQP4 to erythriol, adonitol, mannitol, and glycerol transport already confirmed (Drake et al., 2015; Ishibashi et al., 1997; Sreedharan et al., 2016). Additionally, AQPs have also shown ammonia ($\text{NH}_3/\text{NH}_4^+$) conductance, evident in rat AQP8 and human aquaporins AQP3, AQP7, AQP8, and AQP9, which all readily transport ammonia and some also transport urea (Litman et al., 2009; Saparov et al., 2007). In invertebrate models, the AQP-Bom2 exhibits urea and glycerol conductance where its transcripts were identified in the Malpighian tubules of *B. mori* (Kataoka et al., 2009). To the best of my knowledge, ammonia transport in the Malpighian tubules has not been identified. Therefore, if AaAQP4 possesses the function of transporting ammonia and urea, then transport of these solutes across the apical membrane may be mediated through AaAQP4 in the larval Malpighian tubules. The highly metabolically active Malpighian tubules are predicted to accumulate ammonia as metabolic waste in the cytosol, therefore the secretion of ammonia out of the cells through AaAQP4 would be favourable.

4.6.3 AaAQP5

Of the AaAQP genes expressed in the Malpighian tubules, AaAQP5 transcript abundance was the highest in FW and BW larvae, which was previously demonstrated in the Malpighian tubules of distilled water reared larvae (Marusalin et al., 2012). When compared to other osmoregulatory organs, AaAQP5 transcript abundance was comparable to the abundance in the gastric caeca, anterior midgut, and the anal papillae and did not change in response to BW rearing indicating AaAQP5 is mediating transcellular water transport equally in larvae reared in different salinity environments.

Western blotting of Malpighian tubule protein homogenates probed with AaAQP5 antibody revealed three bands at ~26 kDa, ~60 kDa, and ~75 kDa which were suggested to

represent the monomer, the dimer with post-translational modifications and the trimer, respectively. AaAQP5 protein abundance did not change in response to BW rearing in the Malpighian tubules that may contribute to the sustained fluid secretion rates of the Malpighian tubules with changes to external salinity concentrations (Donini et al., 2006). AaAQP5 localized to the Malpighian tubule basolateral membrane of FW reared larvae that would allow for water to passively be transported from the hemolymph into the principal cell lumen (Figure 32). A previous study demonstrated AaAQP5 localization on the basolateral membrane as well as the apical membrane of Malpighian tubules of larvae reared in distilled water (Misyura et al., 2017). The discrepancy in apical localization of AaAQP5 may potentially demonstrate the regulation of AaAQP5 localization based on the external salinity and resulting osmoregulatory pressure in distilled water in comparison to FW and BW displayed in this study. In distilled water, there is greater passive osmotic accumulation of water in the larvae which the Malpighian tubules must remove to regulate internal ion and solute concentrations mediated through the basolaterally and apically localized AaAQP5. With elevated salinity, intracellular concentration of solutes such as trehalose have been demonstrated, possibly facilitated through basolateral AaAQP5 and kept within the cell by reducing apical AaAQP5 localization. However, the changes in immunofluorescence of AaAQP5 in FW and BW perhaps indicates translocation of AaAQP5 into the apical membrane to transport trehalose out since other osmolytes are accumulated and trehalose is no longer necessary for intracellular solute balance (Edwards, 1982c). In the Malpighian tubules of *A. gambiae*, AgAQP1A and AgAQP1B localized to the basolateral membrane of the proximal Malpighian tubules, which are predicted to function in osmoregulation (Tsujimoto et al., 2013).

4.6.4 AQP Function in the Malpighian tubules

The Malpighian tubules concentrating the hemolymph by removing excess water in FW environments is proposed to transpire through AaAQP1 and AaAQP5 localized at the apical and basolateral membranes, respectively. Similar methods of fluid concentration are apparent in xylem feeding insects which require the concentration of nutrients from the highly dilute media they ingest by the removal of water in the filtering chamber of their gut. This process is enabled by the expression of AQP_{cic} which is highly water specific in the *Cicadella viridis* (Le Caherec et al., 1997).

AaAQP1, AaAQP4, and AaAQP5 displayed localization to the different membranes in the Malpighian tubules implying distinct regulatory mechanisms that reflect the transcellular transport needs of this organ. The changes in AaAQP localization in response to BW rearing may reflect hormonal regulation that modulates the translocation of intracellularly stored AaAQP proteins. This is in contrast to the previously demonstrated AQP expression modulation mediated through hormone stimulation in *R. prolixus* Rp-MIP, where transcript and protein abundance changed in the Malpighian tubules in response to 5-HT (Martini et al., 2004). *Rhodnius neglectus* Malpighian tubule proximal cells were shown to sense hyperosmotic medium resulting in cellular regulatory volume increase to cope with the water loss out of the cell by osmosis. The cells sense extracellular ion concentrations, specifically K⁺ and regulate their function to increase ion absorption (Arenstein et al., 1995). Incubation of *R. prolixus* Malpighian tubules in hyperosmotic medium also demonstrated modulation of Na⁺/K⁺ ATPase activity by 90% via protein kinase C (PKC) (Caruso-Neves et al., 2001). As seen in many physiological systems, there is a potential for the existence of an antagonistic mechanism that senses hypo-osmotic extra-tubular environment, specifically the hemolymph. Perhaps elevated osmolyte

concentrations in the hemolymph including Na^+ , Cl^- , and free amino acids are sensed by the Malpighian tubules and respond by changing translocation of AaAQPs in the membrane, specifically AaAQP4 and AaAQP5, as an alternative to hormonal regulation (Donini et al., 2006; Donini et al., 2007; Edwards, 1982c).

In conclusion, AaAQPs expressed in the Malpighian tubules are predicted to facilitate water and solute transport via the transcellular pathway as demonstrated previously by AaAQP5 (Misyura et al., 2017). Basolaterally localized AaAQP5 allows for water and trehalose to traverse the membrane while apically localized AaAQP1 and AaAQP4 transport water into the Malpighian tubules lumen. Due to the highly abundant transcripts of other AaAQPs detected in the Malpighian tubules, it is essential to localize them in the epithelium and assess their conductance properties and characteristics to infer on their osmoregulatory role.

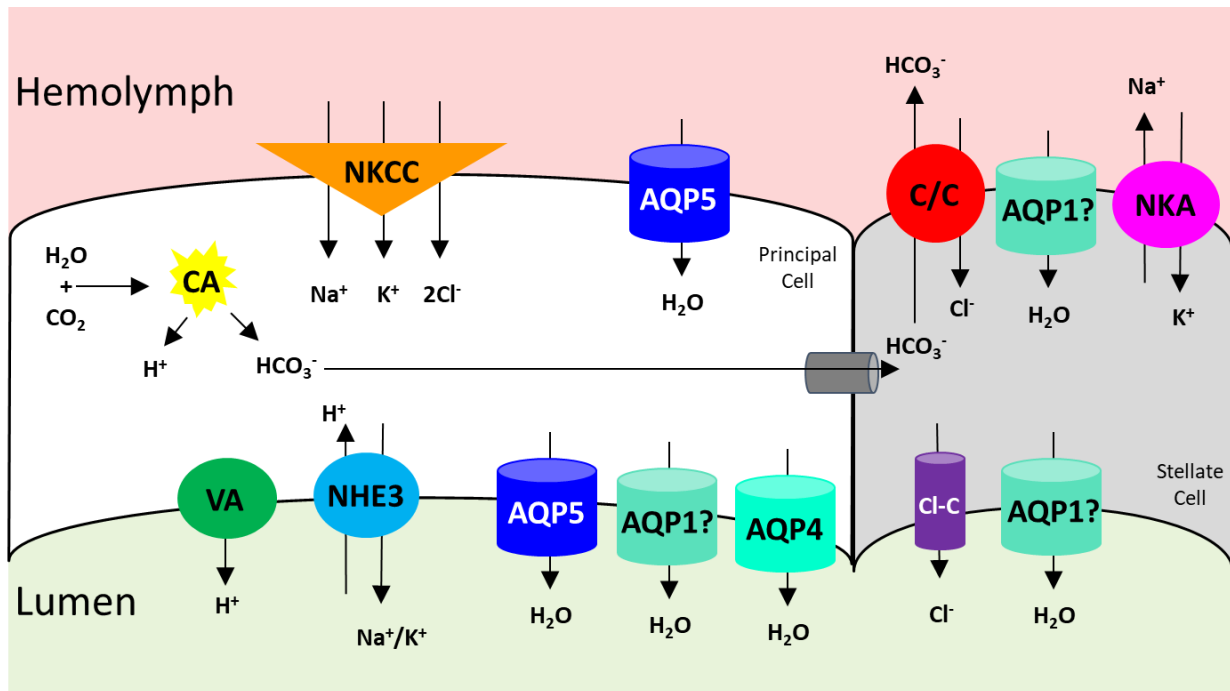


Figure 32: Updated schematic diagram illustrating membrane transport proteins in the Malpighian tubules of larval *Aedes aegypti*. VA: V-type H^+ ATPase, NHE3: Na^+/H^+ exchanger 3, Cl-C: Cl^- channel, CA: carbonic anhydrase, and NKCC: $Na^+/K^+/2Cl^-$ co-transporter C/C: Cl^-/HCO_3^- exchanger, AQP1: *Aedes aegypti* aquaporin 1, AQP4: *Aedes aegypti* aquaporin 4, AQP5: *Aedes aegypti* aquaporin 5. AaAQP1?: AaAQP1 is expressed in stellate cells, however membrane specific localization has not been discerned.

4.7 AaAQPs in the Anal Papillae

Anal papillae actively transport ions from their external habitat into the hemolymph in order to accumulate ions in FW environments. Despite the syncytial epithelium that would diminish passive water absorption into the hemolymph in FW, *A. aegypti* express AaAQPs that allow water movement across the epithelial membrane which is exacerbated by the active transepithelial ion transport (Akhter et al., 2017; Marusalin et al., 2012). Larvae rearing in ranging salinities culminate into several morphological and molecular adaptations of the anal papillae which include AaAQP modifications (Akhter et al., 2017; Donini et al., 2007; Tsujimoto et al., 2013). Similarly, freshwater and seawater dwelling mosquito larvae *Anopheles merus* and

Anopheles quadrimaculatus, respectively, also demonstrate morphological changes in anal papillae with exposure to different environmental salinities, evident by alterations to the convoluted folding pattern of the apical membrane (Coetzee and Sueur, 1988).

4.7.1 Transcript Abundance

Anal papillae contained the second most abundant AaAQP mRNA abundance in the organs assessed in this study, indicating that despite the water accumulation across the epithelium, water and solute permeability across this integument is functionally important. AaAQP2 transcript was highly abundant in the anal papillae of FW and BW larvae as was previously demonstrated in larvae exposed to distilled water and ion poor water (Akhter et al., 2017; Marusalin et al., 2012). AaAQP2 is proposed to possess the dominant role in transepithelial water absorption in the anal papillae in FW environments because of its high water conductance and high transcript abundance when compared to other AaAQP genes (Drake et al., 2015). In contrast, AaAQP1 had the lowest transcript abundance in the three water conditions across the studies, indicating the ability to selectively express AaAQPs with similar transport conductance in the anal papillae (Akhter et al., 2017; Marusalin et al., 2012). AaAQP5 mRNA was previously shown to be less abundant in rearing media with lower salinities than in the present study indicating that differences in expression patterns may be driven by the lesser magnitude of salinity disparity between FW and BW than previous studies of ion poor water and BW (Akhter et al., 2017; Marusalin et al., 2012).

AaAQP3 displayed a trend towards a decrease in transcript abundance and supports previous findings that used ion poor water reared larvae, which had a significant decrease in transcript abundance supporting the notion that AaAQP3 is salinity responsive whereby transcript abundance changes depending on the external salt concentration (Akhter et al., 2017).

AaAQP3 is proposed to contribute to limiting the absorption of Na⁺ and Cl⁻ through the anal papillae down their concentration gradients into the hemolymph in BW (Akhter et al., 2017). Due to the syncytial epithelium of the anal papillae devoid of cellular adhesion requisites, AaAQP3 may contribute to adhesion of the tracheolar cells to the anal papillae epithelium. Alternatively, AaAQP3 may also function in substrate transport; therefore, further assessment of AaAQP3 function needs to be discerned to understand its role in osmoregulation and to understand why transcript abundance changes with salinity (Akhter et al., 2017; Marusalin et al., 2012). AaAQP6 trended towards a decrease, which supported previous findings in ion poor water rearing (Akhter et al., 2017). AaAQP6 substrate specificity or its role in osmoregulation have not been discerned, therefore further assessment of AaAQP6 function is necessary to speculate its role in anal papillae and osmoregulation (Akhter et al., 2017; Yang and Piermarini, 2017).

4.7.2 AaAQP1

AaAQP1 transcript abundance did not change in the anal papillae of BW reared larvae; however, there was a trend towards a decrease, which was not observed in a previous study between ion poor water and BW conditions (Akhter et al., 2017). Western blotting of anal papillae protein homogenates probed with AaAQP1 antibody displayed a band at ~60 kDa which was indicative of a putative dimer supported by the peptide block to be AaAQP1 protein specific. AaAQP1 protein abundance was elevated in BW reared larvae which was supported by the immunofluorescence signal strength of anal papillae probed with AaAQP1 antibody when exposure settings were kept consistent. AaAQP1 localized to the apical membrane of BW reared larvae suggesting apical transport of water into the cells in BW habitats which is perhaps deleterious in FW, therefore AaAQP1 is not observed. AaAQP1 is predicted to allow for water

transport into the cell driven by the high hemolymph osmolarity resulting from the accumulation of ions and solutes in the hemolymph in response to BW as well as the active uptake of ions such as Na^+ , Cl^- and free amino acids at the apical membrane (Donini et al., 2007; Edwards, 1982c). AaAQP1 did not colocalize with the apical membrane marker V-type H^+ ATPase, but rather appeared further towards the external environment than V-type H^+ ATPase immunoreactivity. AaAQP1 may be strictly positioned towards the outermost apical membrane regions and not within the infolding membrane. The V-type H^+ ATPase antibody binds to the cytosolic V_0 domain of the protein, which is positioned further intracellularly than the AaAQP1 antibody cytosolic binding site on the N-terminus. V-type H^+ ATPase function may also be downregulated in BW by the dissociation of V_1 and V_0 subunits or vesicular storage of V-type H^+ ATPase intracellularly (Beyenbach and Piermarini, 2011; Jefferies et al., 2008). V-type H^+ ATPase was shown to respond to 5-HT in the gastric caeca where activation of 5-HT receptors elevated V-type H^+ ATPase functions by facilitating its translocation into the membrane (D'Silva and O'Donnell, 2018). Therefore, if V-type H^+ ATPase is intracellularly stored, then the immunofluorescence signal would be intracellular as opposed to apical, perhaps explain the lack of colocalization of V-type H^+ ATPase and AaAQP1 if the latter remains in the apical membrane. AaAQP1 is the first water transporting AaAQP to localize solely to the apical membrane of the anal papillae implicating apical water absorption directly from the external environment through AaAQP1.

4.7.3 AaAQP4

AaAQP4 transcript abundance decreased in response to BW rearing of larvae when compared to FW larvae, which was also shown previously when AaAQP4 transcript decreased between ion poor water and BW (Akhter et al., 2017). Reduced AaAQP4 transcript abundance

may occur in an effort to accumulate osmolytes in the hemolymph and prevent their diffusion into the external environment. Activation of PKC was shown to inhibit mammalian AQP4 permeability via phosphorylation of the Ser180, as well as decrease mRNA expression of AQP4 and AQP9 (Han et al., 1998; Yamamoto et al., 2001; Zelenina et al., 2002). Based on amino acid sequence analysis, Ser180 is present in AaAQP4, and therefore, implicate PKC activation, decreasing AaAQP4 gene expression through Ser180 phosphorylation.

Western blotting anal papillae protein homogenates with AaAQP4 antibody displayed a resolved band at ~75 kDa in FW samples which was predicted to be a putative dimer with post-translational modifications of the monomers. This would explain the mass discrepancy between the predicted dimer and the observed ~75 kDa band (Kamsteeg et al., 2000; Neely et al., 1999). BW treatment revealed a band at ~58 kDa predicted to be a putative dimer without post-translational modification. The mass transition between FW and BW may indicate post-translational modifications used for AaAQP4 regulation within the epithelium. AQP glycosylation is important for cell surface expression and translocation therefore, AaAQP4 may appear more apparent at the basal surface in FW reared anal papillae possibly due to glycosylation signaling for cell surface expression (Hendriks et al., 2004). Despite AaAQP4 transcript abundance decrease in response to BW rearing, AaAQP4 protein abundance was unaltered indicating asynchronous protein degradation rates in the two external salinity concentration environments as mentioned previously. Therefore, elucidating AaAQP4 regulation would shed light on its function in the anal papillae.

AaAQP4 appeared on the basal membrane in FW sections with diminished immunofluorescence signal in BW anal papillae as was previously demonstrated (Figure 33) (Akhter et al., 2017). AaAQP4 was not found on the apical membrane in FW samples as was

previously shown in ion poor reared larvae, which may be a mechanism of adaptation to the different water conditions in the studies. Anal papillae would benefit from expressing AaAQP4 on the apical membrane to avoid passive water absorption into the hemolymph due to the highly concentrated hemolymph in comparison to the external environment and also because of AaAQP4's poor water transport conductance. Therefore, under more dilute conditions than FW, apical AaAQP4 localization would be beneficial. AaAQP4 localization at the basal membrane is implicated in facilitating trehalose transport into the cell for ATP production used in the active uptake of ions and cellular function in FW conditions (Akhter et al., 2017). Additionally, AaAQP4 has also been proposed to facilitate transepithelial ammonia transport; whereby ammonia is removed from the hemolymph through basal localized AaAQP4 and apically excreted out of the cell through Rh or Amt channels (Akhter et al., 2017; Chasiotis et al., 2016; Durant et al., 2017).

4.7.1 AaAQP5

AaAQP5 transcript abundance was highly elevated in the anal papillae of FW and BW reared larvae when compared to other AaAQP genes, implicating AaAQP5 in water and trehalose transport across the anal papillae epithelium. AaAQP5 was previously demonstrated to express to lesser abundance than other AaAQP genes when larvae were reared in ion poor water or distilled water indicating that AaAQP5 expression in low ion conditions perhaps hinders osmoregulation in the larvae (Akhter et al., 2017; Marusalin et al., 2012). AaAQP5 transcript abundance did not change with BW rearing. A previous study assessing AaAQP5 transcript abundance in ion poor and BW reared larvae demonstrated significantly elevated AaAQP5 transcript abundance in response to increasing external salinity (Akhter et al., 2017). The lack of AaAQP5 transcript abundance changes in the current study may reflect the previously mentioned

discrepancy in salinity concentrations and the magnitude difference between the salt concentrations in the rearing media being compared.

Western blotting with anal papillae protein homogenates probed with AaAQP5 antibody displayed a single resolved band at ~26 kDa which was the predicted AaAQP5 monomer that was confirmed to be AaAQP5 protein based on peptide block results. This band was also identified previously in BW reared larvae supporting antibody specificity (Akhter et al., 2017). AaAQP5 protein abundance was highly elevated in the anal papillae in response to greater external salinity concentrations when compared to FW, which did not follow the trend of AaAQP5 transcript abundance. As previously mentioned this may also be due to the asynchronous protein degradation in the two water conditions despite the stable mRNA abundance. An increase in AaAQP5 protein abundance in BW was also observed when compared to ion poor water larvae. AaAQP5 localized to the basal membrane as previously shown in the same BW reared conditions is proposed to facilitate the transport of water and trehalose from the hemolymph into the cytosol of the anal papillae epithelium (Figure 33) (Akhter et al., 2017). The basal transport of water is predicted to maintain cellular volume based on AaAQP5's previously proposed osmosensing functions (Akhter et al., 2017). AaAQP5 may also transport trehalose intracellularly to maintain cell volume by accumulating trehalose in the cell to maintain the osmotic gradient between the hemolymph and the external environment in BW as well as provide energy for ATP synthesis that energizes ATPases (Elbein et al., 2003; Liu et al., 2013). Tree frog, *Hyla japonica*, AQP-h3BL possesses water and glycerol conductance and is localized to the basolateral surface of skin epithelial cells (Akabane et al., 2007). AQP-h3BL has been implicated in the hydration of the epidermis as well as osmoregulation in the *H. japonica* which may relate to the function of basally localized AaAQP5 (Akabane et al., 2007).

AaAQP5 is a multifunctional AaAQP channels important for homeostasis of water in BW conditions as well as trehalose uptake into tissues for energy use or osmoregulation.

AaAQPs with high water conductance were downregulated in FW water conditions, such as AaAQP1 and AaAQP5 while poor water conducting AaAQP4, was upregulated possibly in an effort to reduce the passive water uptake that would result in hemolymph dilution. Opposite trends were observed in BW conditions where high water permeating AaAQPs were upregulated to allow for passive water transport since the osmotic gradient between the hemolymph and the external environment is reduced or eliminated.

4.8 Conclusions

Larval *A. aegypti* mosquito control efforts have predominantly focused on the elimination and treatment of their freshwater habitats. However, *A. aegypti* populations have been shown to thrive in brackish water and this necessitates the understanding of their physiological plasticity in response to salinity changes to their aquatic habitats. This would enable the development of mosquito control agents that may target diverse habitats with greater potency and specificity. AaAQPs are the channels that facilitate the transport of water across cell membranes and allow animals to osmoregulate; however, this has not been shown in mosquitoes. This study sets the basis for understanding the function of AaAQPs in the osmoregulatory organs of larval *A. aegypti* by mapping the expression of these transporters in larvae that were reared in FW and BW. This comprehensive study delineates the changes in mRNA abundance in the major osmoregulatory organs in response to changes in environmental salinity. Additionally, a complete expression of mRNA, protein, and protein localization is provided for AaAQP1, AaAQP4, and AaAQP5 in the osmoregulatory organs that shed light on the potential functional role of these AaAQPs in facilitating water and solute movement across the transcellular pathway.

AaAQPs were identified in all the osmoregulatory organs examined in both FW and BW aquatic conditions, suggesting their significance in the function of the cells, epithelia, and subsequently organs despite osmoregulatory changes that arise with salinity rearing. The various osmoregulatory organs responded to the elevated external salinity by changing the abundance of mRNA or protein, or both as a potential means for altering the osmoregulatory function of the organs. Additionally, immunolocalization provided evidence that AaAQP1, AaAQP4, and AaAQP5 may be regulated through changing AaAQP membrane localization through translocation in different rearing conditions. However, the pathway responsible for changes in

AaAQP localization within the cellular membrane require further analysis. AaAQP1, AaAQP4 and AaAQP5 membrane localization also revealed transcellular water and solute pathways in the various osmoregulatory organs which, help elucidate organ function and water pathways.

To further understand osmoregulatory function of the various organs highlighted in this study as well as the role AaAQPs play in water and solute permeability, assessment of AaAQP3 and AaAQP6 conductance require further inquiry by heterologous expression in oocytes. Additionally, AaAQP2, AaAQP3, AaAQP4, AaAQP5, and AaAQP6 function with changes to extracellular pH environments would contribute to understanding AaAQP function in the anterior midgut. Finally, assessing AaAQP4 conductance of ammonia would demonstrate its purpose in various osmoregulatory organs such as the Malpighian tubules and the anal papillae, where transcellular ammonia excretion through AaAQP4 would be beneficial. The results provide a basis of understanding for the role of AQPs in the osmoregulatory processes of *A. aegypti* larvae which, through further studies may identify new targets for the development of novel mosquito control agents for larvae prior to their emergence into the disease vector adult life stage.

5. REFERENCES

- Abascal, F., Irisarri, I. and Zardoya, R.** (2014). Diversity and evolution of membrane intrinsic proteins. *Biochim. Biophys. Acta - Gen. Subj.* **1840**, 1468–1481.
- Adler, P. H.** (2009). *Insect biodiversity: Science and society*. Wiley-Blackwell.
- Agre, P., Sasaki, S. and Chrispeels, M. J.** (1993). Aquaporins: a family of water channel proteins. *Am. J. Physiol.* **265**, F461.
- Akabane, G., Ogushi, Y., Hasegawa, T., Suzuki, M. and Tanaka, S.** (2007). Gene cloning and expression of an aquaporin (AQP-h3BL) in the basolateral membrane of water-permeable epithelial cells in osmoregulatory organs of the tree frog. *Am. J. Physiol. Integr. Comp. Physiol.* **292**, R2340–R2351.
- Akhter, H., Misyura, L., Bui, P. and Donini, A.** (2017). Salinity responsive aquaporins in the anal papillae of the larval mosquito, *Aedes aegypti*. *Comp. Biochem. Physiol. -Part A Mol. Integr. Physiol.* **203**, 144–151.
- Aly, C. and Dadd, R.** (1989). Drinking rate regulation in some freshwater mosquito larvae. *Physiol. Entomol.* **14**, 241–256.
- Aoki, M., Kaneko, T., Katoh, F., Hasegawa, S., Tsutsui, N. and Aida, K.** (2003). Intestinal water absorption through aquaporin 1 expressed in the apical membrane of mucosal epithelial cells in seawater-adapted Japanese eel. *J. Exp. Biol.* **206**, 3495–505.
- Arenstein, I. R., Caruso-Neves, C., Onuchic, L. F. and Lopes, A. G.** (1995). Mechanisms of cell volume regulation in the proximal segment of the Malpighian tubule of *Rhodnius neglectus*. *J. Membr. Biol.* **146**, 47–57.
- Asakura, K.** (1980). The anal portion as a salt-excreting organ in a seawater mosquito larva, *Aedes togoi* Theobald. *J. Comp. Physiol. B* **138**, 59–65.

- Azuma, M., Nagae, T., Maruyama, M., Kataoka, N. and Miyake, S.** (2012). Two water-specific aquaporins at the apical and basal plasma membranes of insect epithelia: Molecular basis for water recycling through the cryptonephric rectal complex of lepidopteran larvae. *J. Insect Physiol.* **58**, 523–533.
- Beitz, E., Wu, B., Holm, L. M., Schultz, J. E. and Zeuthen, T.** (2006). Point mutations in the aromatic/arginine region in aquaporin 1 allow passage of urea, glycerol, ammonia, and protons. *Proc. Natl. Acad. Sci. U. S. A.* **103**, 269–74.
- Benedict, M.** (2003). The first releases of transgenic mosquitoes: an argument for the sterile insect technique. *Trends Parasitol.* **19**, 349–355.
- Beyenbach, K.** (1995). Mechanism and regulation of electrolyte transport in Malpighian tubules. *J. Insect Physiol.* **41**, 197–207.
- Beyenbach, K.** (2003). Transport mechanisms of diuresis in Malpighian tubules of insects. *J. Exp. Biol.* **206**, 3845–3856.
- Beyenbach, K. W. and Piermarini, P. M.** (2011). Transcellular and paracellular pathways of transepithelial fluid secretion in Malpighian (renal) tubules of the yellow fever mosquito *Aedes aegypti*. *Acta Physiol. (Oxf)*. **202**, 387–407.
- Beyenbach, K. and Wiczorek, H.** (2006). The V-type H⁺ ATPase: molecular structure and function, physiological roles and regulation. *J. Exp. Biol.* **209**, 557–589.
- Beyenbach, K., Pannabecker, T. and Nagel, W.** (2000). Central role of the apical membrane H⁺-ATPase in electrogenesis and epithelial transport in Malpighian tubules. *J. Exp. Biol* **203**, 1459–1468.
- Beyenbach, K. W., Skaer, H. and Dow, J. A. T.** (2010). The developmental, molecular, and transport biology of Malpighian tubules. *Annu. Rev. Entomol.* **55**, 351–374.

- Bhatt, S., Gething, P. W., Brady, O. J., Messina, J. P., Farlow, A. W., Moyes, C. L., Drake, J. M., Brownstein, J. S., Hoen, A. G., Sankoh, O., et al.** (2013). The global distribution and burden of dengue. *Nature* **496**, 504–7.
- Boassa, D., Stamer, W. D. and Yool, A. J.** (2006). Ion channel function of aquaporin-1 natively expressed in choroid plexus. *J. Neurosci.* **26**, 7811–9.
- Bonenfant, D., Schmelzle, T., Jacinto, E., Crespo, J. L., Mini, T., Hall, M. N. and Jenoe, P.** (2003). Quantitation of changes in protein phosphorylation: a simple method based on stable isotope labeling and mass spectrometry. *Proc. Natl. Acad. Sci. U. S. A.* **100**, 880–5.
- Boudko, D. Y.** (2012). Molecular basis of essential amino acid transport from studies of insect nutrient amino acid transporters of the SLC6 family (NAT-SLC6). *J. Insect Physiol.* **58**, 433–449.
- Boudko, D. Y., Moroz, L. L., Linser, P. J., Trimarchi, J. R., Smith, P. J. and Harvey, W. R.** (2001a). In situ analysis of pH gradients in mosquito larvae using non-invasive, self-referencing, pH-sensitive microelectrodes. *J. Exp. Biol.* **204**, 691–699.
- Boudko, D. Y., Moroz, L. L., Harvey, W. R. and Linser, P. J.** (2001b). Alkalinization by chloride/bicarbonate pathway in larval mosquito midgut. *Proc. Natl. Acad. Sci. U. S. A.* **98**, 15354–9.
- Boudko, D. Y., Tsujimoto, H., Rodriguez, S. D., Meleshkevitch, E. A., Price, D. P., Drake, L. L. and Hansen, I. A.** (2015). Substrate specificity and transport mechanism of amino-acid transceptor Slimfast from *Aedes aegypti*. *Nat. Commun.* **6**, 8546.
- Bradley, T.** (1987). Physiology of osmoregulation in mosquitoes. *Annu. Rev. Entomol.* **32**, 439–462.
- Bradley, T. J. and Phillips, J. E.** (1975). The secretion of hyperosmotic fluid by the rectum of a

- saline-water mosquito larva, *Aedes taeniorhynchus*. *J. Exp. Biol.* **63**, 331–342.
- Bradley, T. J. and Snyder, C.** (1989). Fluid secretion and microvillar ultrastructure in mosquito Malpighian tubules. *Am. J. Physiol.* **257**, R1096-102.
- Bradley, T., Strange, K. and Phillips, J.** (1984). Osmotic and ionic regulation in saline-water mosquito larvae. *Osmoregul. Estuar. Mar. Anim.* **9**, 35–50.
- Brown, D., Hasler, U., Nunes, P., Bouley, R. and Lu, H. A. J.** (2008). Phosphorylation events and the modulation of aquaporin 2 cell surface expression. *Curr. Opin. Nephrol. Hypertens.* **17**, 491–8.
- Cabrero, P., Pollock, V. P., Davies, S. A. and Dow, J. A. T.** (2004). A conserved domain of alkaline phosphatase expression in the Malpighian tubules of dipteran insects. *J. Exp. Biol.* **207**, 3299–305.
- Campbell, E. M., Ball, A., Hoppler, S. and Bowman, A. S.** (2008). Invertebrate aquaporins: a review. *J. Comp. Physiol. B* **178**, 935–55.
- Caruso-Neves, C., Silva, I. V, Morales, M. M. and Lopes, A. G.** (2001). Cytoskeleton elements mediate the inhibition of the (Na⁺/K⁺) ATPase activity by PKC in *Rhodnius prolixus* Malpighian tubules during hyperosmotic shock. *Arch. Insect Biochem. Physiol.* **48**, 81–8.
- Chamberlain, R. and Sudia, W.** (1961). Mechanism of transmission of viruses by mosquitoes. *Annu. Rev. Entomol.* **6**, 371–390.
- Chasiotis, H., Ionescu, A., Misyura, L., Bui, P., Fazio, K., Wang, J., Patrick, M., Weihrauch, D. and Donini, A.** (2016). An animal homolog of plant Mep/Amt transporters promotes ammonia excretion by the anal papillae of the disease vector mosquito, *Aedes aegypti*. *J. Exp. Biol.* **219**, 10.1242/jeb.134494.

- Clark, T. M. and Bradley, T. J.** (1996). Stimulation of Malpighian tubules from larval *Aedes aegypti* by secretagogues. *J. Insect Physiol.* **42**, 593–602.
- Clark, T. M., Koch, A. and Moffett, D. F.** (1999). The anterior and posterior “stomach” regions of larval *Aedes aegypti* midgut: regional specialization of ion transport and stimulation by 5-hydroxytryptamine. *J. Exp. Biol.* **202**, 247–252.
- Clark, T. M., Flis, B. J. and Remold, S. K.** (2004). Differences in the effects of salinity on larval growth and developmental programs of a freshwater and a euryhaline mosquito species (Insecta: Diptera, Culicidae). *J. Exp. Biol.* **207**, 2289–95.
- Clark, T. M., Hutchinson, M. J., Huegel, K. L., Moffett, S. B. and Moffett, D. F.** (2005). Additional morphological and physiological heterogeneity within the midgut of larval *Aedes aegypti* (Diptera: Culicidae) revealed by histology, electrophysiology, and effects of *Bacillus thuringiensis* endotoxin. *Tissue Cell* **37**, 457–468.
- Coetzee, M. and Sueur, D. Le** (1988). Effects of salinity on the larvae of some Afrotropical anopheline mosquitoes. *Med. Vet. Entomol.* **2**, 385–390.
- Corena, M. P., Seron, T. J., Lehman, H. K., Ochrietor, J. D., Kohn, A., Tu, C. and Linser, P. J.** (2002). Carbonic anhydrase in the midgut of larval *Aedes aegypti* : cloning, localization and inhibition. *J. Exp. Biol.* **205**, 591–602.
- D’Silva, N. M. and O’Donnell, M. J.** (2018). The gastric caecum of larval *Aedes aegypti*: stimulation of epithelial ion transport by 5-hydroxytryptamine and cAMP. *J. Exp. Biol.* **221**, jeb172866.
- D’Silva, N. M., Patrick, M. L. and O’Donnell, M. J.** (2017). Effects of rearing salinity on expression and function of ion-motive ATPases and ion transport across the gastric caecum of *Aedes aegypti* larvae. *J. Exp. Biol.* **220**, 3172–3180.

- Dadd, R. H.** (1975). Alkalinity within the midgut of mosquito larvae with alkaline-active digestive enzymes. *J. Insect Physiol.* **21**, 1847–1853.
- Del Duca, O., Nasirian, A., Galperin, V. and Donini, A.** (2011). Pharmacological characterisation of apical Na⁺ and Cl⁻ transport mechanisms of the anal papillae in the larval mosquito *Aedes aegypti*. *J. Exp. Biol.* **214**, 3992–3999.
- Delporte, C. and Steinfeld, S.** (2006). Distribution and roles of aquaporins in salivary glands. *Biochim. Biophys. Acta - Biomembr.* **1758**, 1061–1070.
- Dephoure, N., Gould, K. L., Gygi, S. P. and Kellogg, D. R.** (2013). Mapping and analysis of phosphorylation sites: a quick guide for cell biologists. *Mol. Biol. Cell* **24**, 535–42.
- Donini, A. and O'Donnell, M.** (2005). Analysis of Na⁺, Cl⁻, K⁺, H⁺ and NH₄⁺ concentration gradients adjacent to the surface of anal papillae of the mosquito *Aedes aegypti*: application of self-referencing ion-selective mi. *J. Exp. Biol.* **208**, 603–610.
- Donini, A., Patrick, M. L., Bijelic, G., Christensen, R. J., Ianowski, J. P., Rheault, M. R. and O'Donnell, M. J.** (2006). Secretion of water and ions by malpighian tubules of larval mosquitoes: effects of diuretic factors, second messengers, and salinity. *Physiol. Biochem. Zool.* **79**, 645–55.
- Donini, A., Gaidhu, M. P., Strasberg, D. R. and O'donnell, M. J.** (2007). Changing salinity induces alterations in hemolymph ion concentrations and Na⁺ and Cl⁻ transport kinetics of the anal papillae in the larval mosquito, *Aedes aegypti*. *J. Exp. Biol.* **210**, 983–92.
- Drake, L. L., Boudko, D. Y., Marinotti, O., Carpenter, V. K., Dawe, A. L. and Hansen, I. A.** (2010). The Aquaporin gene family of the yellow fever mosquito, *Aedes aegypti*. *PLoS One* **5**, e15578.
- Drake, L. L., Rodriguez, S. D. and Hansen, I. A.** (2015). Functional characterization of

aquaporins and aquaglyceroporins of the yellow fever mosquito, *Aedes aegypti*. *Sci. Rep.* **5**, 7795.

Duchesne, L., Hubert, J.-F., Verbavatz, J.-M., Thomas, D. and Pietrantonio, P. V. (2003).

Mosquito (*Aedes aegypti*) aquaporin, present in tracheolar cells, transports water, not glycerol, and forms orthogonal arrays in *Xenopus* oocyte membranes. *Eur. J. Biochem.* **270**, 422–429.

Durant, A. C. and Donini, A. (2018). Ammonia excretion in an osmoregulatory syncytium is facilitated by AeAmt2, a novel ammonia transporter in *Aedes aegypti* larvae. *Front. Physiol.* **9**, 339.

Durant, A. C., Chasiotis, H., Misyura, L. and Donini, A. (2017). *Aedes aegypti* Rhesus glycoproteins contribute to ammonia excretion by larval anal papillae. *J. Exp. Biol.* **220**, 588–596.

Echevarría, M., Ramírez-Lorca, R., Hernández, C. S., Gutiérrez, A., Méndez-Ferrer, S., González, E., Toledo-Aral, J. J., Ilundáin, A. A. and Whittombury, G. (2001).

Identification of a new water channel (Rp-MIP) in the Malpighian tubules of the insect *Rhodnius prolixus*. *Pflugers Arch. Eur. J. Physiol.* **442**, 27–34.

Edwards, H. (1982a). Ion concentration and activity in the haemolymph of *Aedes aegypti* larvae. *J. Exp. Biol.* **101**, 143–151.

Edwards, H. (1982b). *Aedes aegypti*: energetics of osmoregulation. *J. Exp. Biol.* **101**, 135–141.

Edwards, H. (1982c). Free amino acids as regulators of osmotic pressure in aquatic insect larvae. *J. Exp. Biol.* **101**, 153–160.

Edwards, H. and Harrison, J. B. (1983). An osmoregulatory syncytium and associated cells in a freshwater mosquito. *Tissue Cell* **15**, 271–280.

- Elbein, A., Pan, Y., Pastuszak, I. and Carroll, D.** (2003). New insights on trehalose: a multifunctional molecule. *Glycobiology* **13**, 17R–27R.
- Endeward, V., Musa-Aziz, R., Cooper, G. J., Chen, L.-M., Pelletier, M. F., Virkki, L. V., Supuran, C. T., King, L. S., Boron, W. F. and Gros, G.** (2006). Evidence that aquaporin 1 is a major pathway for CO₂ transport across the human erythrocyte membrane. *FASEB J.* **20**, 1974–81.
- Finn, R. N. and Cerdá, J.** (2015). Evolution and functional diversity of aquaporins. *Biol. Bull.* **229**, 6–23.
- Finn, R. N., Chauvigné, F., Stavang, J. A., Belles, X. and Cerdà, J.** (2015). Insect glycerol transporters evolved by functional co-option and gene replacement. *Nat. Commun.* **6**, 7814.
- Fischer, M. and Kaldenhoff, R.** (2008). On the pH regulation of plant aquaporins. *J. Biol. Chem.* **283**, 33889–92.
- Fu, D. and Lu, M.** (2007). The structural basis of water permeation and proton exclusion in aquaporins (Review). *Mol. Membr. Biol.* **24**, 366–374.
- Fu, G., Lees, R., Nimmo, D., Aw, D., Jin, L., Gary, P., Berendonk, T., White-Cooper, H., Scaife, S., Phuc, H., et al.** (2010). Female-specific flightless phenotype for mosquito control. *Proc. Natl. Acad. Sci.* **107**, 4550–4554.
- Fushimi, K., Sasaki, S. and Marumo, F.** (1997). Phosphorylation of serine 256 is required for cAMP-dependent regulatory exocytosis of the aquaporin-2 water channel. *J. Biol. Chem.* **272**, 14800–4.
- Gallardo, P., Cid, L. P., Vio, C. P. and Sepúlveda, F. V.** (2001). Aquaporin-2, a regulated water channel, is expressed in apical membranes of rat distal colon epithelium. *Am. J. Physiol. Gastrointest. Liver Physiol.* **281**, G856-63.

- García, F., Kierbel, A., Larocca, M. C., Gradilone, S. A., Splinter, P., LaRusso, N. F. and Marinelli, R. A.** (2001). The water channel aquaporin-8 is mainly intracellular in rat hepatocytes, and its plasma membrane insertion is stimulated by cyclic AMP. *J. Biol. Chem.* **276**, 12147–52.
- Garrett, M. and Bradley, T.** (1984). Ultrastructure of osmoregulatory organs in larvae of the brackish water mosquito, *Culiseta inornata* (Williston). *J. Morphol.* **182**, 257–277.
- Groot, B. De, Frigato, T., Helms, V. and Grubmüller, H.** (2003). The mechanism of proton exclusion in the aquaporin-1 water channel. *J. Mol. Biol.* **333**, 279–293.
- Gu, F., Hata, R., Toku, K., Yang, L., Ma, Y.-J., Maeda, N., Sakanaka, M. and Tanaka, J.** (2003). Testosterone up-regulates aquaporin-4 expression in cultured astrocytes. *J. Neurosci. Res.* **72**, 709–15.
- Han, Z., Wax, M. B. and Patil, R. V.** (1998). Regulation of aquaporin-4 water channels by phorbol ester-dependent protein phosphorylation. *J. Biol. Chem.* **273**, 6001–6004.
- Hartridge, H. and Roughton, F. J. W.** (1923). A Method of Measuring the Velocity of Very Rapid Chemical Reactions. *Proc. R. Soc. A* **104**, 376–394.
- Hendriks, G., Koudijs, M., van Balkom, B. W. M., Oorschot, V., Klumperman, J., Deen, P. M. T. and van der Sluijs, P.** (2004). Glycosylation is important for cell surface expression of the water channel aquaporin-2 but is not essential for tetramerization in the endoplasmic reticulum. *J. Biol. Chem.* **279**, 2975–83.
- Hiroaki, Y., Tani, K., Kamegawa, A., Gyobu, N., Nishikawa, K., Suzuki, H., Walz, T., Sasaki, S., Mitsuoka, K., Kimura, K., et al.** (2006). Implications of the aquaporin-4 structure on array formation and cell adhesion. *J. Mol. Biol.* **355**, 628–639.
- Hofmann** (1993). TMbase - A database of membrane spanning proteins segments. *Biol. Chem.*

Hoppe-Seyler **374**,.

- Hub, J. and Groot, B. De** (2007). Mechanism of selectivity in aquaporins and aquaglyceroporins. *Proc. Natl. Acad. Sci.* **105**, 1198–1203.
- Ishibashi, K., Kuwahara, M., Gu, Y., Kageyama, Y., Tohsaka, A., Suzuki, F., Marumo, F. and Sasaki, S.** (1997). Cloning and functional expression of a new water channel abundantly expressed in the testis permeable to water, glycerol, and urea. *J. Biol. Chem.* **272**, 20782–20786.
- Ishikawa, Y., Eguchi, T., Skowronski, M. T. and Ishida, H.** (1998). Acetylcholine acts on M3 muscarinic receptors and induces the translocation of aquaporin5 water channel via cytosolic Ca²⁺ elevation in rat parotid glands. *Biochem. Biophys. Res. Commun.* **245**, 835–840.
- Jagadeshwaran, U., Onken, H., Hardy, M., Moffett, S. B. and Moffett, D. F.** (2010). Cellular mechanisms of acid secretion in the posterior midgut of the larval mosquito (*Aedes aegypti*). *J. Exp. Biol.* **213**, 295–300.
- Jahn, T., Møller, A., Zeuthen, T., Holm, L., Klærke, D. A., Mohsin, B., Kühlbrandt, W. and Schjoerring, J. K.** (2004). Aquaporin homologues in plants and mammals transport ammonia. *FEBS Lett.* **574**, 31–36.
- Jefferies, K. C., Cipriano, D. J. and Forgac, M.** (2008). Function, structure and regulation of the vacuolar (H⁺)-ATPases. *Arch. Biochem. Biophys.* **476**, 33–42.
- Jonusaite, S., Kelly, S. P. and Donini, A.** (2011). The physiological response of larval *Chironomus riparius* (Meigen) to abrupt brackish water exposure. *J. Comp. Physiol. B Biochem. Syst. Environ. Physiol.* **181**, 343–352.
- Jonusaite, S., Kelly, S. P. and Donini, A.** (2013). Tissue-specific ionomotive enzyme activity

- and K⁺ reabsorption reveal the rectum as an important ionoregulatory organ in larval *Chironomus riparius* exposed to varying salinity. *J. Exp. Biol.* **216**,.
- Jonusaite, S., Donini, A. and Kelly, S. P.** (2016). Occluding junctions of invertebrate epithelia. *J. Comp. Physiol. B.* **186**, 17–43.
- Jonusaite, S., Donini, A. and Kelly, S. P.** (2017a). Salinity alters snakeskin and mesh transcript abundance and permeability in midgut and Malpighian tubules of larval mosquito, *Aedes aegypti*. *Comp. Biochem. Physiol. Part A Mol. Integr. Physiol.* **205**, 58–67.
- Jonusaite, S., Kelly, S. P. and Donini, A.** (2017b). Identification of the septate junction protein gliotactin in the mosquito *Aedes aegypti*: evidence for a role in increased paracellular permeability in larvae. *J. Exp. Biol.* **220**, 2354–2363.
- Jung, J. S., Preston, G. M., Smith, B. L., Guggino, W. B. and Agre, P.** (1994). Molecular structure of the water channel through aquaporin CHIP. The hourglass model. *J. Biol. Chem.* **269**, 14648–54.
- Kambara, K., Takematsu, Y., Azuma, M. and Kobayashi, J.** (2009). cDNA cloning of aquaporin gene expressed in the digestive tract of the Formosan subterranean termite, *Coptotermes formosanus* Shiraki (Isoptera; Rhinotermitidae). *Appl. Entomol. Zool.* **44**, 315–321.
- Kamsteeg, E. J., Heijnen, I., van Os, C. H. and Deen, P. M.** (2000). The subcellular localization of an aquaporin-2 tetramer depends on the stoichiometry of phosphorylated and nonphosphorylated monomers. *J. Cell Biol.* **151**, 919–30.
- Kamsteeg, E.-J., Hendriks, G., Boone, M., Konings, I. B. M., Oorschot, V., van der Sluijs, P., Klumperman, J. and Deen, P. M. T.** (2006). Short-chain ubiquitination mediates the regulated endocytosis of the aquaporin-2 water channel. *Proc. Natl. Acad. Sci. U. S. A.* **103**,

18344–9.

Kang'ethe, W., Aimanova, K. G., Pullikuth, A. K. and Gill, S. S. (2007). NHE8 mediates amiloride-sensitive Na^+/H^+ exchange across mosquito Malpighian tubules and catalyzes Na^+ and K^+ transport in reconstituted proteoliposomes. *Am. J. Physiol. Physiol.* **292**, F1501–F1512.

Kataoka, N., Miyake, S. and Azuma, M. (2009). Aquaporin and aquaglyceroporin in silkworms, differently expressed in the hindgut and midgut of *Bombyx mori*. *Insect Mol. Biol.* **18**, 303–314.

Kaufmann, N., Mathai, J. C., Hill, W. G., Dow, J. A. T., Zeidel, M. L. and Brodsky, J. L. (2005). Developmental expression and biophysical characterization of a *Drosophila melanogaster* aquaporin. *Am. J. Physiol. Cell Physiol.* **289**, C397–407.

Kim, J.-H., Park, S.-H., Moon, Y. W., Hwang, S., Kim, D., Jo, S.-H., Oh, S. B., Kim, J. S., Jahng, J. W., Lee, J.-H., et al. (2009). Histamine H1 receptor induces cytosolic calcium increase and aquaporin translocation in human salivary gland cells. *J. Pharmacol. Exp. Ther.* **330**, 403–12.

Klassen, W. and Curtis, C. (2005). History of the sterile insect technique. *Sterile Insect Tech.* 3–36.

Kraemer, M. U. G., Sinka, M. E., Duda, K. A., Mylne, A., Shearer, F. M., Barker, C. M., Moore, C. G., Carvalho, R. G., Coelho, G. E., Van Bortel, W., et al. (2015). The global distribution of the arbovirus vectors *Aedes aegypti* and *Ae. albopictus*. *Elife* **4**, e08347.

Kwon, T.-H., Frøkiær, J. and Nielsen, S. (2013). Regulation of aquaporin-2 in the kidney: A molecular mechanism of body-water homeostasis. *Kidney Res. Clin. Pract.* **32**, 96–102.

Larsen, E. H., Deaton, L. E., Onken, H., O'Donnell, M., Grosell, M., Dantzler, W. H. and

- Weihrauch, D.** (2014). Osmoregulation and Excretion. In *Comprehensive Physiology*, pp. 405–573. Hoboken, NJ, USA: John Wiley & Sons, Inc.
- Le Caherec, F., Guillam, M. T., Beuron, F., Cavalier, A., Thomas, D., Gouranton, J. and Hubert, J. F.** (1997). Aquaporin-related proteins in the filter chamber of homopteran insects. *Cell Tissue Res.* **290**, 143–51.
- Lines, J. and Kleinschmidt, I.** (2015). Is malaria control better with both treated nets and spraying? *Lancet* **385**, 1375–1377.
- Linser, P. J., Smith, K. E., Seron, T. J. and Neira Oviedo, M.** (2009). Carbonic anhydrases and anion transport in mosquito midgut pH regulation. *J. Exp. Biol.* **212**, 1662–71.
- Litman, T., Sogaard, R. and Zeuthen, T.** (2009). Ammonia and urea permeability of mammalian aquaporins. *Aquaporins* **190**, 327–58.
- Liu, K., Tsujimoto, H., Cha, S.-J., Agre, P. and Rasgon, J. L.** (2011). Aquaporin water channel AgAQP1 in the malaria vector mosquito *Anopheles gambiae* during blood feeding and humidity adaptation. *Proc. Natl. Acad. Sci. U. S. A.* **108**, 6062–6.
- Liu, K., Dong, Y., Huang, Y., Rasgon, J. and Agre, P.** (2013). Impact of trehalose transporter knockdown on *Anopheles gambiae* stress adaptation and susceptibility to *Plasmodium falciparum* infection. *Proc. Natl. Acad. Sci.* **110**, 17504–17509.
- Liu, K., Tsujimoto, H., Huang, Y., Rasgon, J. L. and Agre, P.** (2016). Aquaglyceroporin function in the malaria mosquito *Anopheles gambiae*. *Biol. Cell* **108**, 294–305.
- Lu, H.-L., Kersch, C. and Pietrantonio, P.** (2011). The kinin receptor is expressed in the Malpighian tubule stellate cells in the mosquito *Aedes aegypti* (L.): a new model needed to explain ion transport? *Insect Biochem. Mol. Biol.* **41**, 135–40.
- Mahmood, T. and Yang, P.-C.** (2012). Western blot: technique, theory, and trouble shooting.

- N. Am. J. Med. Sci.* **4**, 429–34.
- Mandell, J. W.** (2003). Phosphorylation State-Specific Antibodies: Applications in Investigative and Diagnostic Pathology. *Am. J. Pathol.* **163**, 1687–1698.
- Marinelli, R. A., Pham, L., Agre, P. and LaRusso, N. F.** (1997). Secretin promotes osmotic water transport in rat cholangiocytes by increasing aquaporin-1 water channels in plasma membrane. Evidence for a secretin-induced vesicular translocation of aquaporin-1. *J. Biol. Chem.* **272**, 12984–12988.
- Marinelli, R. A., Tietz, P. S., Pham, L. D., Rueckert, L., Agre, P. and LaRusso, N. F.** (1999). Secretin induces the apical insertion of aquaporin-1 water channels in rat cholangiocytes. *Am. J. Physiol. - Gastrointest. Liver Physiol.* **276**,.
- Marrades, M. P., Milagro, F. I., Martínez, J. A. and Moreno-Aliaga, M. J.** (2006). Differential expression of aquaporin 7 in adipose tissue of lean and obese high fat consumers. *Biochem. Biophys. Res. Commun.* **339**, 785–789.
- Martini, S. V, Goldenberg, R. C., Fortes, F. S. A., Campos-de-Carvalho, A. C., Falkenstein, D. and Morales, M. M.** (2004). *Rhodnius prolixus* Malpighian tubule's aquaporin expression is modulated by 5-hydroxytryptamine. *Arch. Insect Biochem. Physiol.* **57**, 133–41.
- Marusalin, J., Matier, B. J., Rheault, M. R. and Donini, A.** (2012). Aquaporin homologs and water transport in the anal papillae of the larval mosquito, *Aedes aegypti*. *J. Comp. Physiol. B* **182**, 1047–56.
- Meredith, J. and Phillips, J. E.** (1973). Rectal ultrastructure in salt- and freshwater mosquito larvae in relation to physiological state. *Zeitschrift fur Zellforsch. und Mikroskopische Anat.* **138**, 1–22.

- Milam, C. D., Farris, J. L. and Wilhide, J. D.** (2000). Evaluating mosquito control pesticides for effect on target and nontarget organisms. *Arch. Environ. Contam. Toxicol.* **39**, 324–8.
- Misyura, L., Yerushalmi, G. Y. and Donini, A.** (2017). A mosquito entomoglyceroporin, *Aedes aegypti* AQP5 participates in water transport across the Malpighian tubules of larvae. *J. Exp. Biol.* **220**, jeb.158352.
- Moffett, D. F., Jagadeshwaran, U., Wang, Z., Davis, H. M., Onken, H. and Goss, G. G.** (2012). Signaling by intracellular Ca^{2+} and H^+ in larval mosquito (*Aedes aegypti*) midgut epithelium in response to serosal serotonin and lumen pH. *J. Insect Physiol.* **58**, 506–512.
- Murata, K., Mitsuoka, K., Hirai, T., Walz, T., Agre, P., Heymann, J., Engel, A. and Fujiyoshi, Y.** (2000). Structural determinants of water permeation through aquaporin-1. *Nature* **407**, 599–605.
- Nagae, T., Miyake, S., Kosaki, S. and Azuma, M.** (2013). Identification and characterisation of a functional aquaporin water channel (Anomala cuprea DRIP) in a coleopteran insect. *J. Exp. Biol.* **216**, 2564–72.
- Neely, J. D., Christensen, B. M., Nielsen, S. and Agre, P.** (1999). Heterotetrameric composition of aquaporin-4 water channels. *Biochemistry* **38**, 11156–11163.
- Nejsum, L., Zelenina, M., Aperia, A., Frokiaer, J. and Nielsen, S.** (2005). Bidirectional regulation of AQP2 trafficking and recycling: involvement of AQP2-S256 phosphorylation. *Am. J. Physiol. - Ren. Physiol.* **288**, F930–F938.
- Nemeth-Cahalan, K. L., Kalman, K. and Hall, J.** (2004). Molecular basis of pH and Ca^{2+} regulation of aquaporin water permeability. *J. Gen. Physiol.* **123**, 573–580.
- Németh-Cahalan, K. L. and Hall, J. E.** (2000). pH and calcium regulate the water permeability of aquaporin 0. *J. Biol. Chem.* **275**, 6777–82.

- Nielsen, S., Chou, C. L., Marples, D., Christensen, E. I., Kishore, B. K. and Knepper, M. A.** (1995). Vasopressin increases water permeability of kidney collecting duct by inducing translocation of aquaporin-CD water channels to plasma membrane. *Proc. Natl. Acad. Sci.* **92**, 1013–1017.
- O'Connor, K. and Beyenbach, K.** (2001). Chloride channels in apical membrane patches of stellate cells of Malpighian tubules of *Aedes aegypti*. *J. Exp. Biol.* **204**, 367–378.
- Öberg, F., Sjöhamn, J., Fischer, G., Moberg, A., Pedersen, A., Neutze, R. and Hedfalk, K.** (2011). Glycosylation increases the thermostability of human aquaporin 10 protein. *J. Biol. Chem.* **286**, 31915–23.
- Omasits, U., Ahrens, C. H., Müller, S. and Wollscheid, B.** (2014). Protter: interactive protein feature visualization and integration with experimental proteomic data. *Bioinformatics* **30**, 884–886.
- Onken, H. and Moffett, D. F.** (2009). Revisiting the cellular mechanisms of strong luminal alkalization in the anterior midgut of larval mosquitoes. *J. Exp. Biol.* **212**, 373–7.
- Onken, H. and Moffett, D. F.** (2017). Acid–base loops in insect larvae with extremely alkaline midgut regions. In *Acid-Base Balance and Nitrogen Excretion in Invertebrates*, pp. 239–260. Cham: Springer International Publishing.
- Pannabecker, T.** (1995). Physiology of the Malpighian tubule. *Annu. Rev. Entomol.* **40**, 493–510.
- Pao, G. M., Wu, L.-F., Johnson, K. D., Höfte, H., Chrispeels, M. J., Sweet, G., Sandal, N. N. and Saier, M. H.** (1991). Evolution of the MIP family of integral membrane transport proteins. *Mol. Microbiol.* **5**, 33–37.
- Patrick, M. and Bradley, T.** (2000). Regulation of compatible solute accumulation in larvae of

- the mosquito *Culex tarsalis*: osmolarity versus salinity. *J. Exp. Biol.* **203**, 831–839.
- Patrick, M. L., Aimanova, K., Sanders, H. R. and Gill, S. S.** (2006). P-type Na⁺/K⁺-ATPase and V-type H⁺-ATPase expression patterns in the osmoregulatory organs of larval and adult mosquito *Aedes aegypti*. *J. Exp. Biol.* **209**, 4638–51.
- Peter, R., Van den Bossche, P., Penzhorn, B. and Sharp, B.** (2005). Tick, fly, and mosquito control-lessons from the past, solutions for the future. *Vet. Parasitol.* **132**, 205–216.
- Pfaffl, M. W.** (2001). A new mathematical model for relative quantification in real-time RT-PCR. *Nucleic Acids Res.* **29**, e45.
- Piermarini, P. M., Weihrauch, D., Meyer, H., Huss, M. and Beyenbach, K. W.** (2009). NHE8 is an intracellular cation/H⁺ exchanger in renal tubules of the yellow fever mosquito *Aedes aegypti*. *Am. J. Physiol. Renal Physiol.* **296**, F730-50.
- Piermarini, P. M., Grogan, L. F., Lau, K., Wang, L. and Beyenbach, K. W.** (2010). A SLC4-like anion exchanger from renal tubules of the mosquito (*Aedes aegypti*): evidence for a novel role of stellate cells in diuretic fluid secretion. *Am. J. Physiol. Regul. Integr. Comp. Physiol.* **298**, R642-60.
- Piermarini, P., Hine, R., Matthew, S., Miyauchi, J. and Beyenbach, K.** (2011). Role of an apical K, Cl cotransporter in urine formation by renal tubules of the yellow fever mosquito (*Aedes aegypti*). *Am. J. Physiol. Regul. Integr. Comp. Physiol.* **301**, R1318–R1337.
- Piermarini, P. M., Dunemann, S. M., Rouhier, M. F., Calkins, T. L., Raphemot, R., Denton, J. S., Hine, R. M. and Beyenbach, K. W.** (2015). Localization and role of inward rectifier K(+) channels in Malpighian tubules of the yellow fever mosquito *Aedes aegypti*. *Insect Biochem. Mol. Biol.* **67**, 59–73.
- Pietrantonio, P. V., Jagge, C., Keeley, L. L. and Ross, L. S.** (2000). Cloning of an aquaporin-

- like cDNA and in situ hybridization in adults of the mosquito *Aedes aegypti* (Diptera: Culicidae). *Insect Mol. Biol.* **9**, 407–418.
- Pimentel, D.** (1995). Amounts of pesticides reaching target pests: Environmental impacts and ethics. *J. Agric. Environ. Ethics* **8**, 17–29.
- Preston, G., Jung, J., Guggino, W. and Agre, P.** (1994). Membrane topology of aquaporin CHIP. Analysis of functional epitope-scanning mutants by vectorial proteolysis. *J. Biol. Chem.* **269**, 1668–1673.
- Pullikuth, A. K., Aimanova, K., Kang'ethe, W., Sanders, H. R., Gill, S. S., Motais, R. and Borgese, F.** (2006). Molecular characterization of sodium/proton exchanger 3 (NHE3) from the yellow fever vector, *Aedes aegypti*. *J. Exp. Biol.* **209**, 3529–44.
- Ramsay, J. A.** (1950). Osmotic regulation in mosquito larvae. *J Exp Biol* **27**, 145–157.
- Reichow, S. L., Clemens, D. M., Freitas, J. A., Németh-Cahalan, K. L., Heyden, M., Tobias, D. J., Hall, J. E. and Gonen, T.** (2013). Allosteric mechanism of water-channel gating by Ca^{2+} -calmodulin. *Nat. Struct. Mol. Biol.* **20**, 1085–92.
- Robinson, J. R.** (1950). Osmoregulation in surviving slices from the kidneys of adult rats. *Proc. R. Soc. London (Series B)* **137**, 378–402.
- Roche, J. V. and Törnroth-Horsefield, S.** (2017). Aquaporin protein-protein interactions. *Int. J. Mol. Sci.* **18**, 2255.
- Sabolić, I., Katsura, T., Verbavatz, J. and Brown, D.** (1995). The AQP2 water channel: effect of vasopressin treatment, microtubule disruption, and distribution in neonatal rats. *J. Membr. Biol.* **143**, 165–175.
- Saparov, S. M., Liu, K., Agre, P. and Pohl, P.** (2007). Fast and selective ammonia transport by aquaporin-8. *J. Biol. Chem.* **282**, 5296–301.

- Satmary, W. and Bradley, T.** (1984). The distribution of cell types in the Malpighian tubules of *Aedes taeniorhynchus* (Wiedemann)(Diptera: Culicidae). *Int. J. Insect Morphol. Embryol.* **13**, 209–214.
- Schneider, C. A., Rasband, W. S. and Eliceiri, K. W.** (2012). NIH Image to ImageJ: 25 years of image analysis. *Nat. Methods* **9**, 671–675.
- Scott, B. N., Yu, M.-J., Lee, L. W. and Beyenbach, K. W.** (2004). Mechanisms of K⁺ transport across basolateral membranes of principal cells in Malpighian tubules of the yellow fever mosquito, *Aedes aegypti*. *J. Exp. Biol.* **207**, 1655–63.
- Shakesby, A. J., Wallace, I. S., Isaacs, H. V., Pritchard, J., Roberts, D. M. and Douglas, A. E.** (2009). A water-specific aquaporin involved in aphid osmoregulation. *Insect Biochem. Mol. Biol.* **39**, 1–10.
- Smith, B. and Agre, P.** (1991). Erythrocyte Mr 28,000 transmembrane protein exists as a multisubunit oligomer similar to channel proteins. *J. Biol. Chem.* **266**, 6407–6415.
- Sohal, R. S. and Copeland, E.** (1966). Ultrastructural variations in the anal papillae of *Aedes aegypti* (L.) at different environmental salinities. *J. Insect Physiol.* **12**, 429–434.
- Sreedharan, S., Kothandanb, G. and Sankaranarayananana, K.** (2016). Structural insights into the *Aedes aegypti* aquaporins and aquaglyceroporins—an in silico study. *J. Recept. Signal Transduct.* **36**, 543–557.
- Staniscuaski, F., Paluzzi, J.-P., Real-Guerra, R., Carlini, C. R. and Orchard, I.** (2013). Expression analysis and molecular characterization of aquaporins in *Rhodnius prolixus*. *J. Insect Physiol.* **59**, 1140–1150.
- Stobbart, R. H.** (1971). Evidence for Na⁺/H⁺ and Cl⁻/HCO₃⁻ exchanges during independent sodium and chloride uptake by the larva of the mosquito *Aedes aegypti* (L.). *J Exp Biol* **54**,

19–27.

- Sumner, D. M. and Belaine, G.** (2005). Evaporation, precipitation, and associated salinity changes at a humid, subtropical estuary. *Estuaries* **28**, 844–855.
- Tada, J., Sawa, T., Yamanaka, N., Shono, M., Akamatsu, T., Tsumura, K., Parvin, M. N., Kanamori, N. and Hosoi, K.** (1999). Involvement of vesicle-cytoskeleton interaction in AQP5 trafficking in AQP5-gene-transfected HSG cells. *Biochem. Biophys. Res. Commun.* **266**, 443–447.
- Tajkhorshid, E., Nollert, P., Jensen, M., Miercke, L., O’Connell, J., Stroud, R. and Schulten, K.** (2002). Control of the selectivity of the aquaporin water channel family by global orientational tuning. *Science (80-.)*. **296**, 525–530.
- Tamma, G., Klussmann, E., Maric, K., Aktories, K., Svelto, M., Rosenthal, W. and Valenti, G.** (2001). Rho inhibits cAMP-induced translocation of aquaporin-2 into the apical membrane of renal cells. *Am. J. Physiol. - Ren. Physiol.* **281**, F1092–F1101.
- Tatsumi, K., Tsuji, S., Miwa, H., Morisaku, T., Nuriya, M., Orihara, M., Kaneko, K., Okano, H. and Yasui, M.** (2009). *Drosophila big brain* does not act as a water channel, but mediates cell adhesion. *FEBS Lett.* **583**, 2077–2082.
- Terra, W. R., Ferreira, C. and de Bianchi, A. G.** (1979). Distribution of digestive enzymes among the endo- and ectoperitrophic spaces and midgut cells of *Rhynchosciara* and its physiological significance. *J. Insect Physiol.* **25**, 487–494.
- Terris, J., Ecelbarger, C. A., Marples, D., Knepper, M. A. and Nielsen, S.** (1995). Distribution of aquaporin-4 water channel expression within rat kidney. *Am J Physiol Ren. Physiol* **269**, F775-785.
- Thompson, S. and Borchardt, D.** (2003). Glucogenic blood sugar formation in an insect

- Manduca sexta* L.: asymmetric synthesis of trehalose from ¹³C enriched pyruvate. *Comp. Biochem. Physiol. Part B Biochem. Mol. Biol.* **135**, 461–671.
- Tomkowiak, E. and Pienkowska, J. R.** (2010). The current knowledge of invertebrate aquaporin water channels with particular emphasis on insect AQPs. *Adv. Cell Biol.* **2**, 91–104.
- Tsujimoto, H., Liu, K., Linser, P. J., Agre, P. and Rasgon, J. L.** (2013). Organ-specific splice variants of aquaporin water channel AgAQP1 in the malaria vector *Anopheles gambiae*. *PLoS One* **8**, e75888.
- van Balkom, B. W. M., Savelkoul, P. J. M., Markovich, D., Hofman, E., Nielsen, S., van der Sluijs, P. and Deen, P. M. T.** (2002). The role of putative phosphorylation sites in the targeting and shuttling of the aquaporin-2 water channel. *J. Biol. Chem.* **277**, 41473–9.
- Verkman, A. and Mitra, A.** (2000). Structure and function of aquaporin water channels. *Am. J. Physiol. - Ren. Physiol.* **278**, F13–F28.
- Virkki, L. V., Cooper, G. J. and Boron, W. F.** (2001). Cloning and functional expression of an MIP (AQP0) homolog from killifish (*Fundulus heteroclitus*) lens. *Am. J. Physiol. Integr. Comp. Physiol.* **281**, R1994–R2003.
- Volkman, A. and Peters, W.** (1989a). Investigations on the midgut caeca of mosquito larvae—II. Functional aspects. *Tissue Cell* **21**, 253–261.
- Volkman, A. and Peters, W.** (1989b). Investigations on the midgut caeca of mosquito larvae—I. Fine structure. *Tissue Cell* **21**, 243–251.
- Walz, T., Smith, B. L., Zeidel, M. L., Engel, A. and Agre, P.** (1994). Biologically active two-dimensional crystals of aquaporin CHIP. *J. Biol. Chem.* **269**, 1583–6.
- Welinder, C. and Ekblad, L.** (2011). Coomassie staining as loading control in Western blot

- analysis. *J. Proteome Res.* **10**, 1416–1419.
- Weng, X., Huss, M., Wieczorek, H. and Beyenbach, K.** (2003). The V-type H⁺-ATPase in Malpighian tubules of *Aedes aegypti*: localization and activity. *J. Exp.* **206**, 2211–2219.
- Wieczorek, H., Putzenlechner, M., Zeiske, W. and Klein, U.** (1991). A vacuolar-type proton pump energizes K⁺/H⁺ antiport in an animal plasma membrane. *J. Biol. Chem.* **266**, 15340–15347.
- Wigglesworth, V. B.** (1932). The function of the anal gills of the mosquito larva. *J. Exp. Biol.* **10**, 16–26.
- Wright, P. A.** (1995). Nitrogen excretion: three end products, many physiological roles. *J. Exp. Biol.* **198**, 273–281.
- Wu, B. and Beitz, E.** (2007). Aquaporins with selectivity for unconventional permeants. *Cell. Mol. life Sci.* **64**, 2413–2421.
- Yamamoto, N., Sobue, K., Miyachi, T., Inagaki, M., Miura, Y., Katsuya, H. and Asai, K.** (2001). Differential regulation of aquaporin expression in astrocytes by protein kinase C. *Mol. Brain Res.* **95**, 110–116.
- Yang, L. and Piermarini, P. M.** (2017). Molecular expression of aquaporin mRNAs in the northern house mosquito, *Culex pipiens*. *J. Insect Physiol.* **96**, 35–44.
- Yanochko, G. M. and Yool, A. J.** (2002). Regulated cationic channel function in *Xenopus* oocytes expressing *Drosophila* big brain. *J. Neurosci.* **22**, 2530–40.
- Yanochko, G. M. and Yool, A. J.** (2004). Block by extracellular divalent cations of *Drosophila* big brain channels expressed in *Xenopus* oocytes. *Biophys. J.* **86**, 1470–8.
- Yasui, M., Hazama, A., Kwon, T.-H., Nielsen, S., Guggino, W. B. and Agre, P.** (1999). Rapid gating and anion permeability of an intracellular aquaporin. *Nature* **402**, 184–187.

Yi, S.-X., Benoit, J. B., Elnitsky, M. A., Kaufmann, N., Brodsky, J. L., Zeidel, M. L.,

Denlinger, D. L. and Lee, R. E. (2011). Function and immuno-localization of aquaporins in the Antarctic midge *Belgica antarctica*. *J. Insect Physiol.* **57**, 1096–105.

Zelenina, M., Zelenin, S., Bondar, A. A., Brismar, H. and Aperia, A. (2002). Water permeability of aquaporin-4 is decreased by protein kinase C and dopamine. *Am. J. Physiol. Renal Physiol.* **283**, F309-18.

Zhuang, Z., Linser, P. J. and Harvey, W. R. (1999). Antibody to H(+) V-ATPase subunit E colocalizes with portosomes in alkaline larval midgut of a freshwater mosquito (*Aedes aegypti*). *J. Exp. Biol.* **202**, 2449–2460.